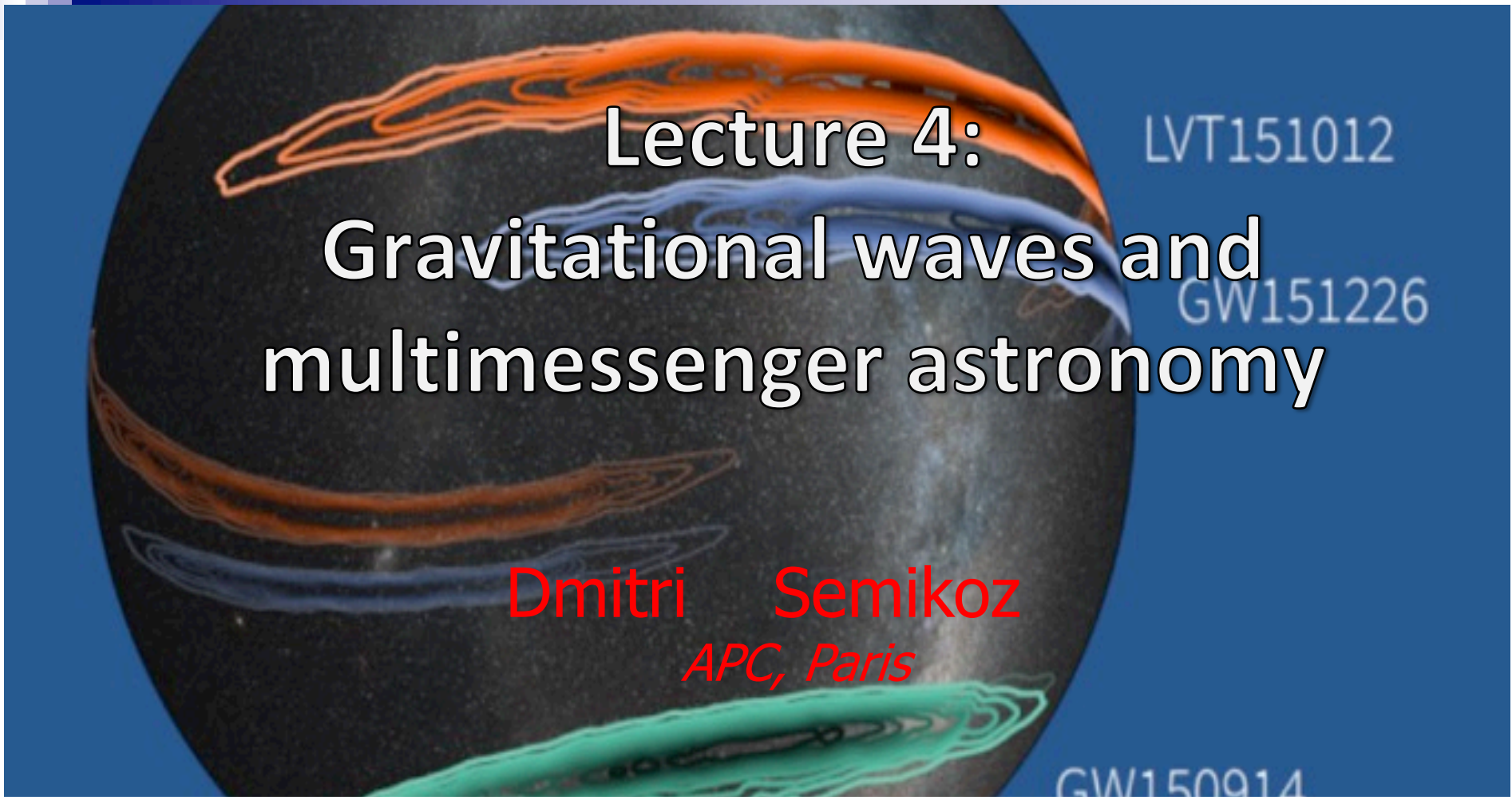

Lecture 4: Gravitational waves and multimessenger astronomy

Dmitri Semikoz
APC, Paris

Overview:

- *Introduction: history GW*
- *Ground based Experiments on Gravitational waves and first detection*
- *Phenomenology of Gravitational Waves*
- *LISA space mission*
- *Pulsar timing Arrays,*
- *HO measurement, NANOGrav signal*
- *Gravitational Waves from neutron star merge and multi-messenger signal.*

INTRODUCTION: histrory of Gravitational Wave searches

General Relativity

1915: Einstein's Theory of General Relativity

1916: Einstein paper on linear approximation to general relativity with multiple applications, including gravitational waves.

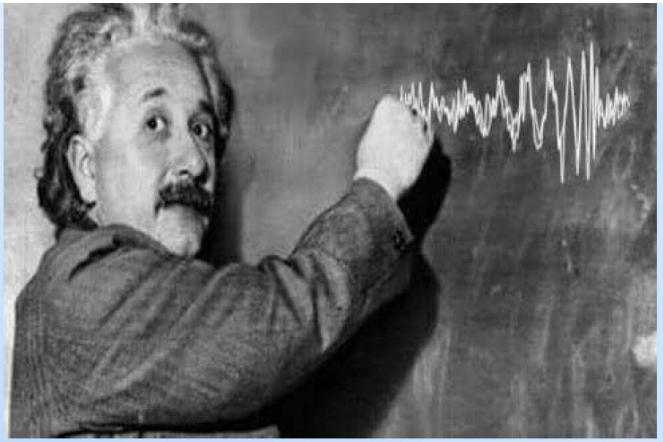

688 Sitzung der physikalisch-mathematischen Klasse vom 22. Juni 1916

Näherungsweise Integration der Feldgleichungen der Gravitation.

Von A. Einstein.

Gravitational waves

$$A = \frac{\varkappa}{24\pi} \sum_{\alpha\beta} \left(\frac{\partial^3 J_{\alpha\beta}}{\partial t^3} \right)^2 . \qquad (21)$$

Würde man die Zeit in Sekunden, die Energie in Erg messen, so würde zu diesem Ausdruck der Zahlenfaktor $\frac{1}{c^4}$ hinzutreten. Berücksichtigt man außerdem, daß $\varkappa = 1.87 \cdot 10^{-27}$, so sieht man, daß A in allen nur denkbaren Fällen einen praktisch verschwindenden Wert haben muß.

"… in all conceivable cases, ***A*** must have a practically vanishing value."

Gravitational waves are predicted by Einstein, but he recognizes that they are too small.

Gravitational waves

154 Gesamtsitzung vom 14. Februar 1918. — Mitteilung vom 31. Januar

Über Gravitationswellen.

Von A. Einstein.

On Gravitational Waves – 1918

Einstein works out the remaining details on gravitational waves: emission (quadrupole), polarizations, they carry energy, etc

Dabei ist zur Abkürzung

$$\mathfrak{J}_{\mu\nu} = \int x_\mu x_\nu \rho \, dV_0 \qquad (23)$$

gesetzt; $\mathfrak{J}_{\mu\nu}$ sind die Komponenten des (zeitlich variabeln) Trägheitsmomentes des materiellen Systems.

$$\gamma'_{23} = -\frac{\varkappa}{4\pi R}\ddot{\mathfrak{J}}_{23}.$$

Are Gravitational Waves Real?

Continued debate on whether gravitational waves really exist up until 1957 Chapel Hill conference.

Felix Pirani paper and presentation: relative acceleration of particle pairs can be associated with the Riemann tensor. The interpretation of the attendees was that non-zero components of the Riemann tensor were due to gravitational waves.

Sticky bead (Felix Pirani, Richard Feynman, Hermann Bondi)

Joe Weber of the University of Maryland, and from this inspiration started to think about gravitational wave detection.

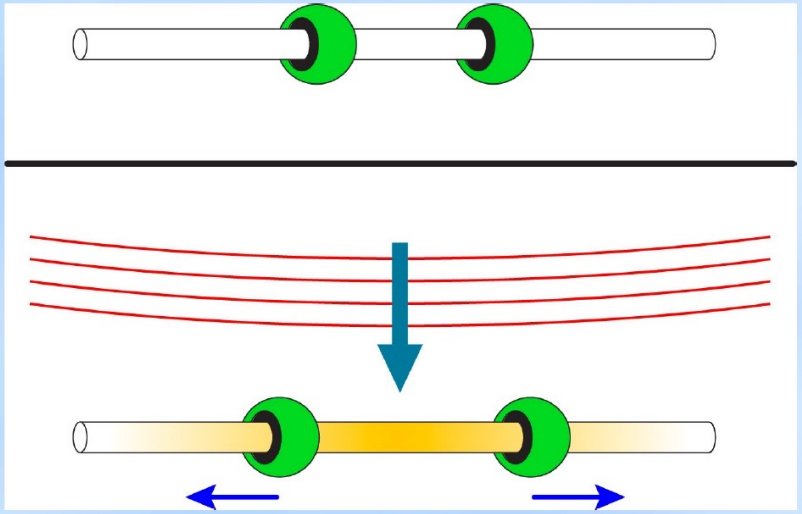

What Are Gravitational Waves?

- General relativity (1916) prediction.
- Gravity is not really a force in GR, but a space-time deformation.
- Masses locally deform space-time.
- Accelerated masses emit gravitational waves, ripples in space time.
- Space-time is rigid:

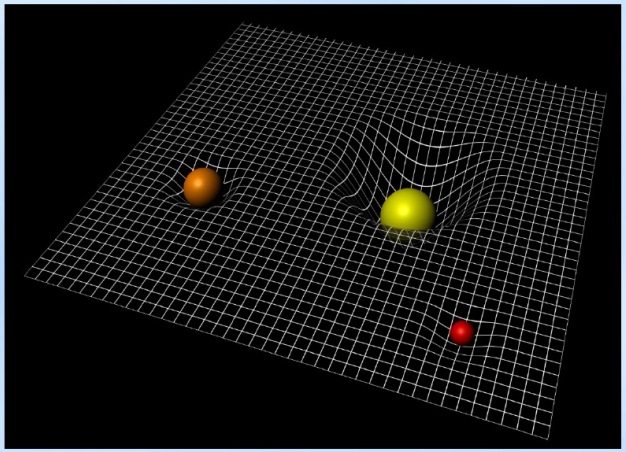

The amplitude of the deformation is tiny.

Need cataclysmic events in order to expect to measure something on Earth … $h \sim 10^{-21}$

- Gravitational Wave sources: mainly astrophysical in the 10 Hz -10 kHz bandwidth

Binary Pulsar PSR 1913+16

$M1 = 1.438\ M_o$

$M2 = 1.390\ M_o$

8 hour orbit
Orbit decays by 3mm per orbit.

Discovered in 1974 by Russell Hulse and Joseph Taylor, then at University Massachusetts.

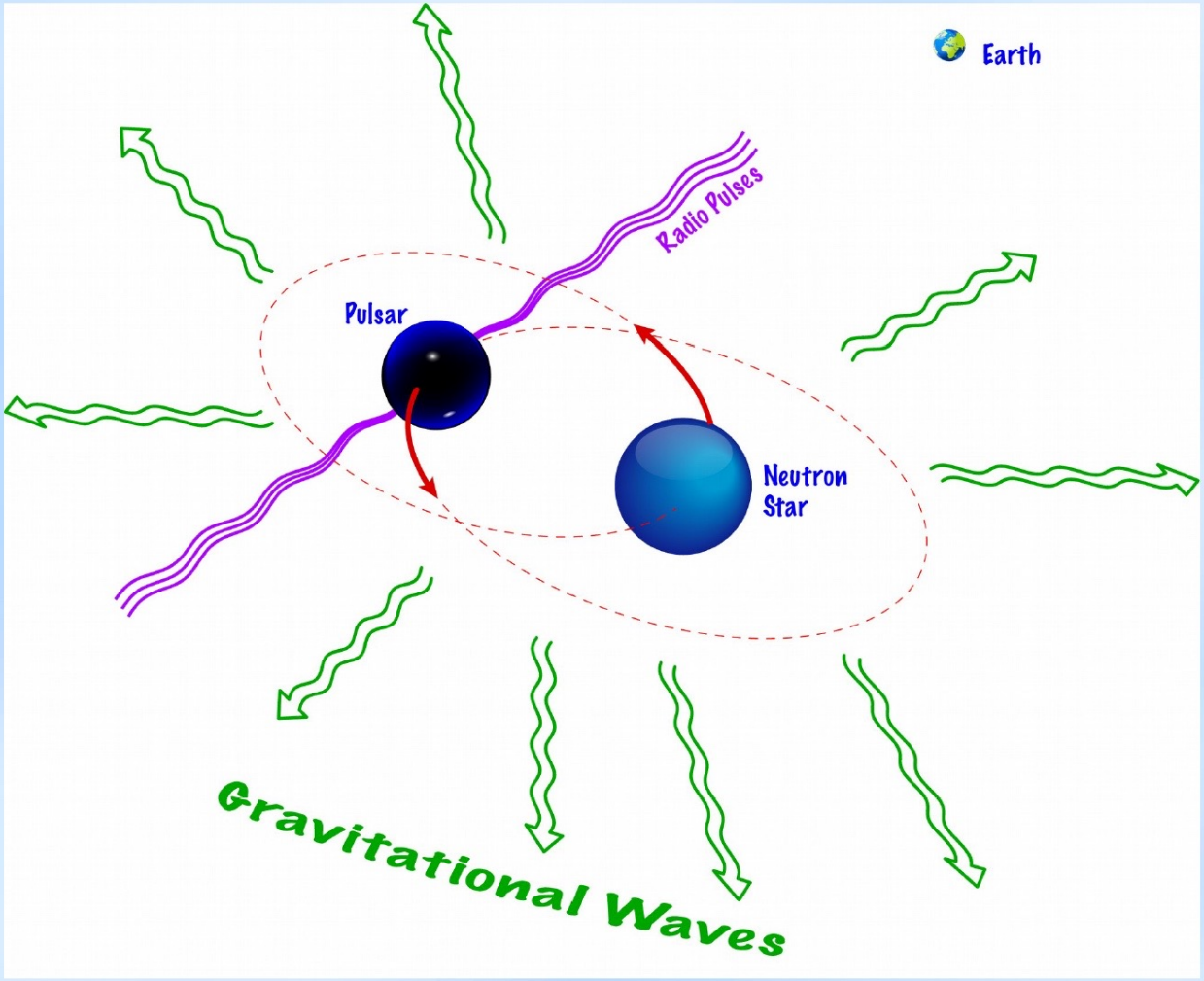

A Nobel Prize for ...

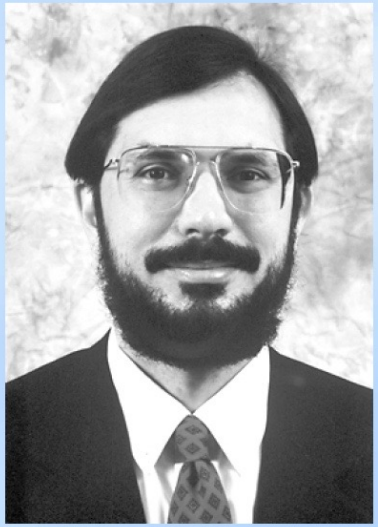

“… for the discovery of a new type of pulsar, a discovery that has opened up new possibilities for the study of gravitation.” 1993

For more on this Nobel, see, "The Nobel pulsar", Nelson Christensen. Science, Vol. 348 no. 6236 p. 766 (2015).

First Proof That Gravitational Waves Exist - 1982

THE ASTROPHYSICAL JOURNAL, 253:908–920, 1982 February 15

A NEW TEST OF GENERAL RELATIVITY: GRAVITATIONAL RADIATION AND THE BINARY PULSAR PSR 1913+16

J. H. TAYLOR AND J. M. WEISBERG
Department of Physics and Astronomy, University of Massachusetts, Amherst; and Joseph Henry Laboratories, Physics Department, Princeton University
Received 1981 July 2; accepted 1981 August 28

ABSTRACT

Observations of pulse arrival times from the binary pulsar PSR 1913+16 between 1974 September and 1981 March are now sufficient to yield a solution for the component masses and the absolute size of the orbit. We find the total mass to be almost equally distributed between the pulsar and its unseen companion, with $m_p = 1.42 \pm 0.06\ M_\odot$ and $m_c = 1.41 \pm 0.06\ M_\odot$. These values are used, together with the well determined orbital period and eccentricity, to calculate the rate at which the orbital period should decay as energy is lost from the system via gravitational radiation. According to the general relativistic quadrupole formula, one should expect for the PSR 1913+16 system an orbital period derivative $\dot{P}_b = (-2.403 \pm 0.005) \times 10^{-12}$. Our observations yield the measured value $\dot{P}_b = (-2.30 \pm 0.22) \times 10^{-12}$. The excellent agreement provides compelling evidence for the existence of gravitational radiation, as well as a new and profound confirmation of the general theory of relativity.

Subject headings: gravitation — pulsars — relativity

Gravitational Wave Proof

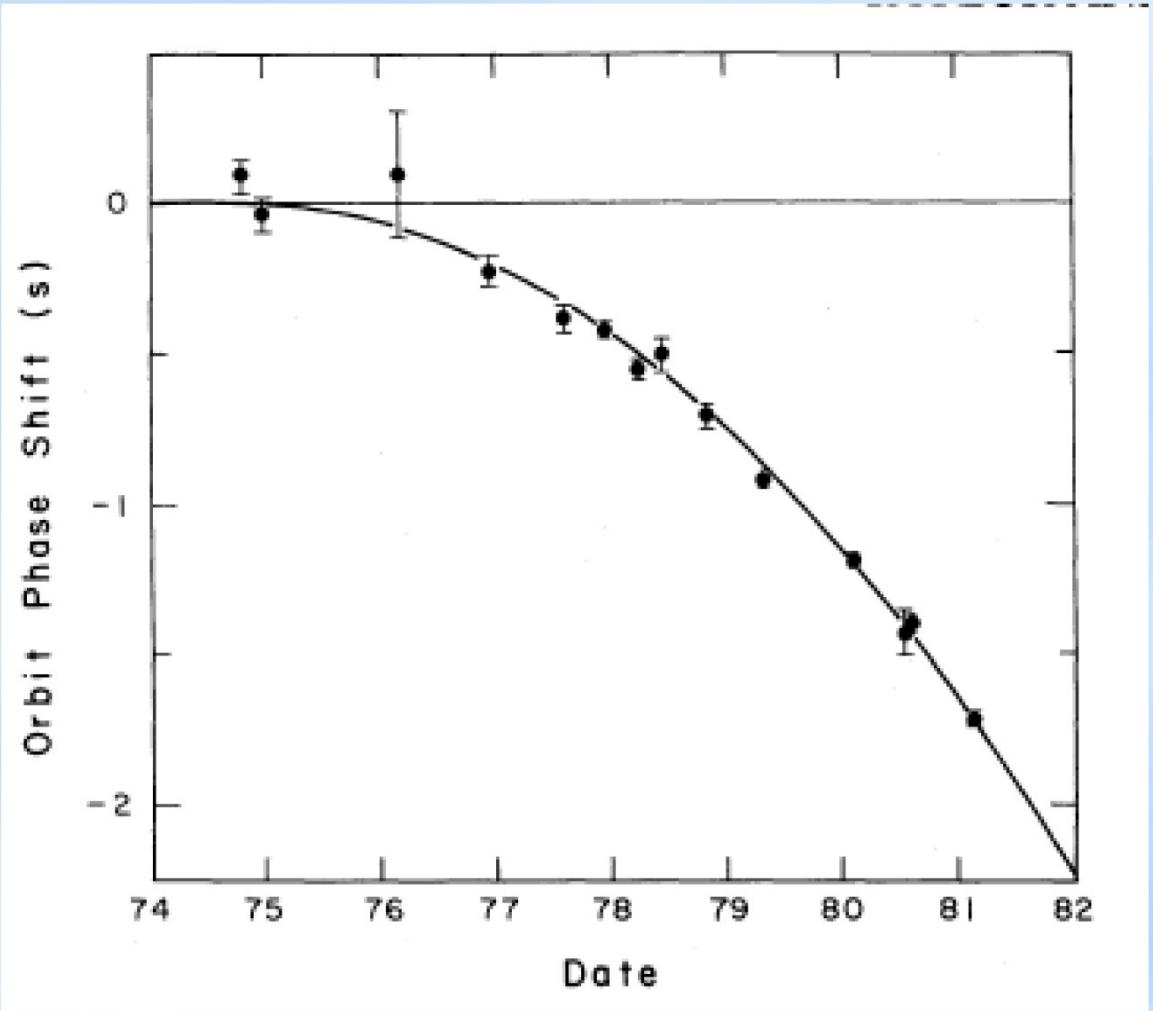

Taylor and Weisberg, 1982

Binary Pulsar Studies Continue

The Astrophysical Journal, 829:55 (10pp), 2016 September 20 doi:10.3847/0004-637X/829/1/55

RELATIVISTIC MEASUREMENTS FROM TIMING THE BINARY PULSAR PSR B1913+16

J. M. Weisberg and Y. Huang
Department of Physics and Astronomy, Carleton College, Northfield, MN 55057, USA; jweisber@carleton.edu
Received 2016 January 19; revised 2016 April 20; accepted 2016 June 1; published 2016 September 21

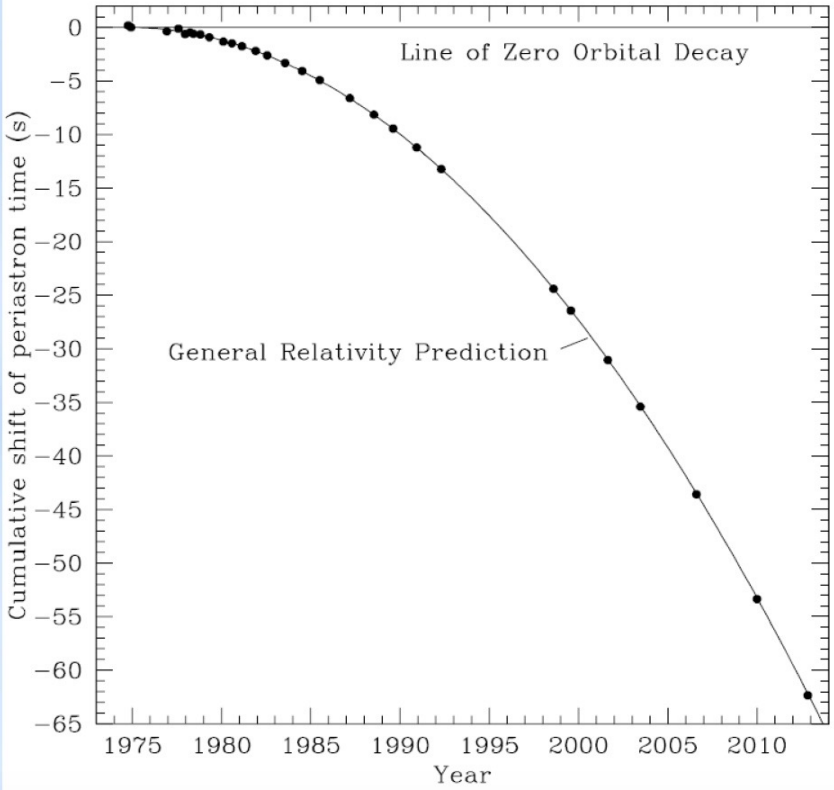

"The points, with error bars too small to show, represent our measurements"

Gravitational Wave Detection

Inspired and motivated by the Chapel Hill Conference, Joe Weber of the University of Maryland constructs the first gravitational wave detectors.

"In 1958 I was able to prove, using Einstein's equations that a gravitational wave would change the dimensions of an extended body."

EVIDENCE FOR DISCOVERY OF GRAVITATIONAL RADIATION*

J. Weber
Department of Physics and Astronomy, University of Maryland, College Park, Maryland 20742
(Received 29 April 1969)

Coincidences have been observed on gravitational-radiation detectors over a base line of about 1000 km at Argonne National Laboratory and at the University of Maryland. The probability that all of these coincidences were accidental is incredibly small. Experiments imply that electromagnetic and seismic effects can be ruled out with a high level of confidence. These data are consistent with the conclusion that the detectors are being excited by gravitational radiation.

K. Thorne 1980

1960s & 70s: Detection claims and theoretical studies on sources

The future looks promising—but by no means certain! The search for gravitational waves is a game requiring long, hard effort with a definite risk of total failure—but with very great payoff if it succeeds.

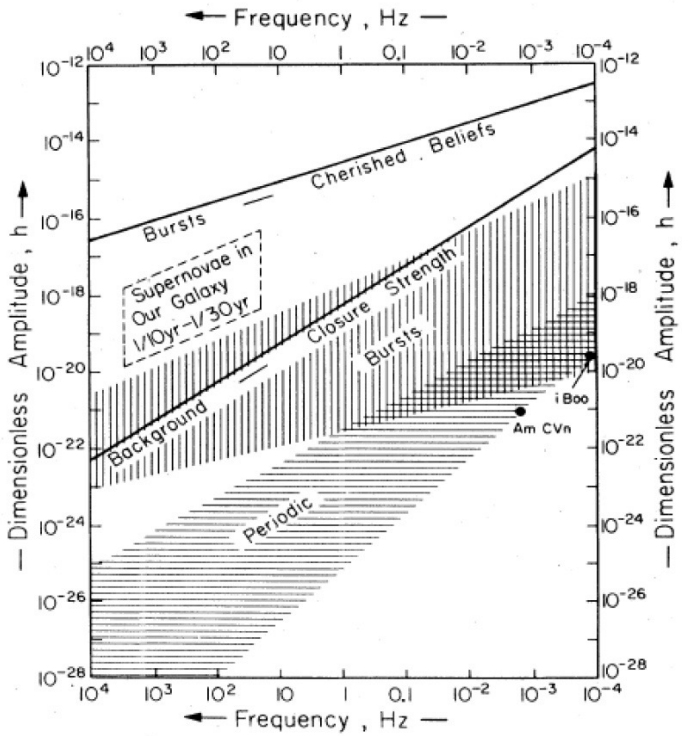

FIG. 3. Estimates of the strengths of the gravitational waves that bathe the Earth. See text for explanation of the lines and hatched regions.

Interferometric GW Detectors

First suggestion: 1962 two Soviet physicists, V.I. Pustovoit and M.E. Gertsenshtein, noted that the use of a Michelson interferometer would be a possible means to detect gravitational waves over a frequency range that was broader than the Weber bars.

1970's, Robert Forward (student of Weber) at Hughes Ai
Michelson interferometer to search for gravitational wave
(MIT) and astronaut Philip Chapman (also at MIT) for ins

The wideband interfe

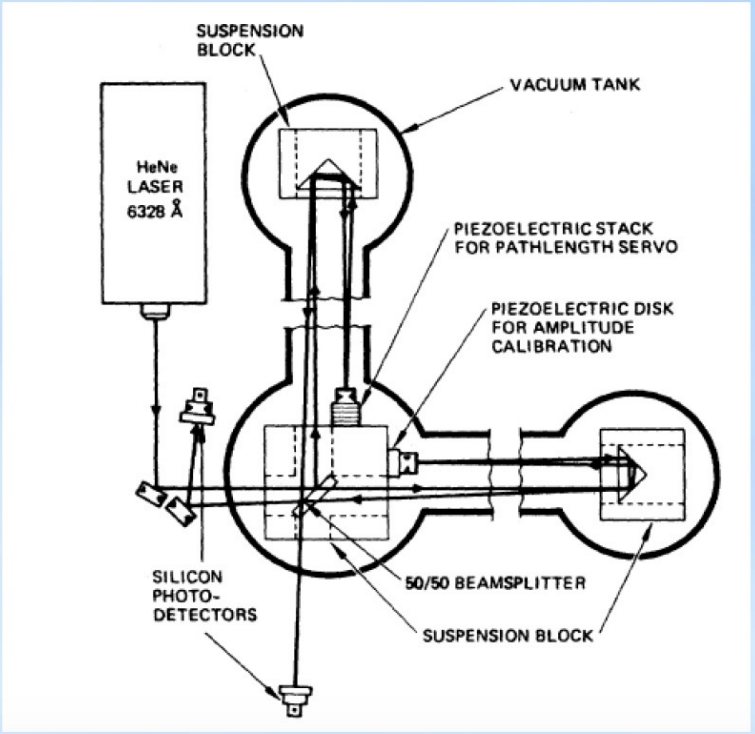

VII. CALIBRATION OF EAR

When the interferometer was working well, we were able to hear single-frequency 3- to 10-kHz tones of 10-fm rms amplitude introduced into the interferometer by the piezoelectric displacement transducer.

Since the noise level of the interferometer in that band is about 0.9 fm/$Hz^{1/2}$, this means that the audio system, including our ear-brain combination, had an effective detection bandwidth of about 120 Hz.

Rai Weiss Interferometer Study

1972: Weiss produces the first detailed study for a realistic interferometric gravitational wave detector.

Systematically addresses a number of realistic noise sources:

- Amplitude Noise in the Laser Output Power
- Laser Phase Noise or Frequency Instability
- Mechanical Thermal Noise in the Antenna
- Radiation-Pressure Noise from the Laser Light
- Seismic Noise
- Thermal-Gradient Noise
- Cosmic-Ray Noise
- Gravitational-Gradient Noise
- Electric Field and Magnetic Field Noise

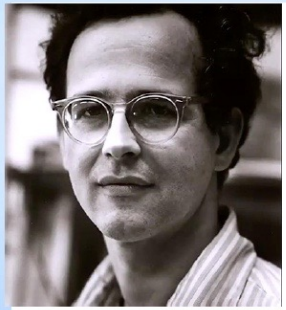

Fig. V-20. Proposed antenna.

Prototype Interferometric Detectors

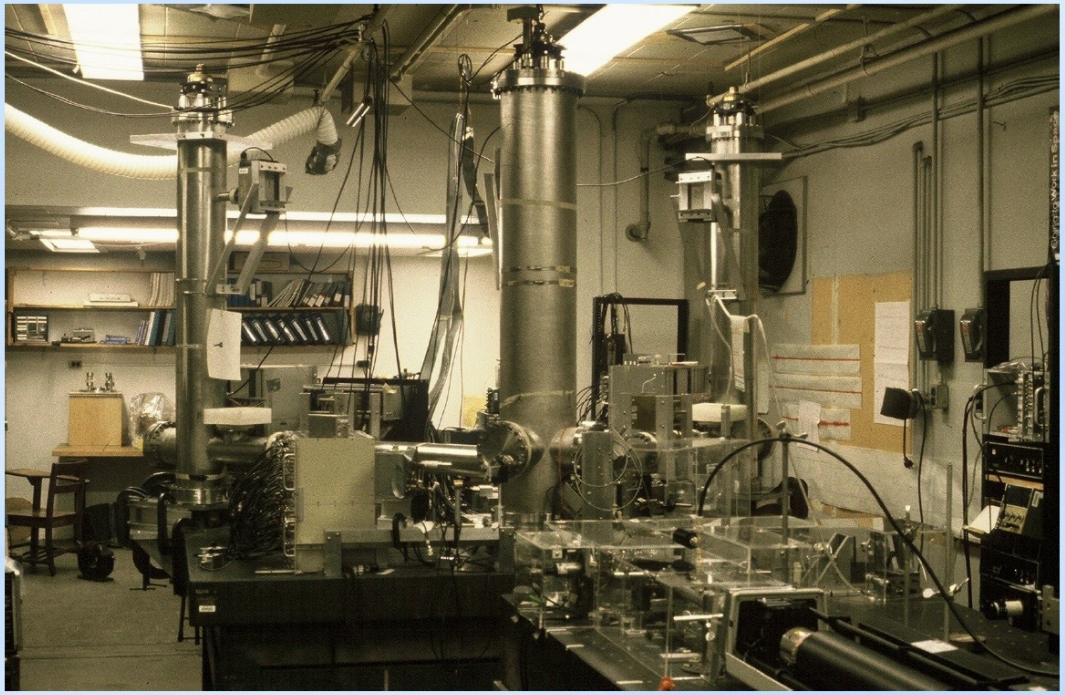

MIT 1.5 m delay line Michelson Interferometer

1970s and 80s:
Interferometers constructed at
Garching
Glasgow
MIT
Caltech

The interferometer technology started progressing rapidly.

1980s LIGO is Born

Thorne, Drever (Caltech)

Weiss (MIT)

National Science Foundation

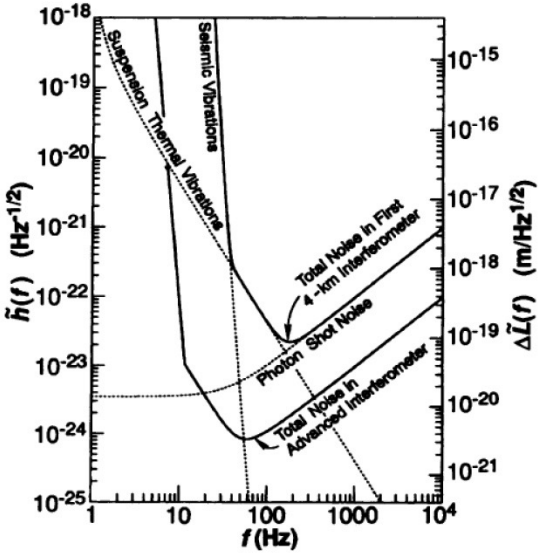

Fig. 7. The expected total noise in each of LIGO's first 4-km interferometers (upper solid curve) and in a more advanced interferometer (lower solid curve). The dashed curves show various contributions to the first interferometer's noise.

SCIENCE • VOL. 256 • 17 APRIL 1992

While in Europe … Virgo

A. Brillet (Orsay, Nice)
Lasers, Optics

A. Giazotto (Pisa)
Vibration Isolation

cnrs

INFN

The Detectors

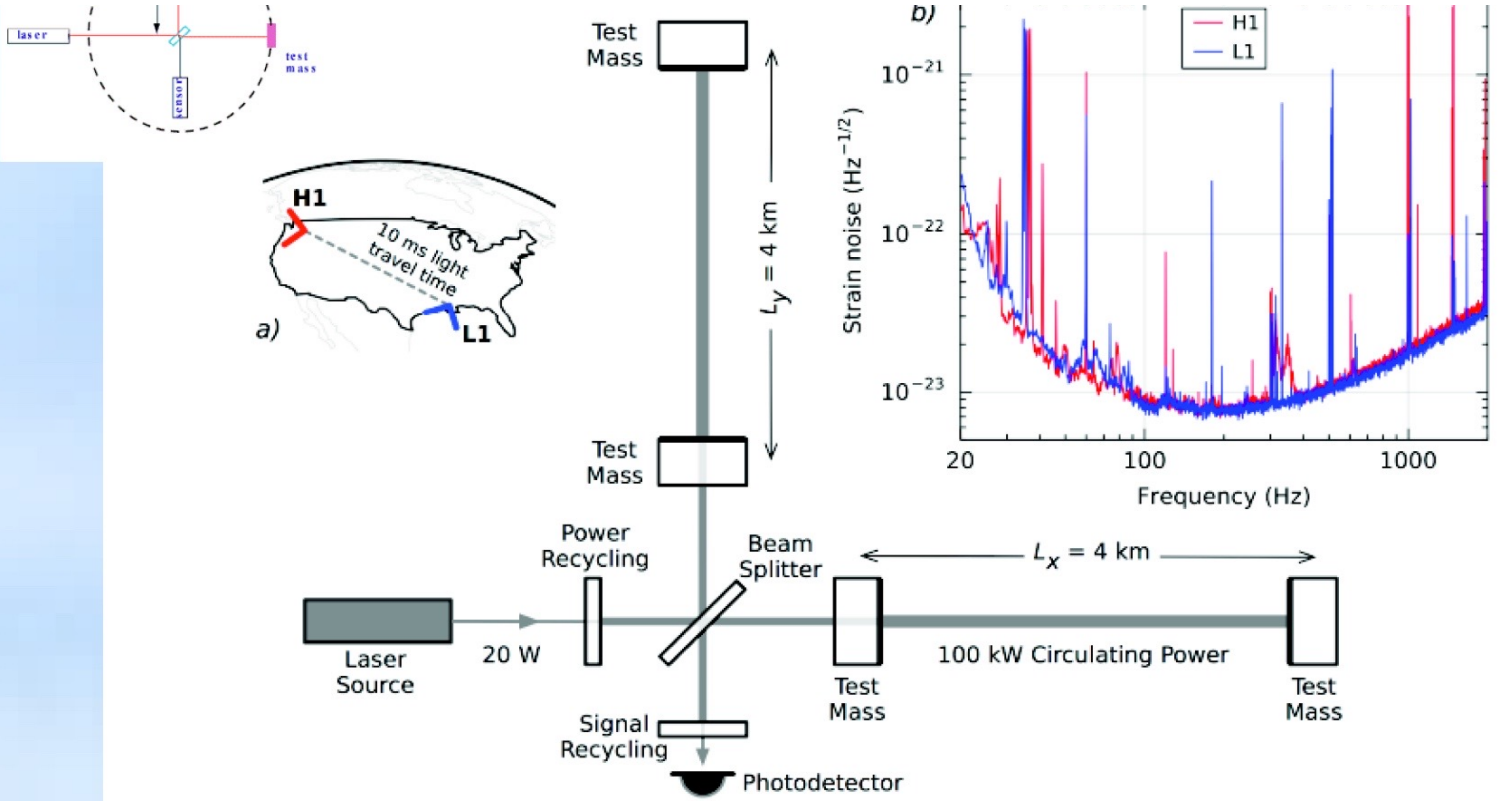

Advanced LIGO – Advanced Virgo

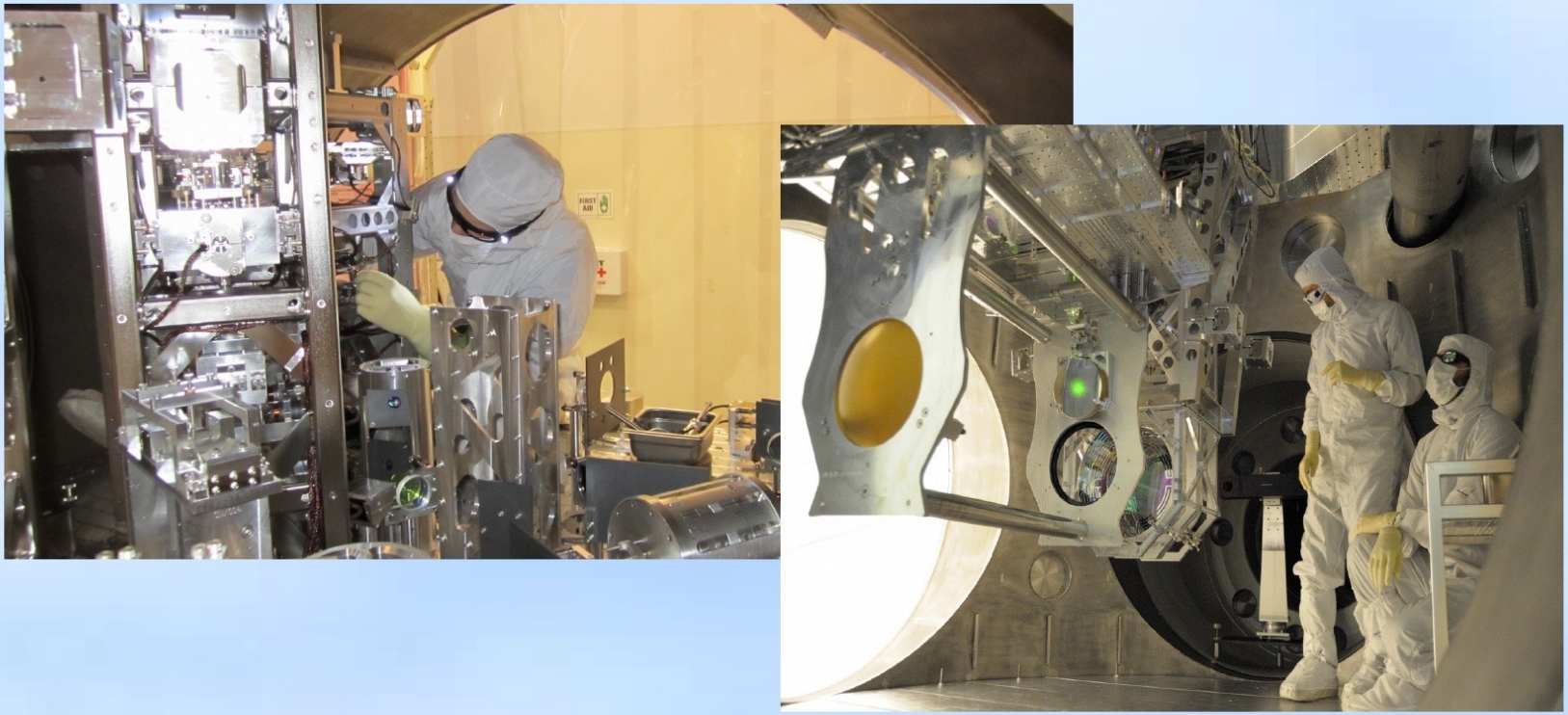

Built on the experience gained from the first generation detectors

Advanced LIGO

- Advanced LIGO commissioned 2010-2015.
  - » Increased laser power
  - » Sophisticated seismic/vibration suppression
  - » Quadruple pendula suspensions
  - » Larger mirrors, better suspension material
  - » More complex and versatile interferometer configuration.

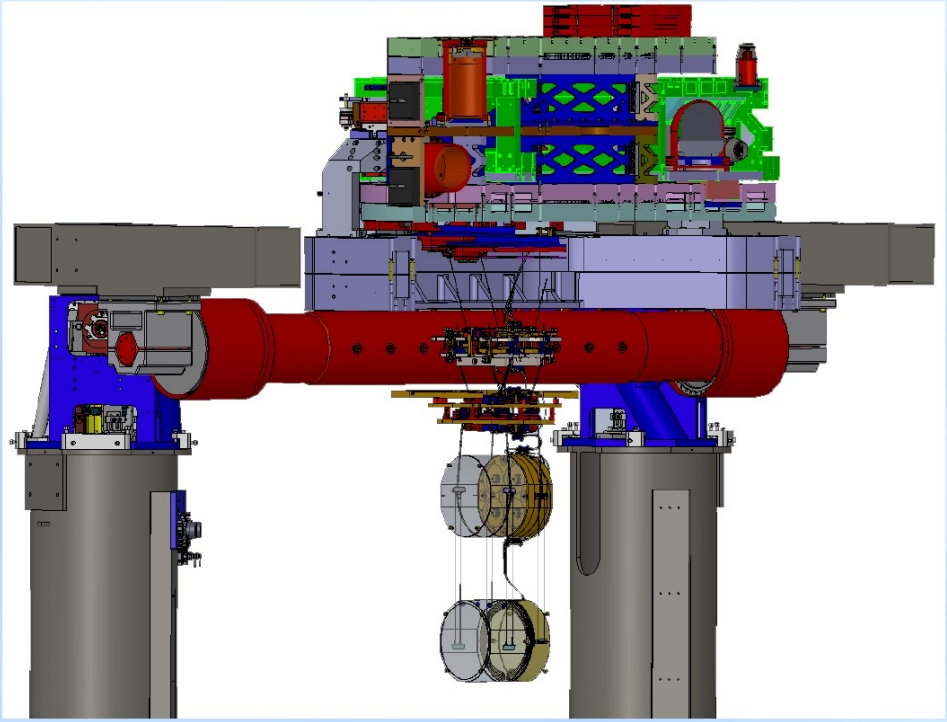

Advanced Virgo

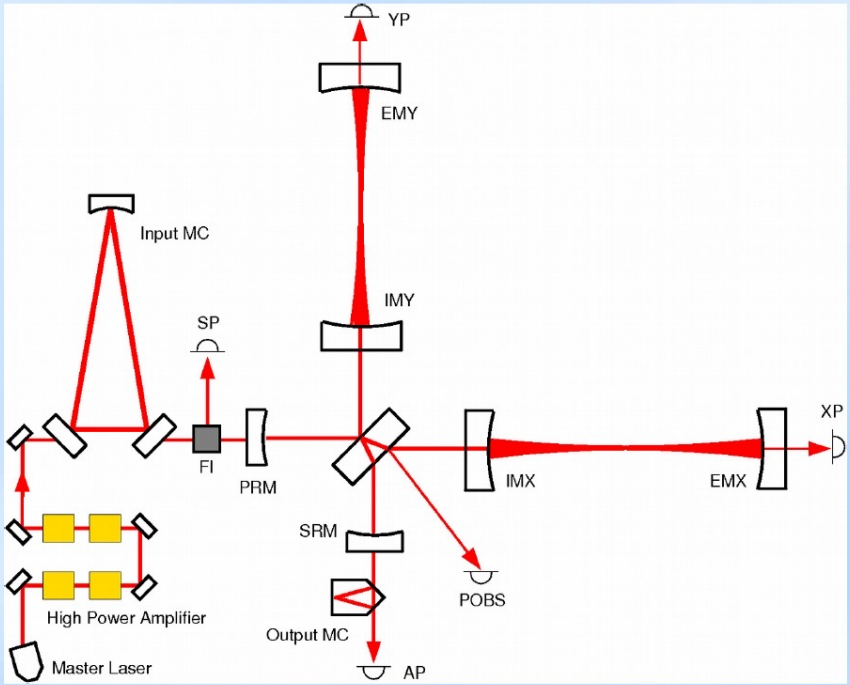

- Larger mirrors; better optical quality.
- Higher finesse of the arm cavities
- Increased laser power.
- Coming on-line in Spring 2017.

Advanced Virgo

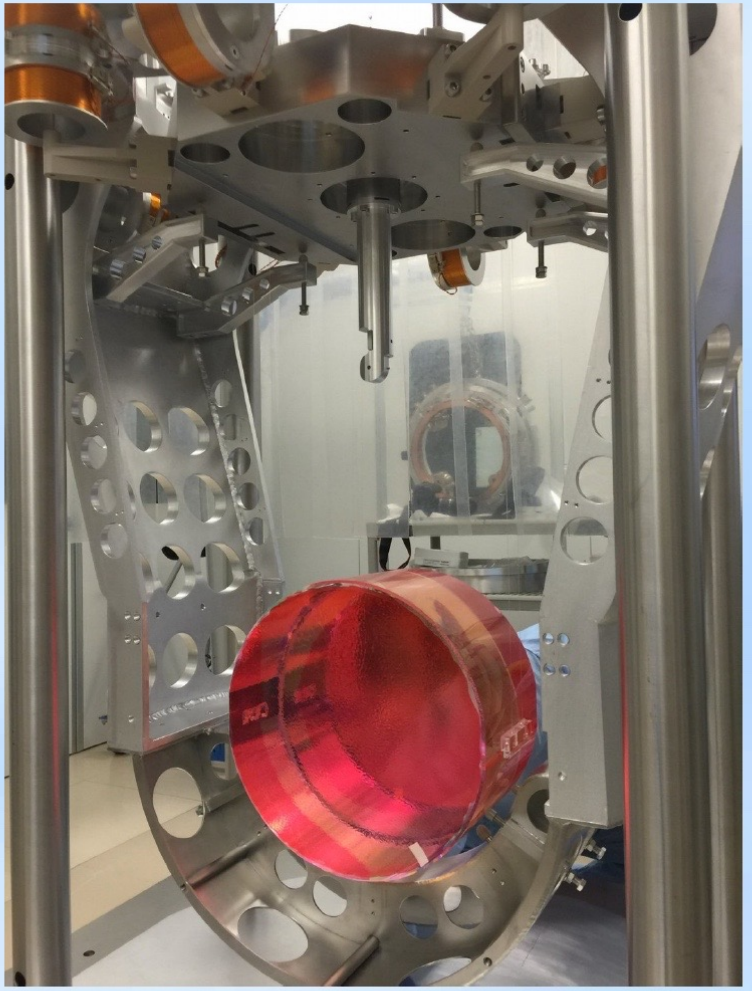

Mirror

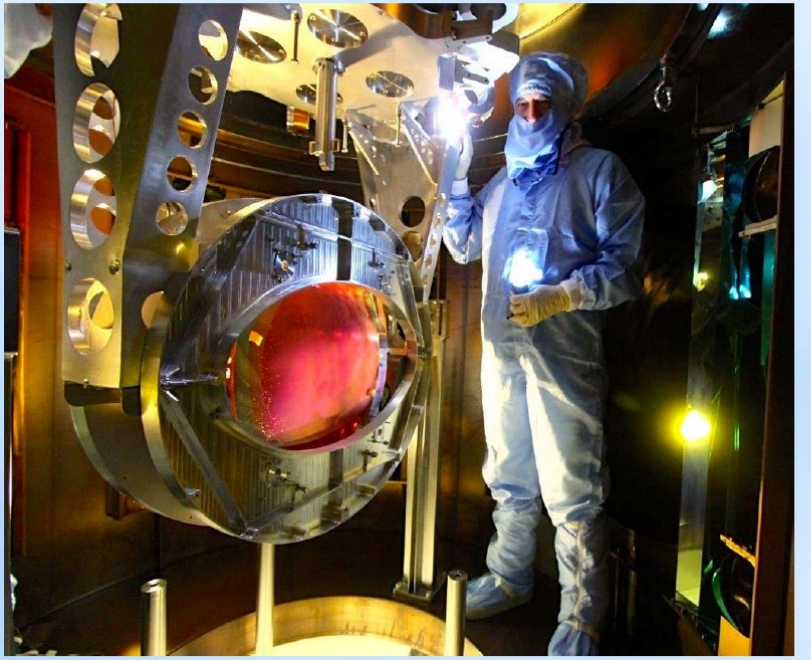

Beamsplitter

The optical components are very large, but their quality is exquisite.

GW150914

- Band-pass filter:

  35-350 Hz
- L1-H1 time delay of about 7ms.
- Chirp signal, typical of binary coalescences.
- Detected by online burst-search pipelines.
- Confirmed later matched template searches.
- Combined SNR: 24.

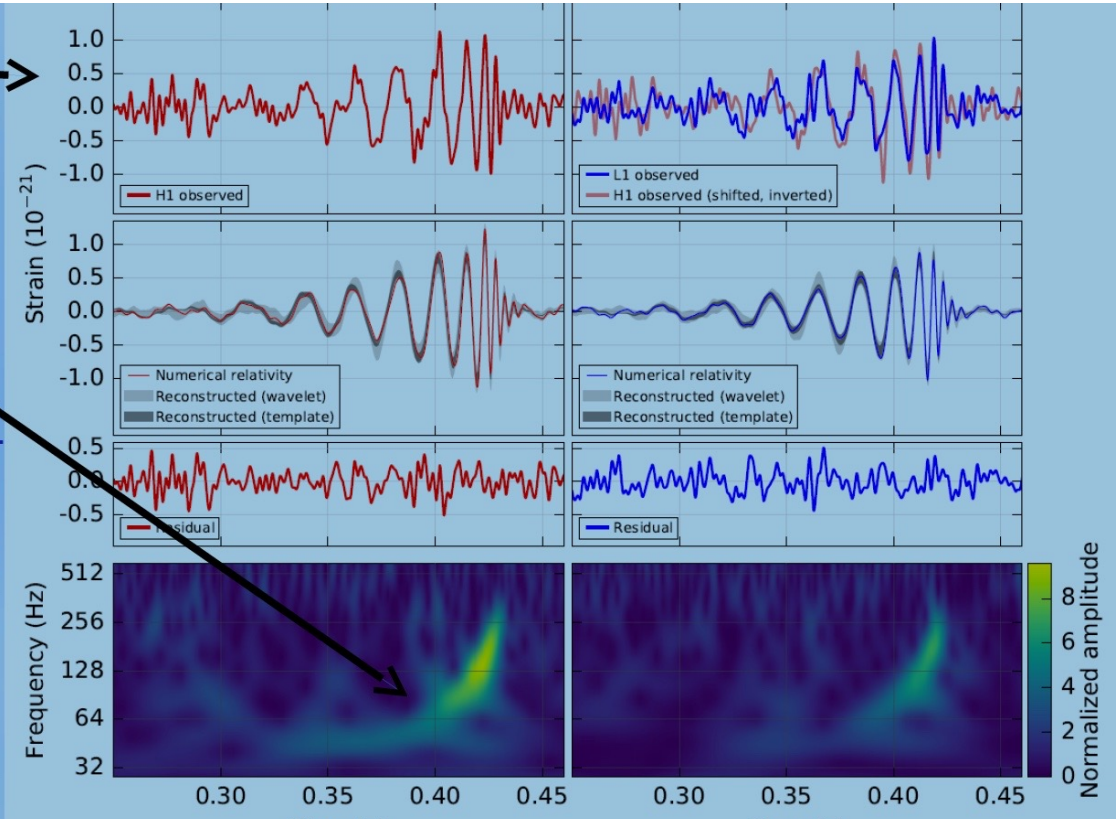

The Results

Observation of Gravitational Waves from a Binary Black Hole Merger

B. P. Abbott *et al.*[*]
(LIGO Scientific Collaboration and Virgo Collaboration)
(Received 21 January 2016; published 11 February 2016)

On September 14, 2015 at 09:50:45 UTC the two detectors of the Laser Interferometer Gravitational-Wave Observatory simultaneously observed a transient gravitational-wave signal. The signal sweeps upwards in frequency from 35 to 250 Hz with a peak gravitational-wave strain of 1.0×10^{-21}. It matches the waveform predicted by general relativity for the inspiral and merger of a pair of black holes and the ringdown of the resulting single black hole. The signal was observed with a matched-filter signal-to-noise ratio of 24 and a false alarm rate estimated to be less than 1 event per 203 000 years, equivalent to a significance greater than 5.1σ. The source lies at a luminosity distance of 410^{+160}_{-180} Mpc corresponding to a redshift $z = 0.09^{+0.03}_{-0.04}$. In the source frame, the initial black hole masses are $36^{+5}_{-4}M_{\odot}$ and $29^{+4}_{-4}M_{\odot}$, and the final black hole mass is $62^{+4}_{-4}M_{\odot}$, with $3.0^{+0.5}_{-0.5}M_{\odot}c^2$ radiated in gravitational waves. All uncertainties define 90% credible intervals. These observations demonstrate the existence of binary stellar-mass black hole systems. This is the first direct detection of gravitational waves and the first observation of a binary black hole merger.

DOI: 10.1103/PhysRevLett.116.061102

Primary black hole mass	$36^{+5}_{-4}M_{\odot}$
Secondary black hole mass	$29^{+4}_{-4}M_{\odot}$
Final black hole mass	$62^{+4}_{-4}M_{\odot}$
Final black hole spin	$0.67^{+0.05}_{-0.07}$
Luminosity distance	410^{+160}_{-180} Mpc
Source redshift z	$0.09^{+0.03}_{-0.04}$

Phenomenology of GW

When GW passes through space deforms it

When GW passes through space deforms it

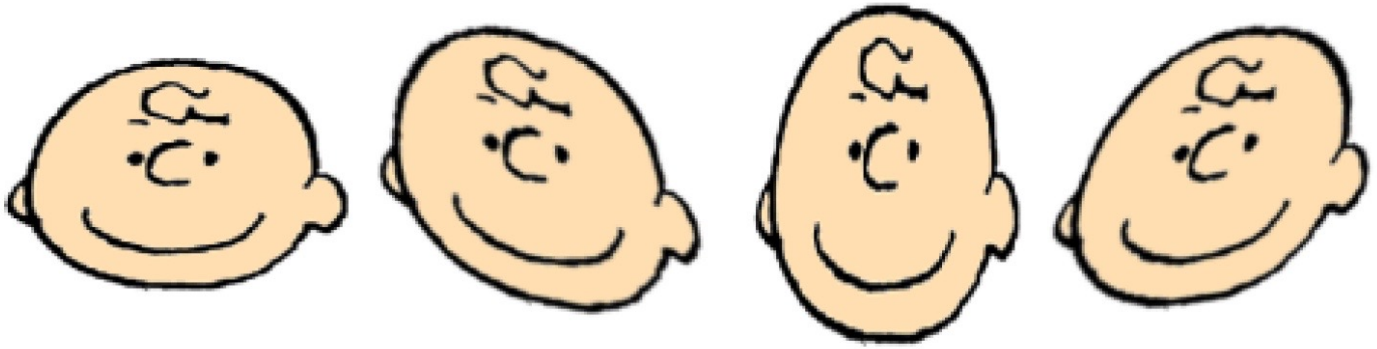

When GW passes through space deforms it

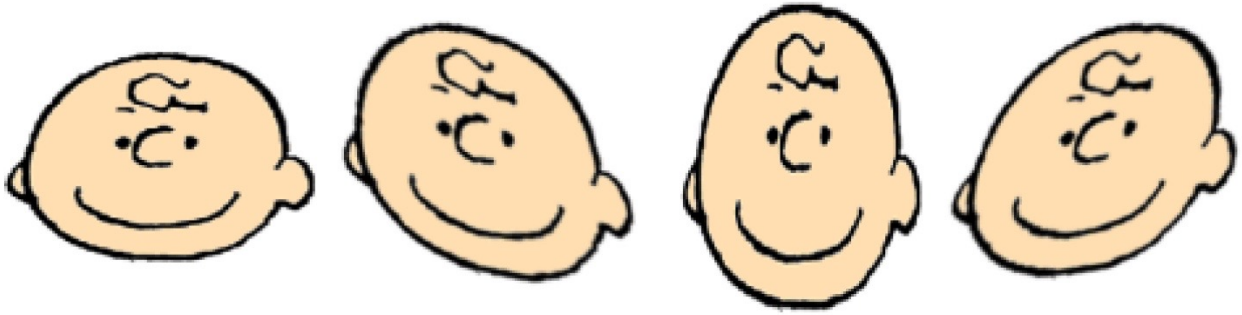

But deformations are very small: strain=relative deformation

$$h = DL/L \sim 1e\text{-}21$$

For $L_{Sun\text{-}Earth}$~ 1.5e13 cm

$h\ L_{Sun\text{-}Earth}$ ~ 1e-21 x 1.5e13 ~ 1.5e-08cm

size of H atom at distance Sun-Earth

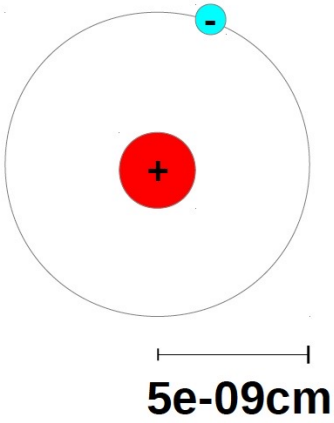

Some math:

Consider Einstein equation

$$R_{\mu\nu} - \frac{1}{2} g_{\mu\nu} R = \frac{8\pi G}{c^4} T_{\mu\nu}$$

Consider a small perturbation of the flat Cartesian metric
Weak field (far from source)

$$g_{\mu\nu} = \eta_{\mu\nu} + h_{\mu\nu} \qquad with\, |h_{\mu\nu}| \ll 1$$

Using gauge invariance and assuming vacuum (*T*=0 no mass no energy)

Equation of WAVES!!

$$\Box h = -\frac{16\pi G}{c^4} T_{\mu\nu} = 0$$

If you want to know more about GR formalism:
https://arxiv.org/pdf/1607.04202.pdf

By integrating equation

$$\Box h = -\frac{16\pi G}{c^4} T_{\mu\nu}$$

$$h^{ij}(t,\vec{x}) \sim \frac{2\,G}{r\,c^4}\frac{d^2}{dt^2} I^{ij}(t - r/c)$$

Distance source-observer

Moment of inertia, or second mass moment, or quadrupole moment of mass $I^{ij} = \int dx^3\, \rho(t,\vec{x})\, x^i\, x^j$

Retarded time

→ **not all accelerating masses do this job but only those with <u>QUADRUPOLE</u>**

If you do calculation, monopole and dipole disappear

→ **for a gravitational wave to form, there must be an ASYMMETRY IN MASS DISTRIBUTION**

What are the astrophysical objects with non-zero quadrupole?

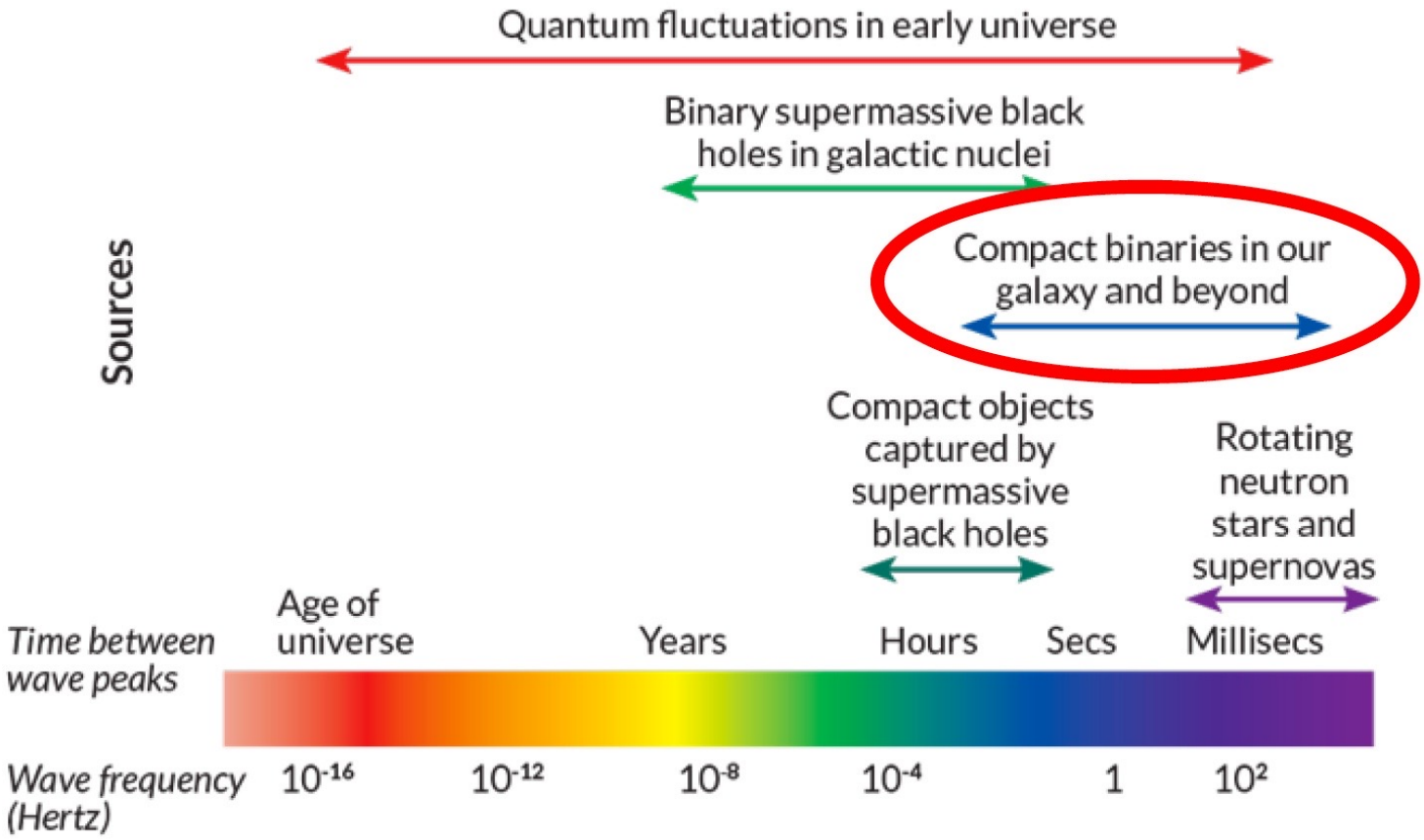

Primordial gravitational waves / Quantum fluctuations:

<< 1 sec from Big Bang, due to INFLATION of the Universe
Freq. ~ 10^-16 – 10^2 Hz
extremely “faint” (small amplitude)

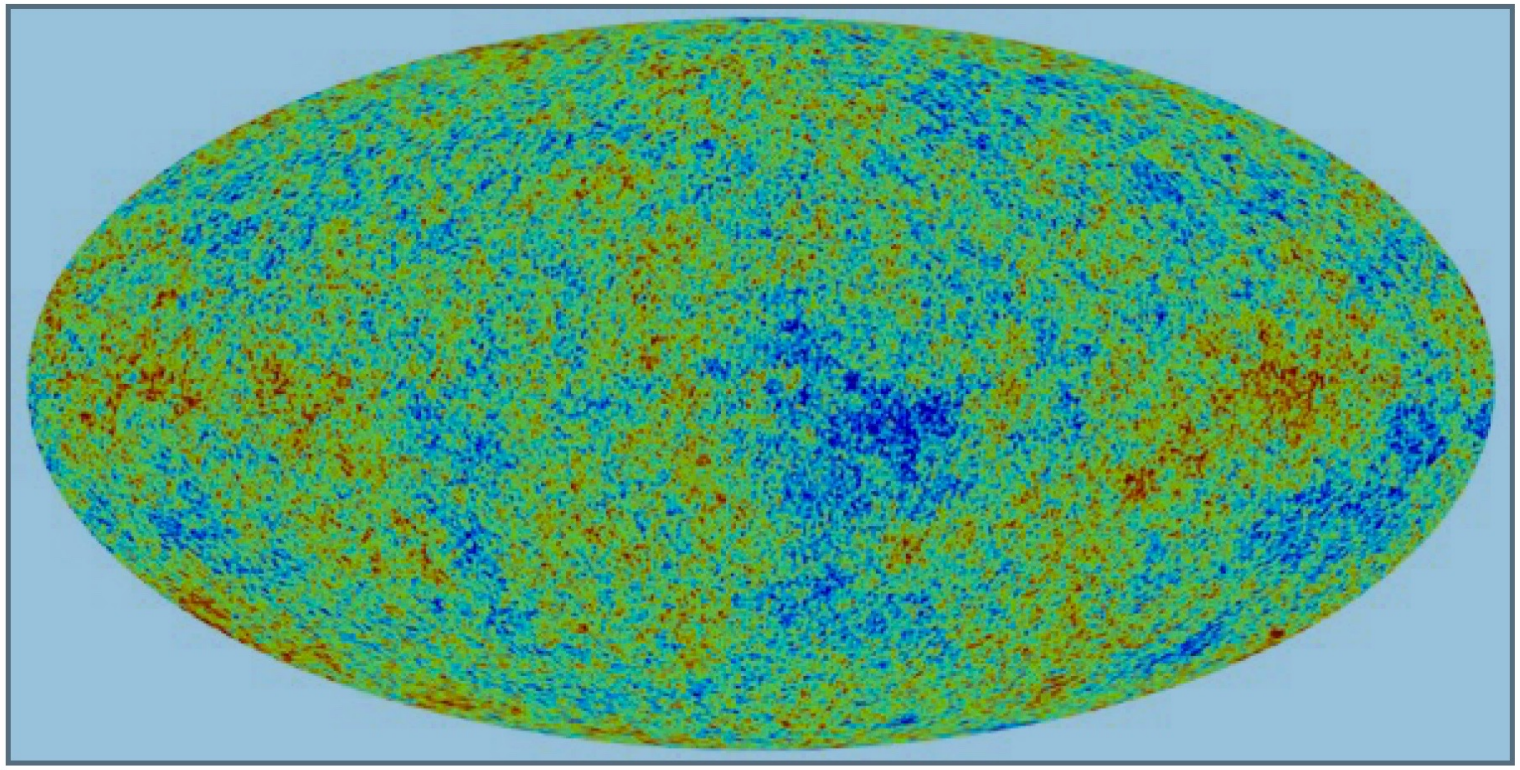

Mergers of super-massive black holes (SMBHs, >10^5 Msun):

Black holes at centre of galaxies might form Keplerian binaries and might merge

Freq. ~ 10^-10 – 0.1 Hz

Mergers of super-massive black holes (SMBHs, >10^5 Msun):

Black holes at centre of galaxies might form Keplerian binaries and might merge

Freq. ~ 10^-10 – 0.1 Hz

Mergers of compact object binaries (black holes <10^5 Msun, neutron stars):

Black holes (BHs) and neutron stars (NSs) born from stars might merge
Freq. ~ 10^-4 – 10^3 Hz

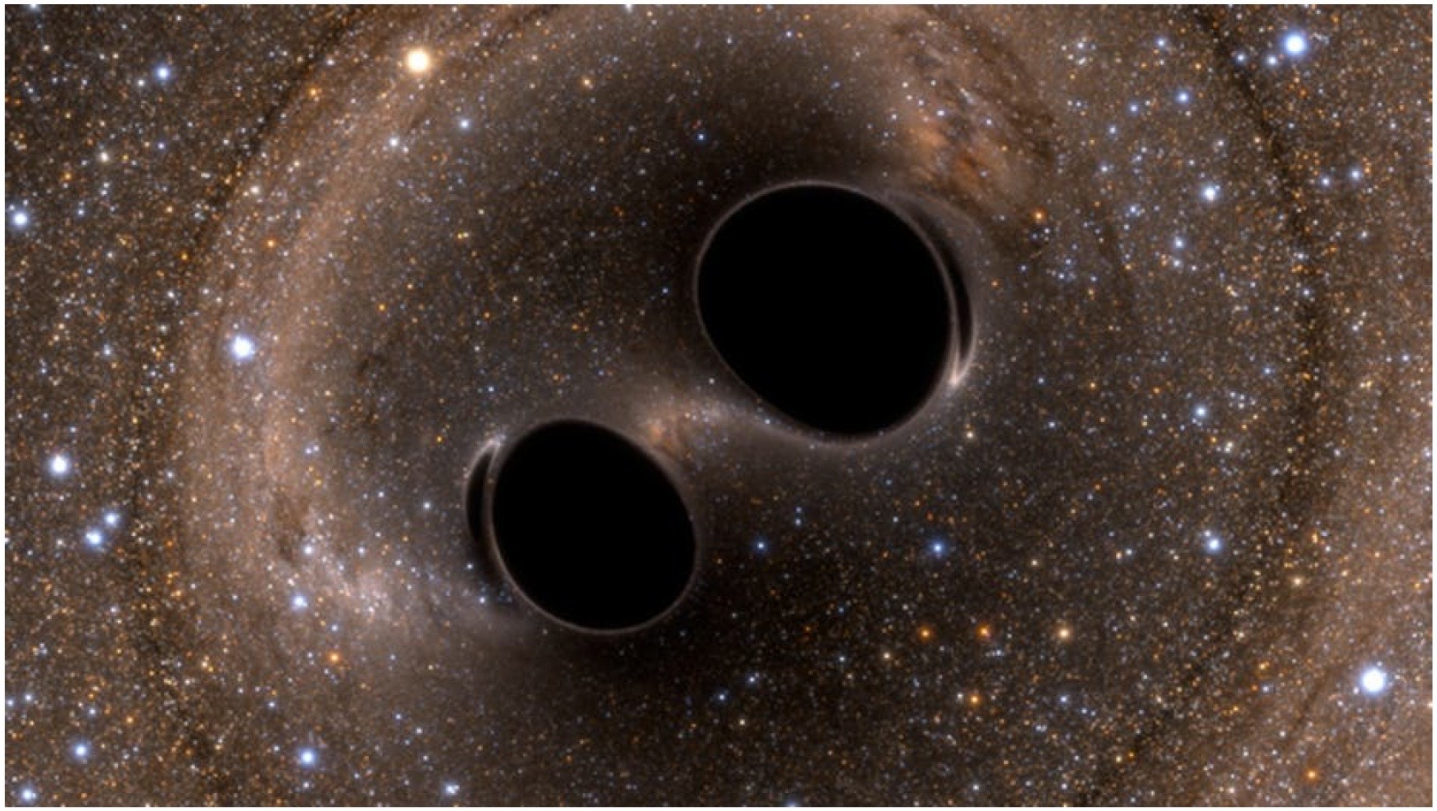

Mergers of SMBHs and stellar-mass BHs:

Small BHs might orbit SMBHs and be captured by them

Freq. ~ 10^-4 – 0.1 Hz

Mergers of SMBHs and stellar-mass BHs:

Small BHs might orbit SMBHs and be captured by them

Freq. ~ 10^-4 – 0.1 Hz

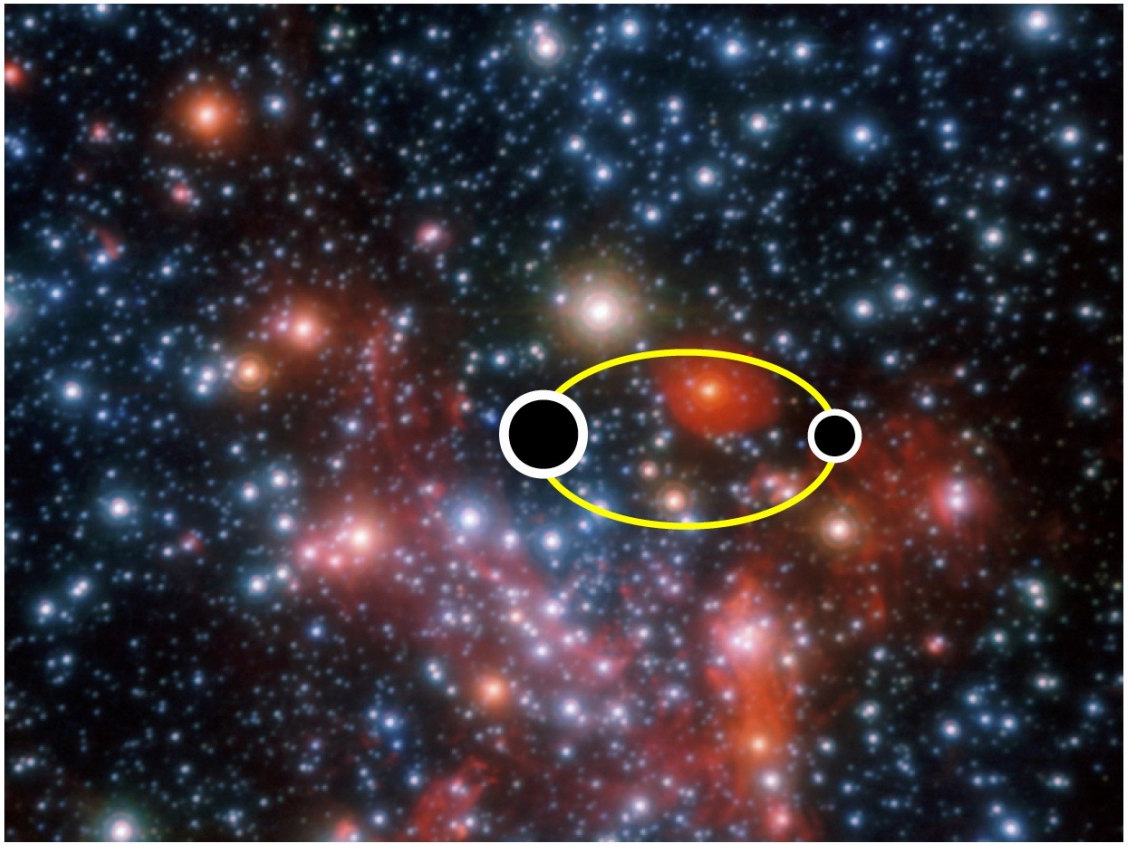

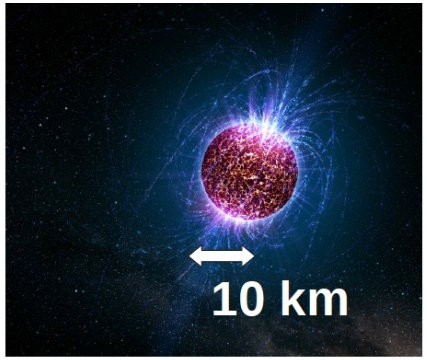

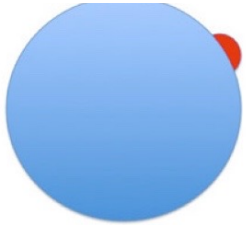

Asymmetric supernova explosions:
Freq. ~ 10 – 10^2 Hz

Mergers of super-massive black holes (SMBHs, >10^5 Msun)

Mergers of compact object binaries

Only GWs observed so far

Mergers of SMBHs and BHs

Neutron stars with crustal asymmetries

Asymmetric supernova explosions

Some essential math about GWs from BINARIES:

It can be shown that $$h^{ij}(t,\vec{x}) \sim \frac{2\,G}{r\,c^4}\frac{d^2}{dt^2}\,I^{ij}(t-r/c)$$

can be expressed in spherical coordinates (*r, ϕ, θ*)
for a KEPLERIAN BINARY with reduced mass μ = *m1 m2/(m1+m2)*
with semi-major axis *a*, with orbital frequency ω_{orb}
and eccentricity *e* = 0 as

$$h_+(t,\theta,\phi,r) = \frac{1}{r}\,\frac{4\,G\,\mu\,\omega_{orb}^2\,a^2}{c^4}\,\frac{1+\cos^2\theta}{2}\,\cos\left(2\,\omega_{orb}\,t_{ret}+\phi\right)$$

$$h_x(t,\theta,\phi,r) = \frac{1}{r}\,\frac{4\,G\,\mu\,\omega_{orb}^2\,a^2}{c^4}\,\cos\theta\,\sin\left(2\,\omega_{orb}\,t_{ret}+\phi\right)$$

where $t_{ret} = t - r/c$ $\qquad$ $\omega_{orb}^2 = \frac{G\,(m_1+m_2)}{a^3}$

This equation tells us:

– **GWs are POLARIZED (h_+, h_x)**

– **FREQUENCY TERM DEPENDS only ON 2 ω_{orb}**

→ **frequency of GWs $\omega_{GW} = 2\,\omega_{orb}$**

(true for most evolution)

– **AMPLITUDE of GWs:**

$$h = \frac{1}{2}\sqrt{h_+^2 + h_x^2} = \frac{2\,G\,\mu\,\omega_{orb}^2\,a^2}{c^4}\,\frac{1}{r}\sqrt{\frac{(1+\cos^2\theta)^2}{4} + cos^2\theta}$$

$$h = \frac{1}{2}\sqrt{h_+^2 + h_x^2} = \frac{2\,G^2\,m_1\,m_2}{a\,c^4}\,\frac{1}{r}\sqrt{\frac{(1+\cos^2\theta)^2}{4} + cos^2\theta}$$

– **AMPLITUDE of GWs:**

$$h = \frac{1}{2}\sqrt{h_+^2 + h_x^2} = \frac{2\,G^2\,m_1\,m_2}{a\,c^4}\,\frac{1}{r}\sqrt{\frac{(1+\cos^2\theta)^2}{4} + cos^2\theta}$$

*** the bigger the amplitude (strain), the easier the detection**

*** the farther the binary, the smaller the amplitude**

*** the larger the masses, the larger the amplitude**

*** the smaller the semi-major axis, the larger the amplitude**

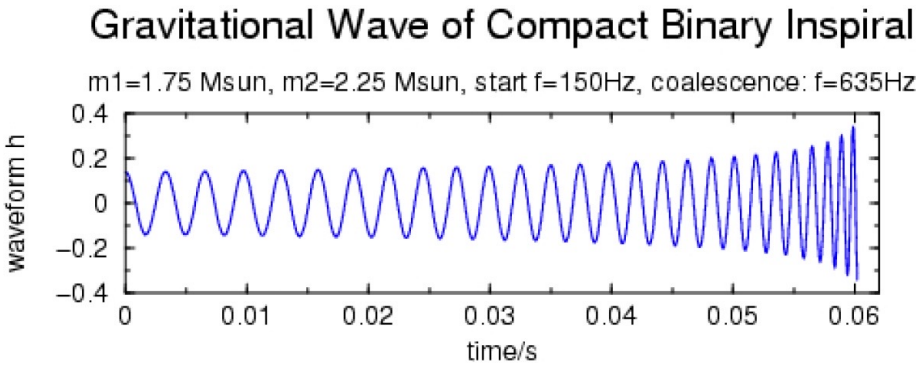

– EMISSION of GWs implies LOSS of ORBITAL ENERGY:

$$E_{orb} = -\frac{G\, m_1\, m_2}{2\, a}$$

THE BINARY SHRINKS WHILE EMITTING GWs
TILL IT MERGES

https://www.youtube.com/watch?v=g8s81MzzJ5c

– **EMISSION of GWs implies LOSS of ORBITAL ENERGY:**
THE BINARY SHRINKS WHILE EMITTING GWs
TILL IT MERGES

– **If the binary shrinks ($a \rightarrow 0$), frequency becomes higher**

– **If the binary shrinks amplitude increases**

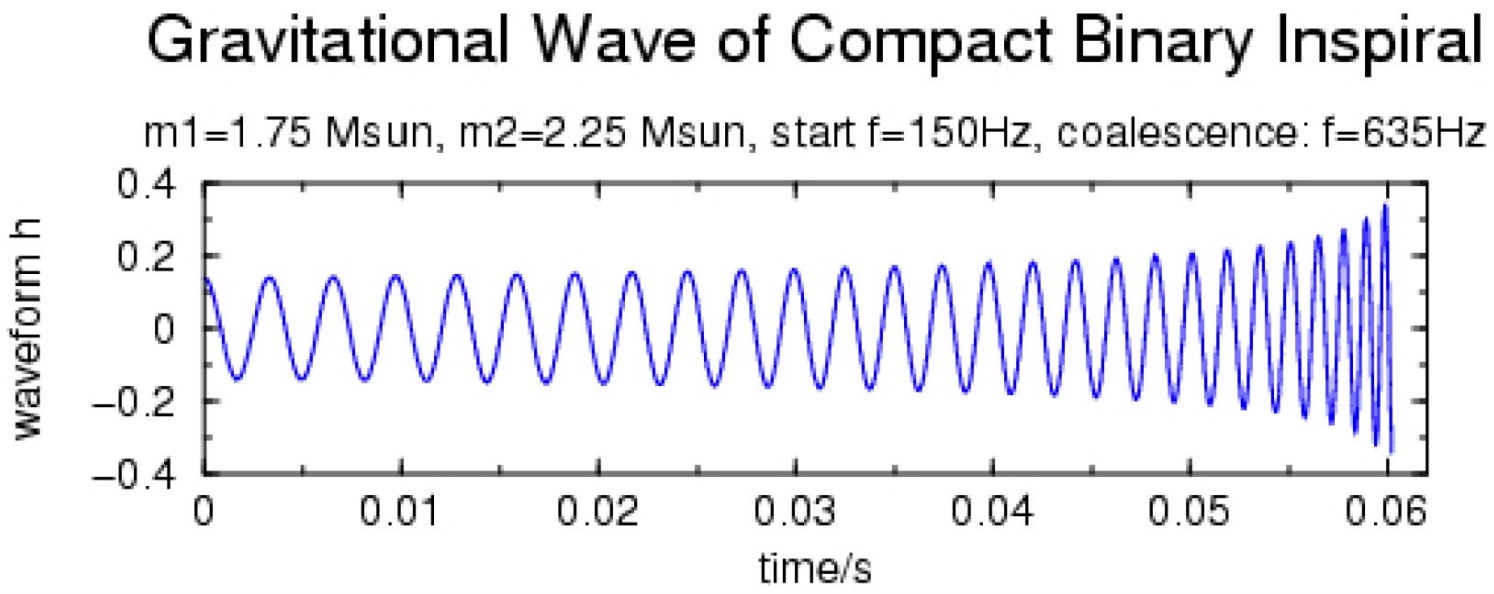

– EMISSION of GWs implies LOSS of ORBITAL ENERGY:

Power radiated by GWs:

From GR

$$P_{GW} = \frac{32}{5}\frac{G^4}{c^5}\frac{1}{a^5}\,m_1^2\,m_2^2\,(m_1+m_2)$$

$$P_{GW} = \frac{dE_{orb}}{dt} = \frac{G\,m_1\,m_2}{2\,a^2}\frac{da}{dt}$$

From Kepler and Newton

$$\Rightarrow \quad \frac{da}{dt} = \frac{64}{5}\frac{G^3}{c^5}\,a^{-3}\,m_1\,m_2\,(m_1+m_2)$$

Integrating differential equation:

$$t_{GW} = \frac{5}{256}\frac{c^5}{G^3}\frac{a^4}{m_1\,m_2\,(m_1+m_2)}$$

Timescale for a system to merge by GW emission

For binaries with general eccentricity *e*

$$t_{GW} = \frac{5}{256}\,\frac{c^5}{G^3}\,\frac{a^4\,(1-e^2)^{7/2}}{m_1\,m_2\,(m_1+m_2)}$$

Peters 1964

Timescale depends on semi-major axis, eccentricity, masses

Timescale extremely long

EXERCISE: calculate tGW for 2 neutron stars with mass equal to the Sun mass (1 Msun) orbiting at the distance between Sun and Earth (1 AU)

$$a(t) = a_0 \left[1 - \frac{256/5\, G^3\, m_1\, m_2\, (m_1 + m_2)\, t}{c^5\, (1 - e^2)^{7/2}\, a_0^4} \right]^{1/4}$$

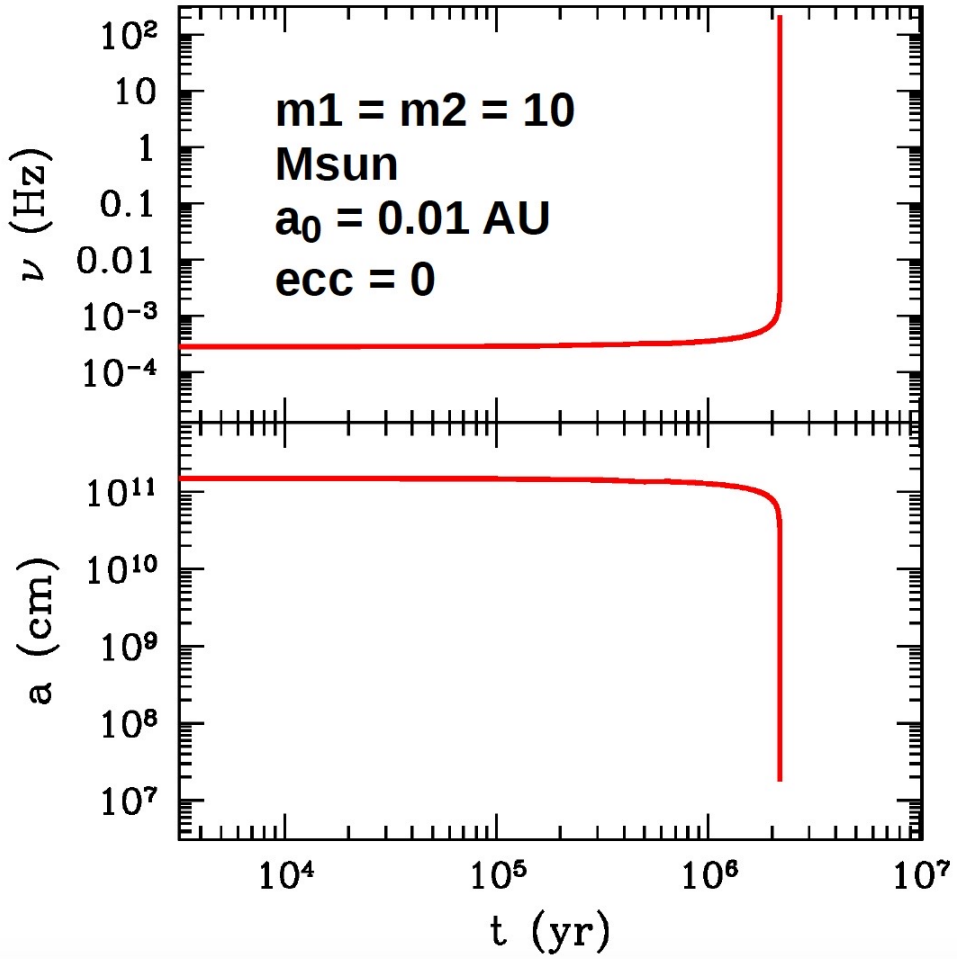

Previous equations are not always true!

Only before merger when binary can be considered Keplerian

i.e. only during inspiral

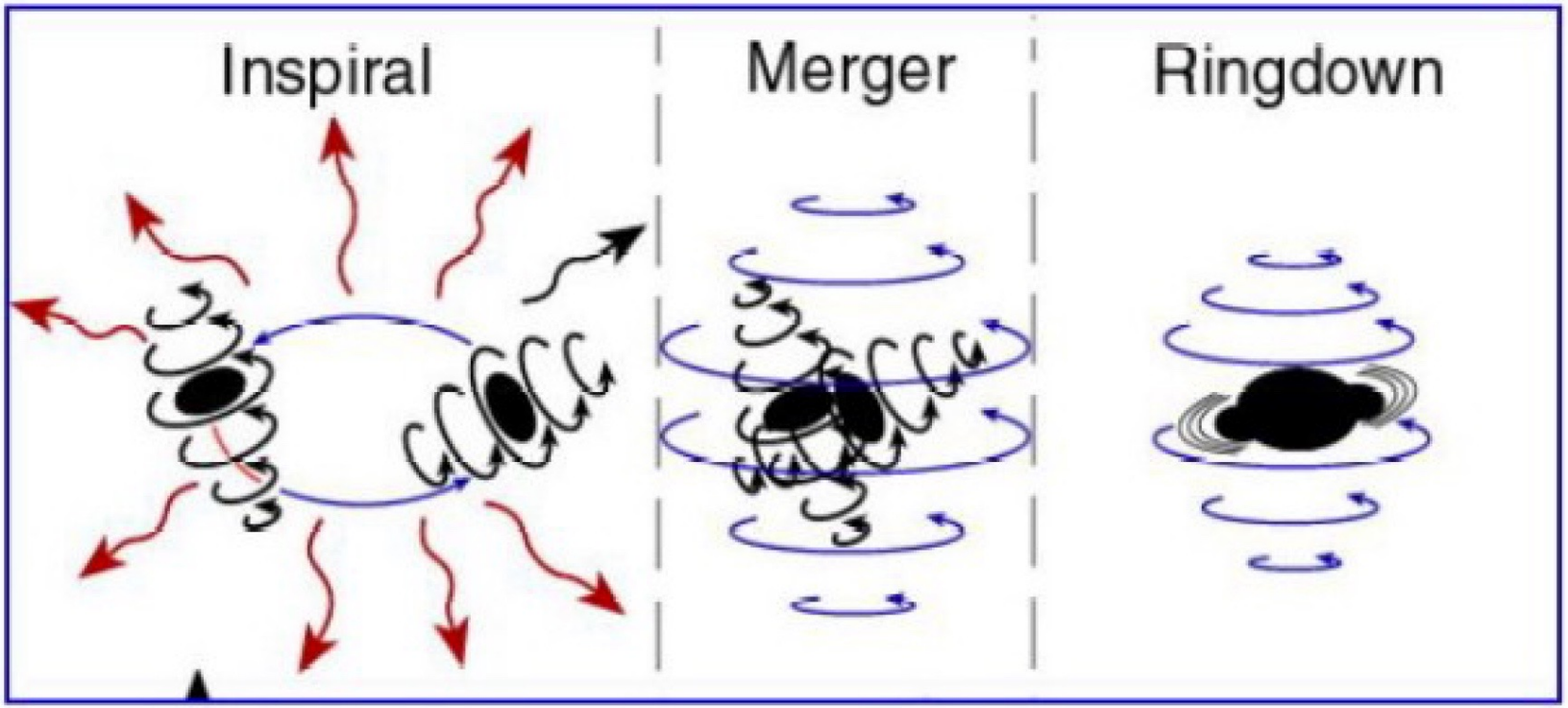

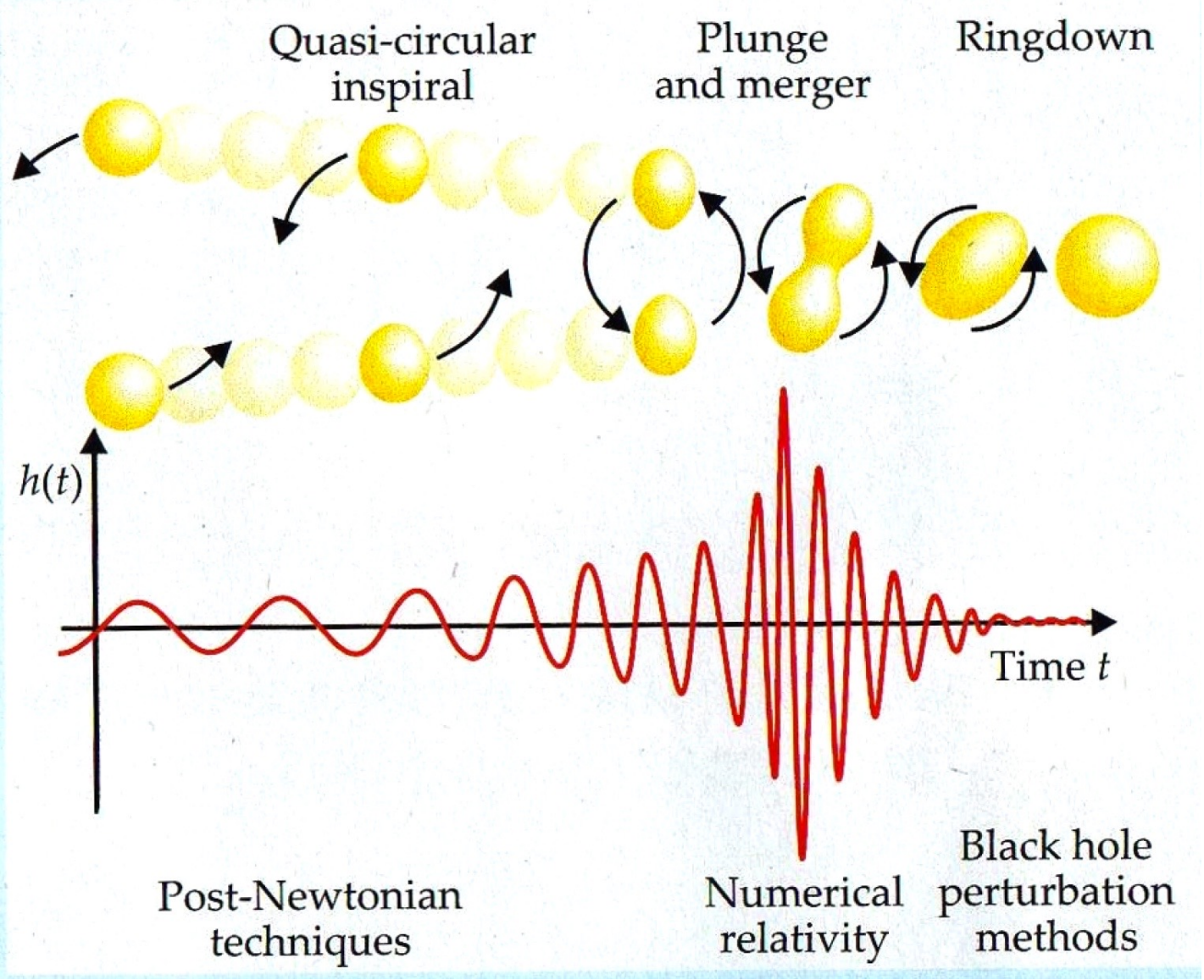
Quasi-circular inspiral
Plunge and merger
Ringdown
h(t)
Time t
Post-Newtonian techniques
Numerical relativity
Black hole perturbation methods

Templates for GWs from BBH coalescence

(Brady, Craighton, Thorne 1998)

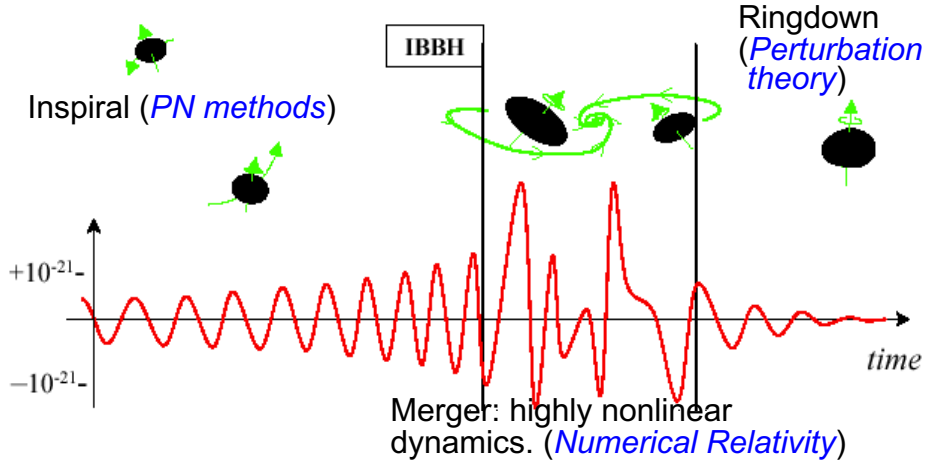

Merger: highly nonlinear dynamics. (*Numerical Relativity*)

(Buonanno & Damour 2000)

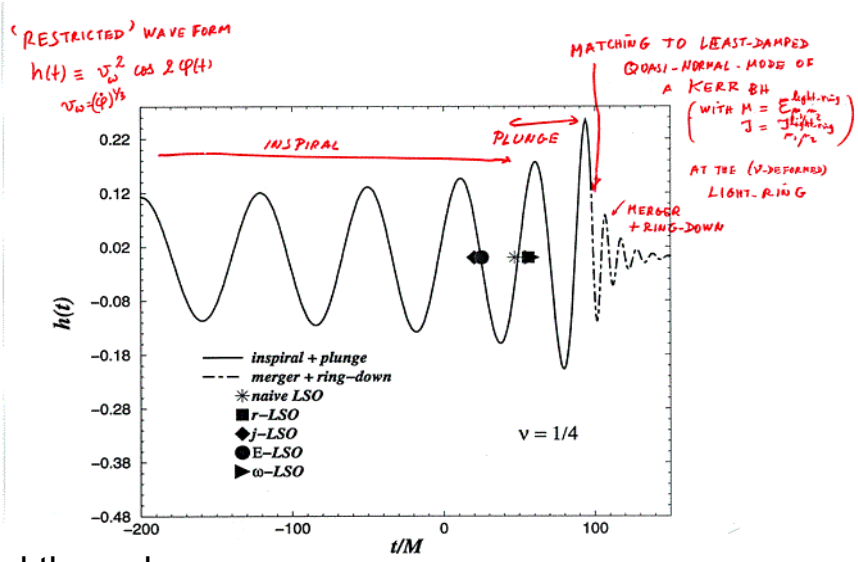

Numerical Relativity, the 2005 breakthrough:
Pretorius, Campanelli et al., Baker et al. …

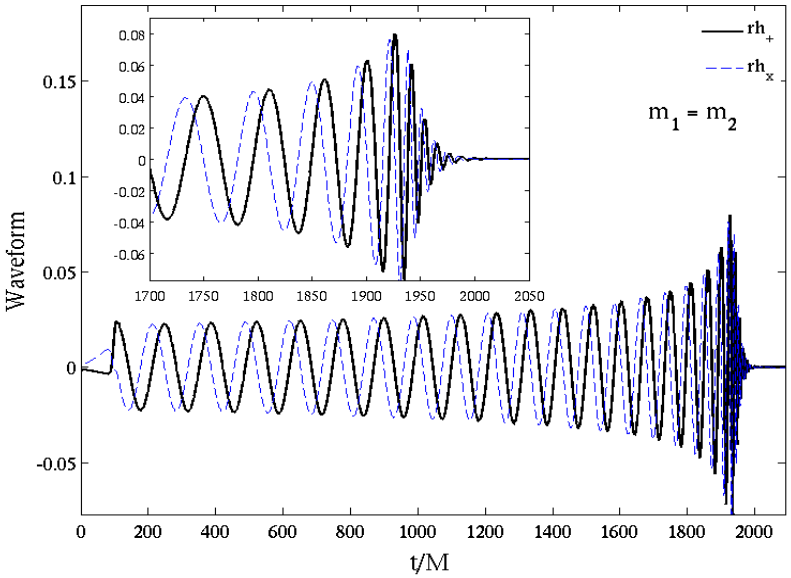

NUMERICAL RELATIVITY WAVEFORM

Numerical Relativity: >= 2005 (Pretorius, Campanelli et al., Baker et al.)

Very accurate data: Caltech-Cornell spectral code (with some caveats): M. Scheel et al., 2008

Spectral code

Extrapolation (radius & resolution) Phase error: < 0.02 rad (inspiral) <0.1 ra (ringdown)

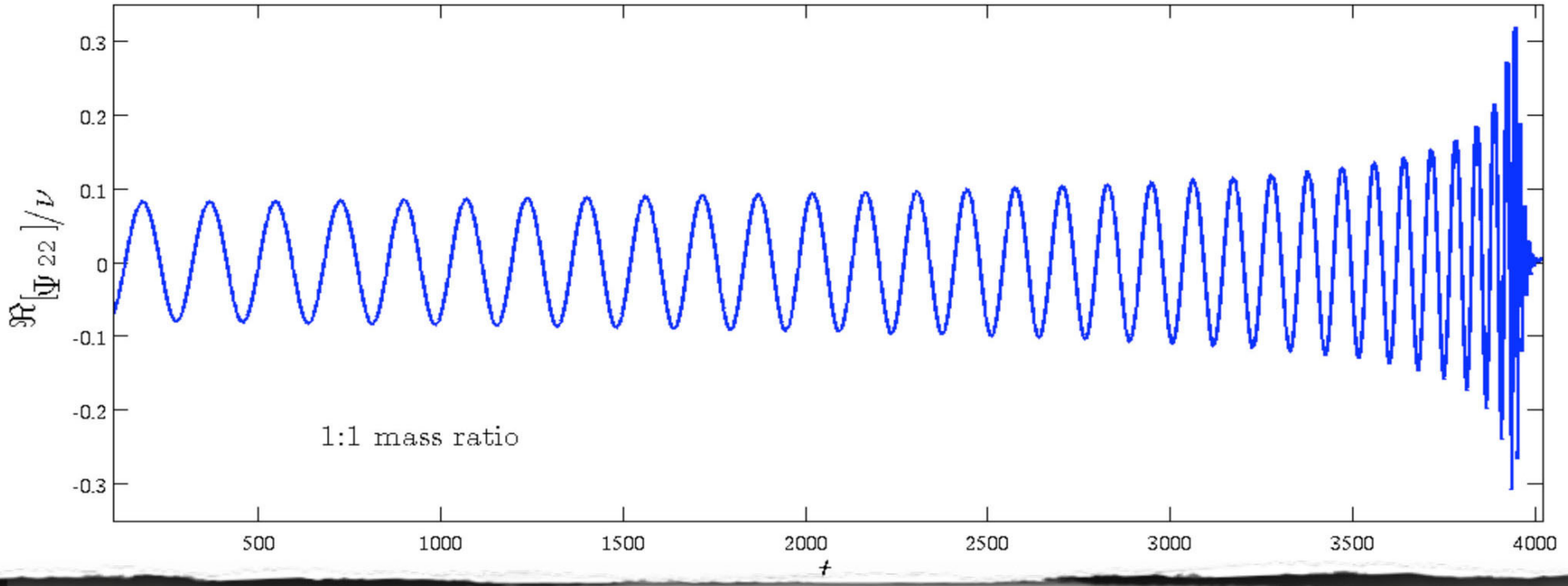

Importance of an analytical formalism

- **Theoretical:** physical understanding of the coalescence process, especially in complicated situations (arbitrary spins)
- **Practical:** need many thousands of accurate GW templates for detection & data analysis;
  need some "analytical" representation of waveform templates as $f(m_1, m_2, \mathbf{S_1}, \mathbf{S_2})$
- Solution: **synergy between analytical & numerical relativity**

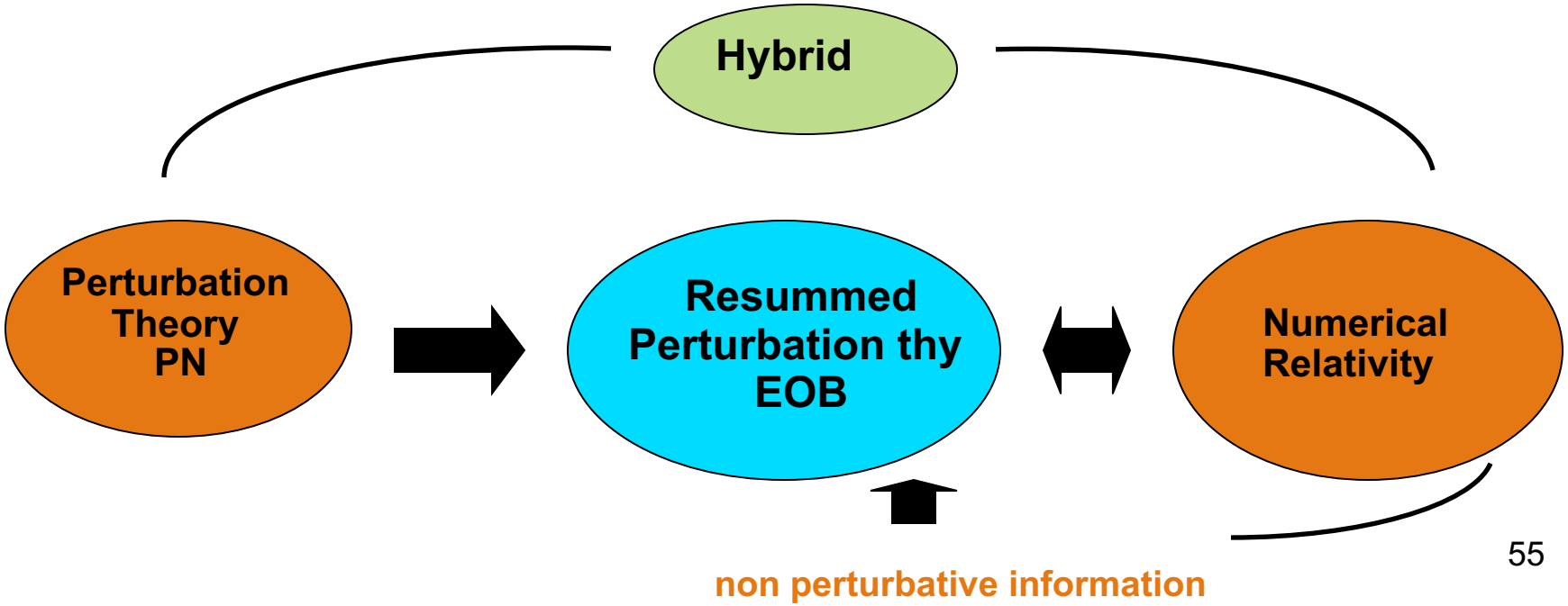

An improved analytical approach

EFFECTIVE ONE BODY (EOB)

approach to the two-body problem

Buonanno,Damour 99	(2 PN Hamiltonian)
Buonanno,Damour 00	(Rad.Reac. full waveform)
Damour, Jaranowski,Schäfer 00	(3 PN Hamiltonian)
Damour 01, Buonanno, Chen, Damour 05,…	(spin)
Damour, Nagar 07, Damour, Iyer, Nagar 08	(factorized waveform)
Buonanno, Cook, Pretorius 07, Buonanno, Pan …	(comparison to NR)
Damour, Nagar 10	(tidal effects)

Binary black hole coalescence: Analytical Relativity

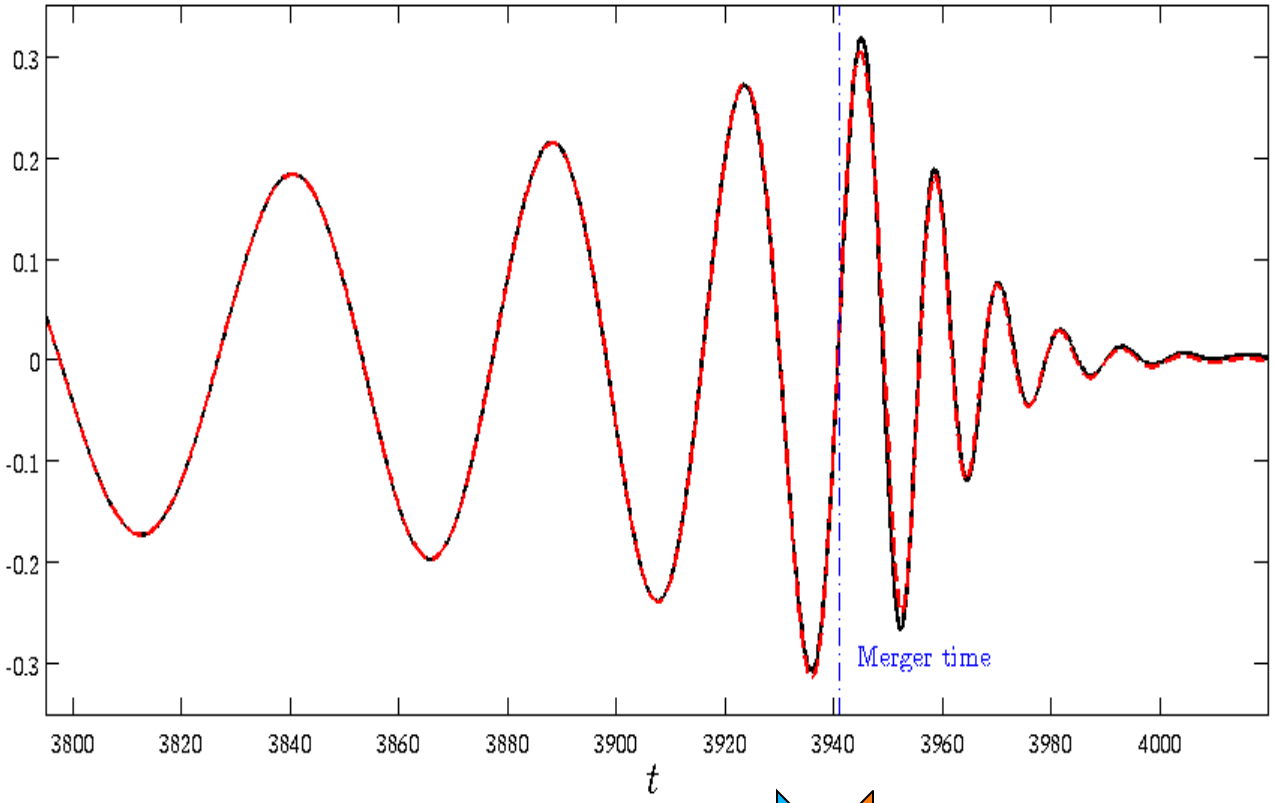

Inspiral + « plunge »

Ringdown

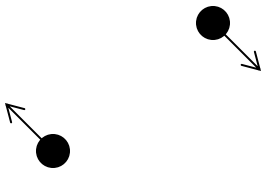

Two orbiting point-masses:
Resummed dynamics

Ringing BH

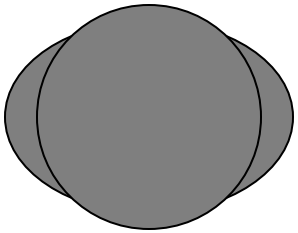

Motion of two point masses

$$S = \int d^D x \frac{R(g)}{16\pi G} - \sum_A \int m_A \sqrt{-g_{\mu\nu}(y_A) dy_A^\mu \, dy_A^\nu}$$

Dimensional continuation : $D = 4 + \varepsilon \ , \ \varepsilon \in \mathbb{C}$

Dynamics : up to 3 loops, i.e. 3 PN

Jaranowski, Schäfer 98
Blanchet, Faye 01
Damour, Jaranowski Schäfer 01
Itoh, Futamase 03
Blanchet, Damour, Esposito-Farèse 04
Foffa, Sturani 11
4PN & 5PN log terms (Damour 10, Blanchet et al 11)
4PN (Jaranowski&Schaefer 13,
Foffa&Sturani 13, Bini&Damour 13)

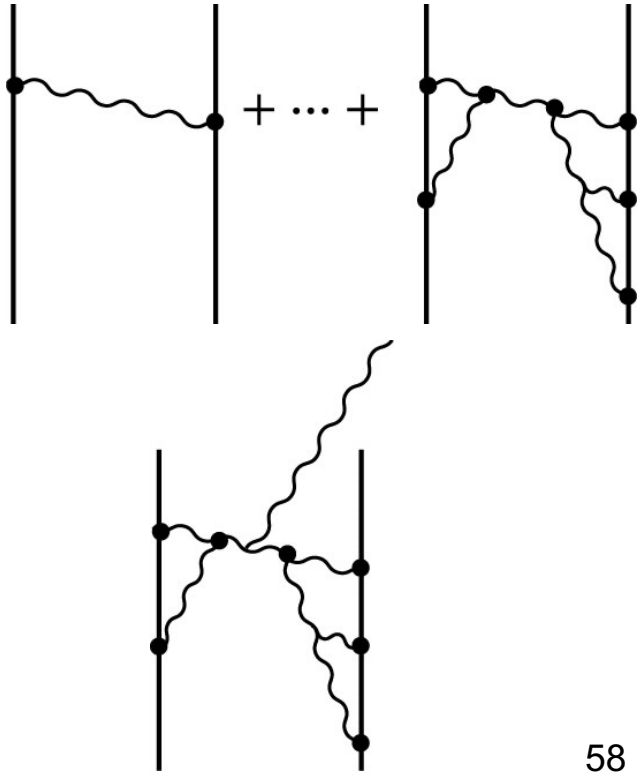

Radiation : up to 3 PN

Blanchet, Iyer, Joguet, 02,
Blanchet, Damour, Esposito-Farèse, Iyer 04
Blanchet, Faye, Iyer, Sinha 08

2-body Taylor-expanded 3PN Hamiltonian [JS98, DJS00,01]

$$H_{\rm N}(\mathbf{x}_a,\mathbf{p}_a)=\sum_a \frac{\mathbf{p}_a^2}{2\,m_a}-\frac{1}{2}\sum_a\sum_{b\neq a}\frac{G\,m_a\,m_b}{r_{ab}}\,.$$

$$H_{\rm 1PN}(\mathbf{x}_a,\mathbf{p}_a)=-\frac{1}{8}\frac{(\mathbf{p}_1^2)^2}{m_1^3}+\frac{1}{8}\frac{Gm_1m_2}{r_{12}}\left[-12\,\frac{\mathbf{p}_1^2}{m_1^2}+14\,\frac{(\mathbf{p}_1\cdot\mathbf{p}_2)}{m_1m_2}+2\,\frac{(\mathbf{n}_{12}\cdot\mathbf{p}_1)(\mathbf{n}_{12}\cdot\mathbf{p}_2)}{m_1m_2}\right]+\frac{1}{4}\frac{Gm_1m_2}{r_{12}}\frac{G(m_1+m_2)}{r_{12}}+(1\longleftrightarrow 2),$$

1PN

$$\begin{aligned}H_{\rm 2PN}(\mathbf{x}_a,\mathbf{p}_a)=&\frac{1}{16}\frac{(\mathbf{p}_1^2)^3}{m_1^5}+\frac{1}{8}\frac{Gm_1m_2}{r_{12}}\left[5\,\frac{(\mathbf{p}_1^2)^2}{m_1^4}-\frac{11}{2}\frac{\mathbf{p}_1^2\,\mathbf{p}_2^2}{m_1^2m_2^2}-\frac{(\mathbf{p}_1\cdot\mathbf{p}_2)^2}{m_1^2m_2^2}+5\,\frac{\mathbf{p}_1^2\,(\mathbf{n}_{12}\cdot\mathbf{p}_2)^2}{m_1^2m_2^2}\right.\\&\left.-6\,\frac{(\mathbf{p}_1\cdot\mathbf{p}_2)\,(\mathbf{n}_{12}\cdot\mathbf{p}_1)(\mathbf{n}_{12}\cdot\mathbf{p}_2)}{m_1^2m_2^2}-\frac{3}{2}\frac{(\mathbf{n}_{12}\cdot\mathbf{p}_1)^2(\mathbf{n}_{12}\cdot\mathbf{p}_2)^2}{m_1^2m_2^2}\right]\\&+\frac{1}{4}\frac{G^2m_1m_2}{r_{12}^2}\left[m_2\left(10\frac{\mathbf{p}_1^2}{m_1^2}+19\frac{\mathbf{p}_2^2}{m_2^2}\right)-\frac{1}{2}(m_1+m_2)\frac{27\,(\mathbf{p}_1\cdot\mathbf{p}_2)+6\,(\mathbf{n}_{12}\cdot\mathbf{p}_1)(\mathbf{n}_{12}\cdot\mathbf{p}_2)}{m_1m_2}\right]\\&-\frac{1}{8}\frac{Gm_1m_2}{r_{12}}\frac{G^2(m_1^2+5m_1m_2+m_2^2)}{r_{12}^2}+(1\longleftrightarrow 2).\end{aligned}$$

2PN

$$\begin{aligned}H_{\rm 3PN}^{\rm reg}(\mathbf{x}_a,\mathbf{p}_a)=&-\frac{5}{128}\frac{(\mathbf{p}_1^2)^4}{m_1^7}+\frac{1}{32}\frac{Gm_1m_2}{r_{12}}\left[-14\,\frac{(\mathbf{p}_1^2)^3}{m_1^6}+4\,\frac{\left((\mathbf{p}_1\cdot\mathbf{p}_2)^2+4\,\mathbf{p}_1^2\,\mathbf{p}_2^2\right)\mathbf{p}_1^2}{m_1^4m_2^2}+\frac{\left(\mathbf{p}_1^2\,\mathbf{p}_2^2-2\,(\mathbf{p}_1\cdot\mathbf{p}_2)^2\right)(\mathbf{p}_1\cdot\mathbf{p}_2)}{m_1^3m_2^3}\right.\\&-10\,\frac{\left(\mathbf{p}_1^2\,(\mathbf{n}_{12}\cdot\mathbf{p}_2)^2+\mathbf{p}_2^2\,(\mathbf{n}_{12}\cdot\mathbf{p}_1)^2\right)\mathbf{p}_1^2}{m_1^4m_2^2}+24\,\frac{\mathbf{p}_1^2\,(\mathbf{p}_1\cdot\mathbf{p}_2)(\mathbf{n}_{12}\cdot\mathbf{p}_1)(\mathbf{n}_{12}\cdot\mathbf{p}_2)}{m_1^4m_2^2}+2\,\frac{\mathbf{p}_1^2\,(\mathbf{p}_1\cdot\mathbf{p}_2)(\mathbf{n}_{12}\cdot\mathbf{p}_2)^2}{m_1^3m_2^3}\\&+\frac{\left(7\,\mathbf{p}_1^2\,\mathbf{p}_2^2-10\,(\mathbf{p}_1\cdot\mathbf{p}_2)^2\right)(\mathbf{n}_{12}\cdot\mathbf{p}_1)(\mathbf{n}_{12}\cdot\mathbf{p}_2)}{m_1^3m_2^3}+6\,\frac{\mathbf{p}_1^2\,(\mathbf{n}_{12}\cdot\mathbf{p}_1)^2(\mathbf{n}_{12}\cdot\mathbf{p}_2)^2}{m_1^4m_2^2}\\&\left.+15\,\frac{(\mathbf{p}_1\cdot\mathbf{p}_2)(\mathbf{n}_{12}\cdot\mathbf{p}_1)^2(\mathbf{n}_{12}\cdot\mathbf{p}_2)^2}{m_1^4m_2^3}-18\,\frac{\mathbf{p}_1^2\,(\mathbf{n}_{12}\cdot\mathbf{p}_1)(\mathbf{n}_{12}\cdot\mathbf{p}_2)^3}{m_1^3m_2^3}+5\,\frac{(\mathbf{n}_{12}\cdot\mathbf{p}_1)^3(\mathbf{n}_{12}\cdot\mathbf{p}_2)^3}{m_1^3m_2^3}\right]\\&+\frac{G^2m_1m_2}{r_{12}^2}\left[\frac{1}{16}(m_1-27m_2)\frac{(\mathbf{p}_1^2)^2}{m_1^4}-\frac{115}{16}m_1\frac{\mathbf{p}_1^2\,(\mathbf{p}_1\cdot\mathbf{p}_2)}{m_1^3m_2}+\frac{1}{48}m_2\frac{25\,(\mathbf{p}_1\cdot\mathbf{p}_2)^2+371\,\mathbf{p}_1^2\,\mathbf{p}_2^2}{m_1^2m_2^2}\right.\\&+\frac{17}{16}\frac{\mathbf{p}_1^2(\mathbf{n}_{12}\cdot\mathbf{p}_1)^2}{m_1^3}-\frac{1}{8}m_1\frac{\left(15\,\mathbf{p}_1^2\,(\mathbf{n}_{12}\cdot\mathbf{p}_2)+11\,(\mathbf{p}_1\cdot\mathbf{p}_2)\,(\mathbf{n}_{12}\cdot\mathbf{p}_1)\right)(\mathbf{n}_{12}\cdot\mathbf{p}_1)}{m_1^3m_2}+\frac{5}{12}\frac{(\mathbf{n}_{12}\cdot\mathbf{p}_1)^4}{m_1^3}\\&-\frac{3}{2}m_1\frac{(\mathbf{n}_{12}\cdot\mathbf{p}_1)^3(\mathbf{n}_{12}\cdot\mathbf{p}_2)}{m_1^3m_2}+\frac{125}{12}m_2\frac{(\mathbf{p}_1\cdot\mathbf{p}_2)\,(\mathbf{n}_{12}\cdot\mathbf{p}_1)(\mathbf{n}_{12}\cdot\mathbf{p}_2)}{m_1^2m_2^2}+\frac{10}{3}m_2\frac{(\mathbf{n}_{12}\cdot\mathbf{p}_1)^2(\mathbf{n}_{12}\cdot\mathbf{p}_2)^2}{m_1^2m_2^2}\\&\left.-\frac{1}{48}(220m_1+193m_2)\frac{\mathbf{p}_1^2(\mathbf{n}_{12}\cdot\mathbf{p}_2)^2}{m_1^2m_2^2}\right]+\frac{G^3m_1m_2}{r_{12}^3}\left[-\frac{1}{48}\left(466\,m_1^2+\left(473-\frac{3}{4}\pi^2\right)m_1m_2+150\,m_2^2\right)\frac{\mathbf{p}_1^2}{m_1^2}\right.\\&+\frac{1}{16}\left(77(m_1^2+m_2^2)+\left(143-\frac{1}{4}\pi^2\right)m_1m_2\right)\frac{(\mathbf{p}_1\cdot\mathbf{p}_2)}{m_1m_2}+\frac{1}{16}\left(61\,m_1^2-\left(43+\frac{3}{4}\pi^2\right)m_1m_2\right)\frac{(\mathbf{n}_{12}\cdot\mathbf{p}_1)^2}{m_1^2}\\&\left.+\frac{1}{16}\left(21(m_1^2+m_2^2)+\left(119+\frac{3}{4}\pi^2\right)m_1m_2\right)\frac{(\mathbf{n}_{12}\cdot\mathbf{p}_1)(\mathbf{n}_{12}\cdot\mathbf{p}_2)}{m_1m_2}\right]\\&+\frac{1}{8}\frac{G^4m_1m_2^3}{r_{12}^4}\left[\left(\frac{227}{3}-\frac{21}{4}\pi^2\right)m_1+m_2\right]+(1\longleftrightarrow 2).\end{aligned}\qquad(12)$$

3PN

Taylor-expanded 3PN waveform

Blanchet,Iyer, Joguet 02, Blanchet, Damour, Esposito-Farese, Iyer 04, Kidder 07, Blanchet et al. 08

$$h^{22} = -8\sqrt{\frac{\pi}{5}}\frac{G\nu m}{c^2 R}e^{-2i\phi}x\Big\{1 - x\Big(\frac{107}{42} - \frac{55}{42}\nu\Big) + x^{3/2}\Big[2\pi + 6i\ln\Big(\frac{x}{x_0}\Big)\Big] - x^2\Big(\frac{2173}{1512} + \frac{1069}{216}\nu - \frac{2047}{1512}\nu^2\Big)$$
$$- x^{5/2}\Big[\Big(\frac{107}{21} - \frac{34}{21}\nu\Big)\pi + 24i\nu + \Big(\frac{107i}{7} - \frac{34i}{7}\nu\Big)\ln\Big(\frac{x}{x_0}\Big)\Big]$$
$$+ x^3\Big[\frac{27\,027\,409}{646\,800} - \frac{856}{105}\gamma_E + \frac{2}{3}\pi^2 - \frac{1712}{105}\ln 2 - \frac{428}{105}\ln x$$
$$- 18\Big[\ln\Big(\frac{x}{x_0}\Big)\Big]^2 - \Big(\frac{278\,185}{33\,264} - \frac{41}{96}\pi^2\Big)\nu - \frac{20\,261}{2772}\nu^2 + \frac{114\,635}{99\,792}\nu^3 + \frac{428i}{105}\pi + 12i\pi\ln\Big(\frac{x}{x_0}\Big)\Big] + O(\epsilon^{7/2})\Big\},$$

$$x = (M\Omega)^{2/3} \sim v^2/c^2$$

$$M = m_1 + m_2$$
$$\nu = m_1 m_2/(m_1 + m_2)^2$$

Simple way to estimate frequency at merger:
Last stable circular orbit around a black hole

$$r_{\rm LSCO} = 6\,\frac{G\,(m_1+m_2)}{c^2}$$

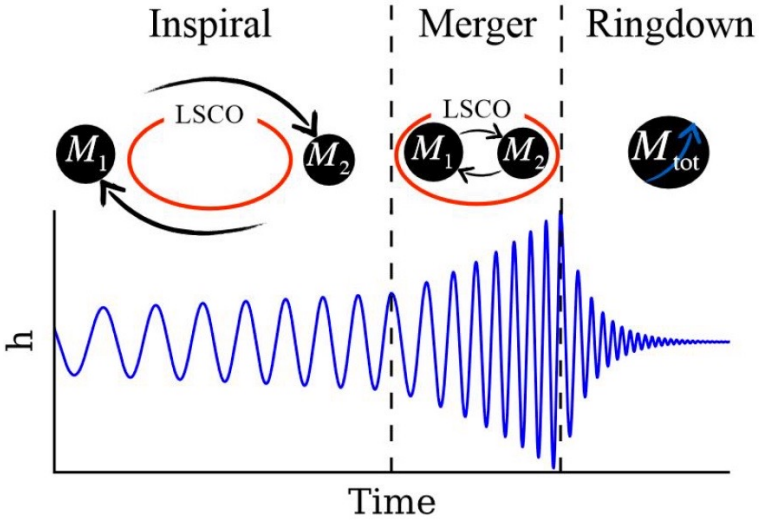

$$\omega_{\rm GW,LSCO} = 2\sqrt{\frac{G\,(m_1+m_2)}{r_{\rm LSCO}^3}} = \frac{2\,c^3}{6^{3/2}\,G\,(m_1+m_2)}$$

$$\omega_{\rm GW,LSCO} = 460\,{\rm Hz}\,\frac{60\,M_{\rm sun}}{(m_1+m_2)}$$

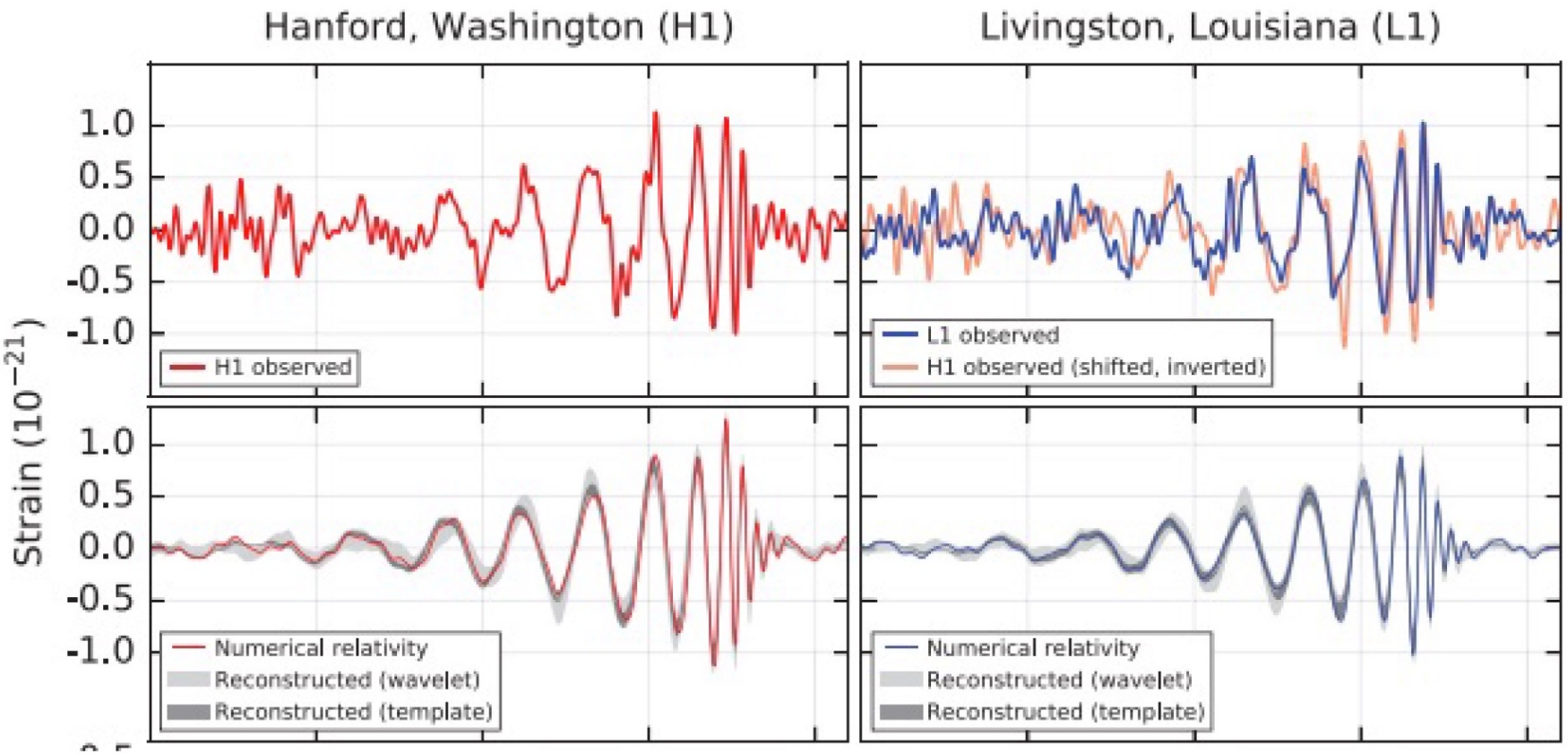

Abbott et al. 2016

Detectors:

Advanced LIGO (Livingstone + Hanford, US)
Advanced Virgo (Pisa, Italy)

Michelson interferometers

Design started in the '90s
First science runs ~ 2007 (no detection)
Being upgraded in 2007 – 2015
First run advanced detectors 2015

Time schedule

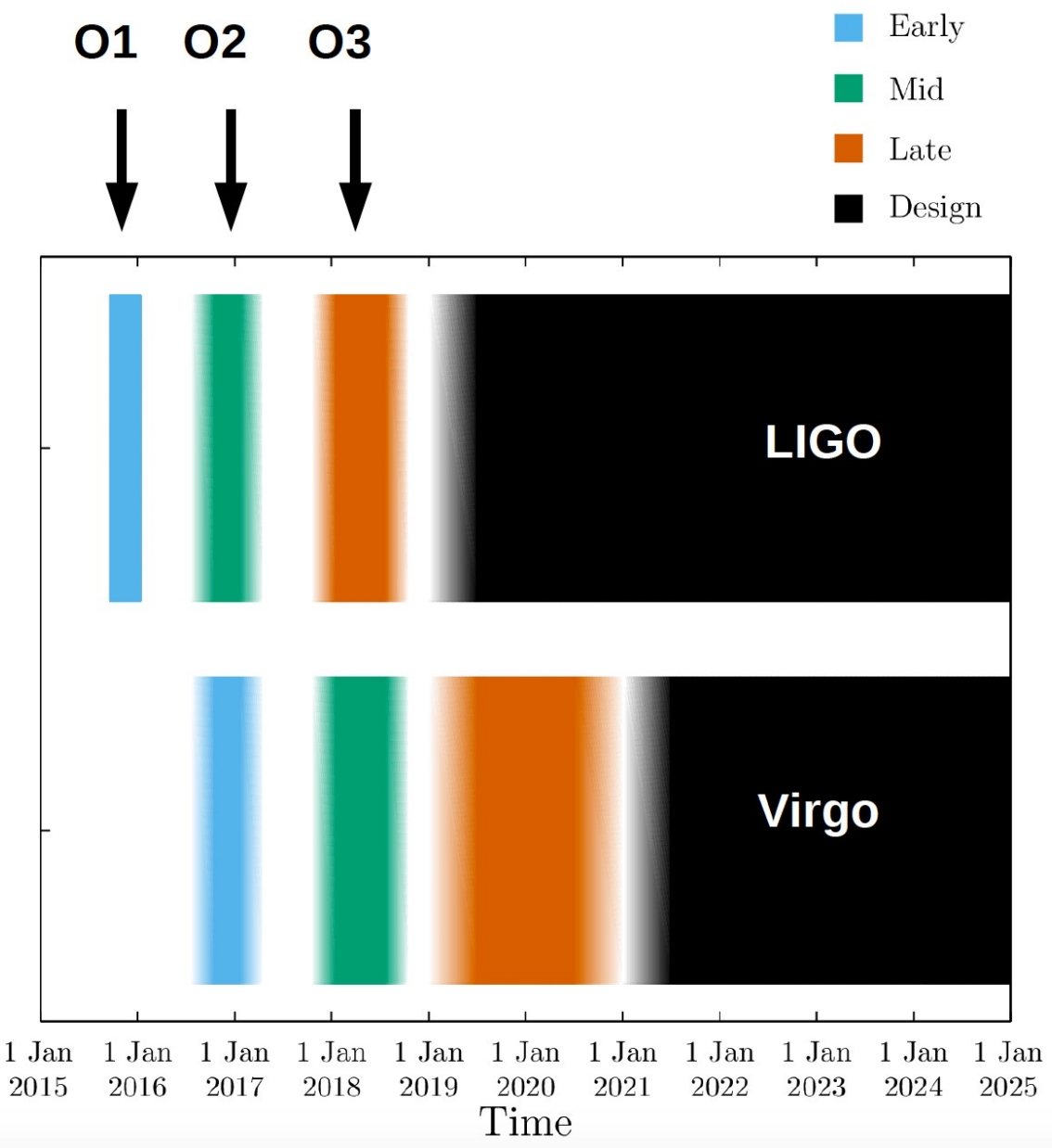

Frequency range: ~ 10 – 10'000 Hz

Suitable for mergers of compact binaries

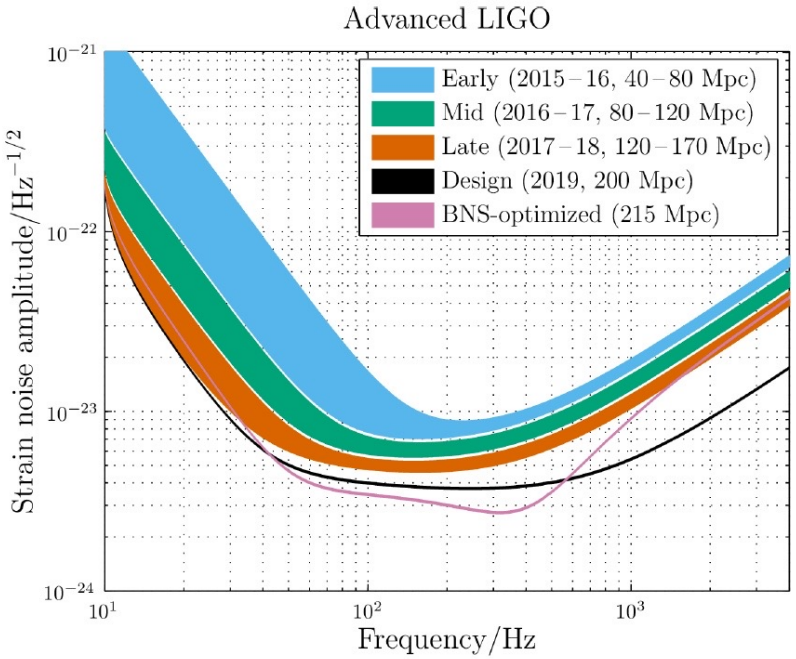

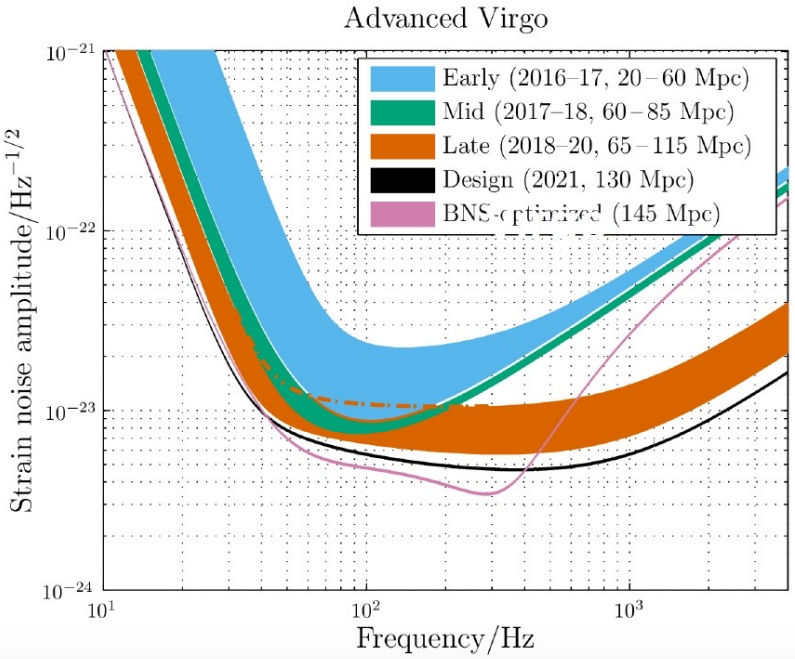

Noise level of LIGO & Virgo
(Noise power spectral density)

Summary of detections:

2015/09/12	first LIGO run	
2015/09/14	GW150914	black holes (BHs)
2015/10/12	LVT151012	maybe BHs
2015/12/26	GW151226	BHs
2015/01 – 2016/11	detectors switched off	
2017/01/04	GW170104	BHs
2017/08/01	Virgo joins LIGO	
2017/08/14	GW170814	BHs
2017/08/17	GW170817	neutron stars (NSs)
2017/08/25 – now	detectors switched off	

Properties of the first detections:

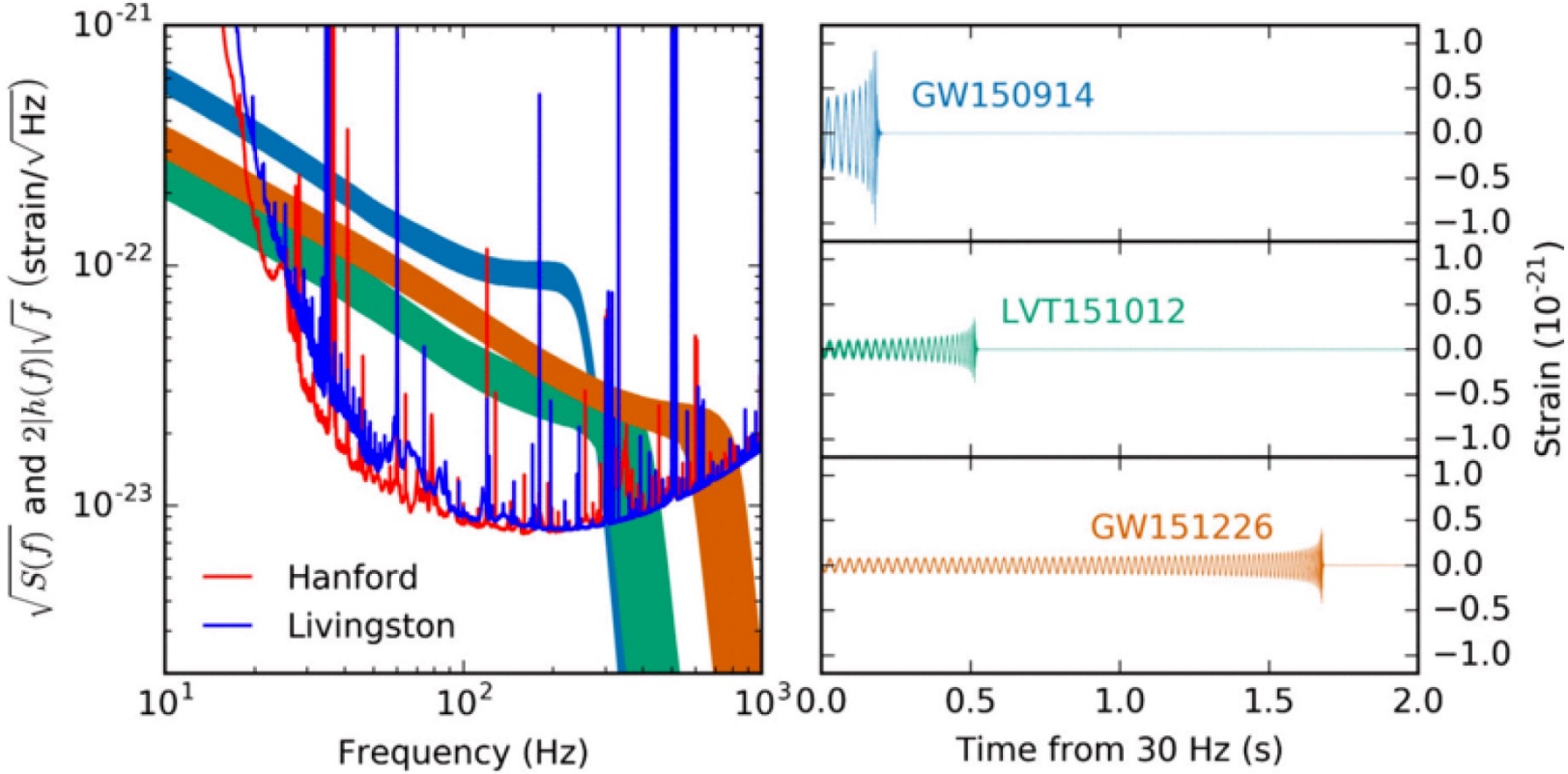

From Abbott et al. (2016)
https://journals.aps.org/prx/abstract/10.1103/PhysRevX.6.041015#fulltext

GW detection

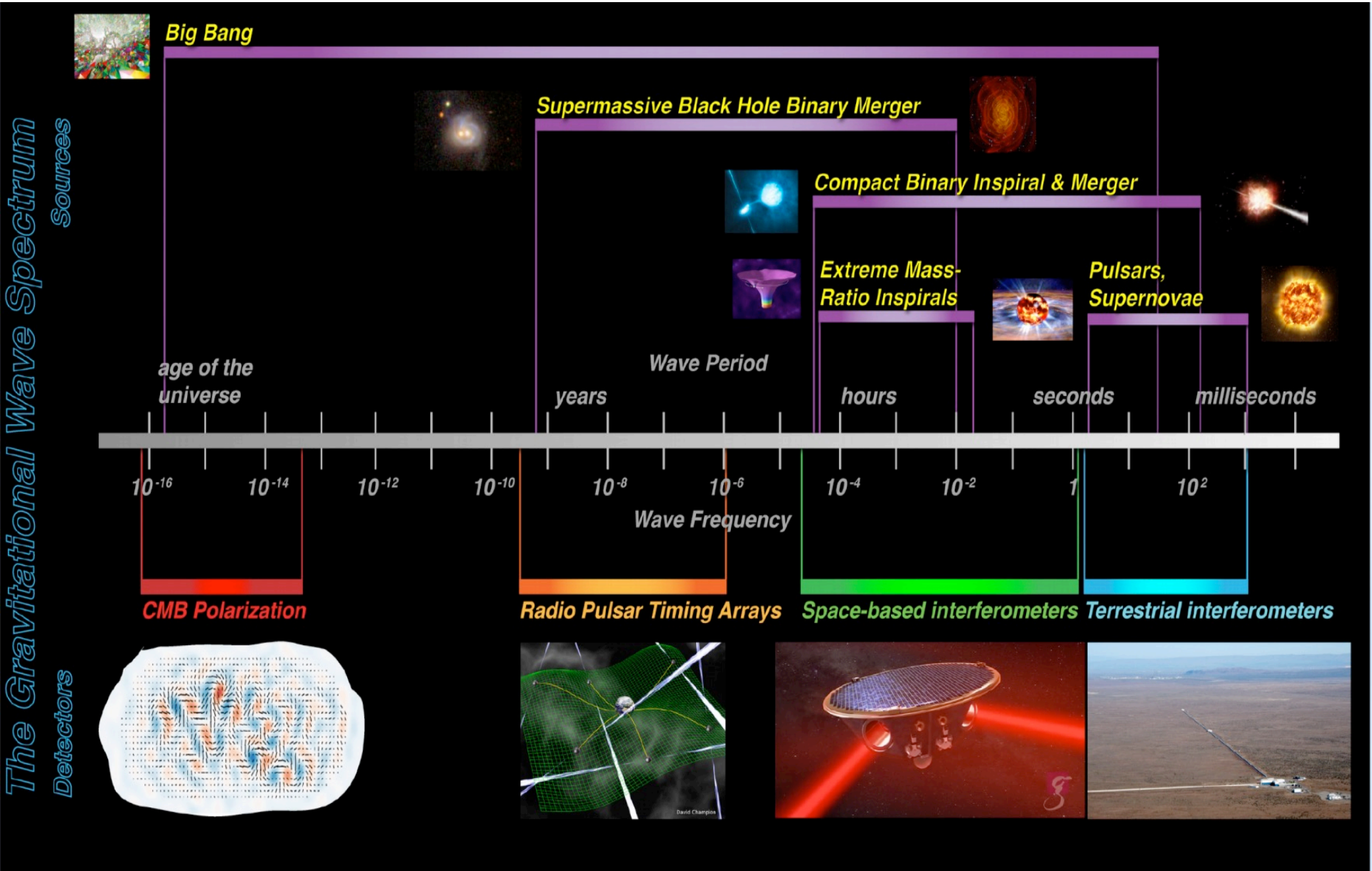

GW detection

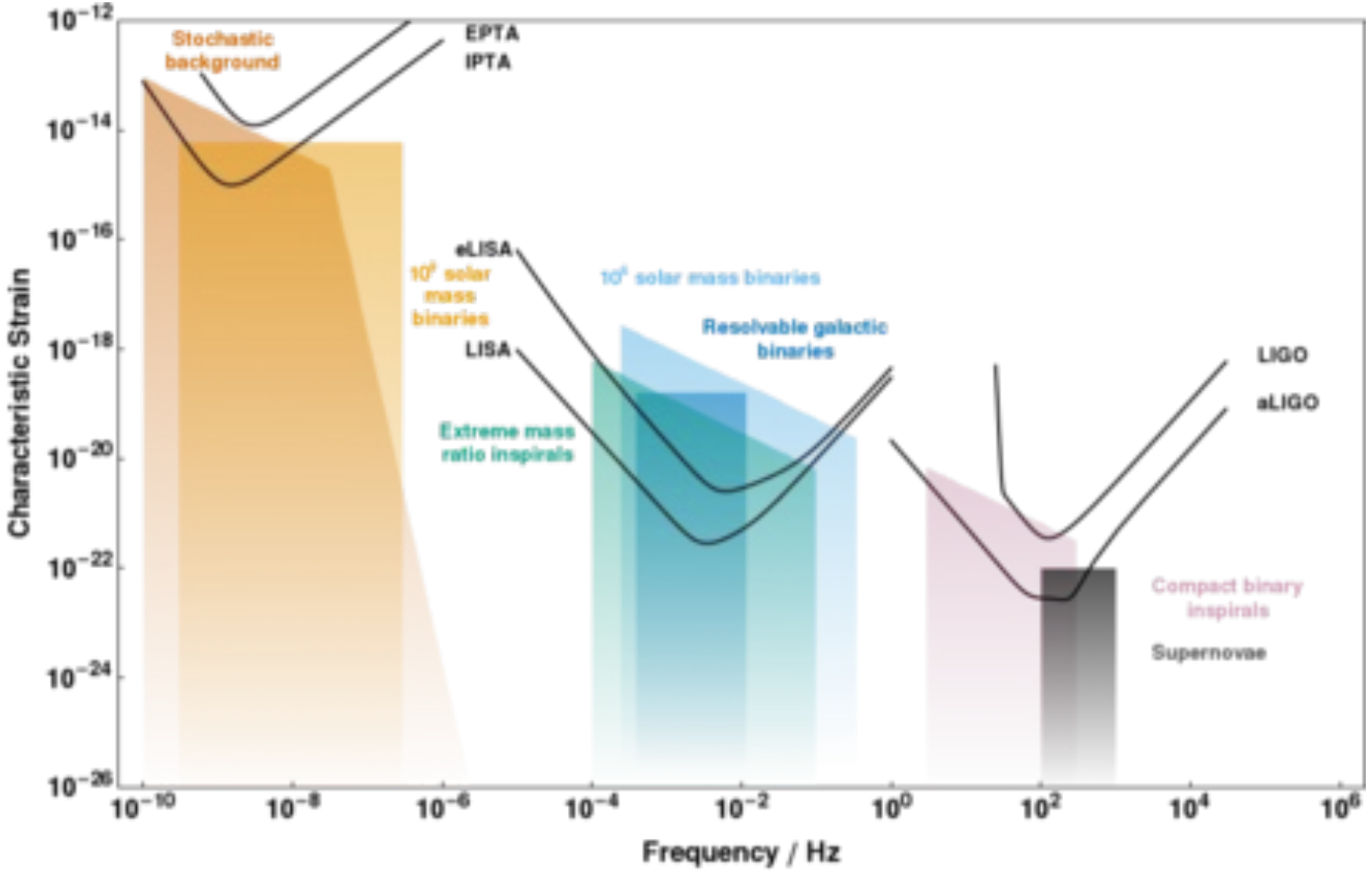

Localization LIGO O1 Events

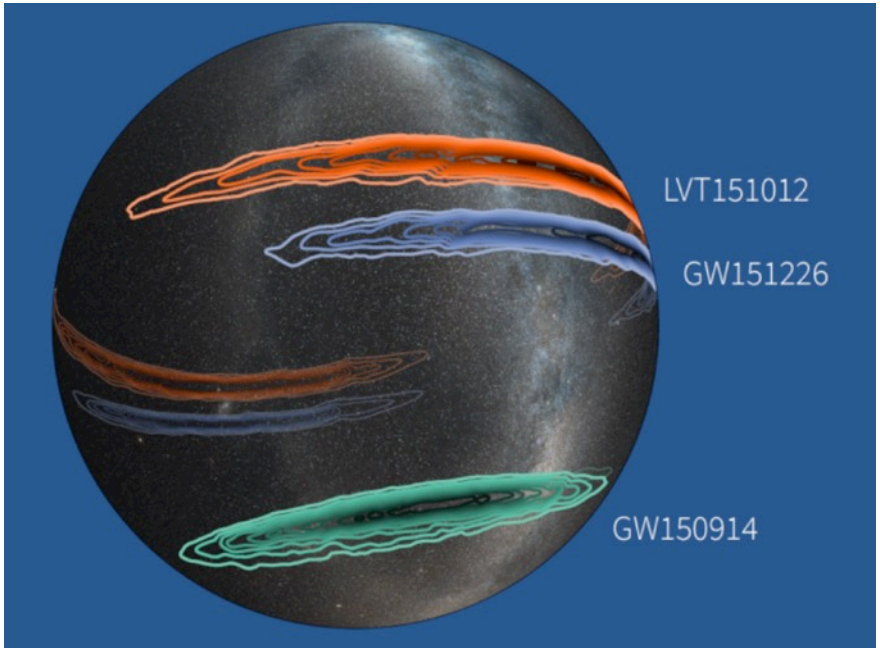

for GW150914: Astrophys. J. Lett. 826, L13 (2016)

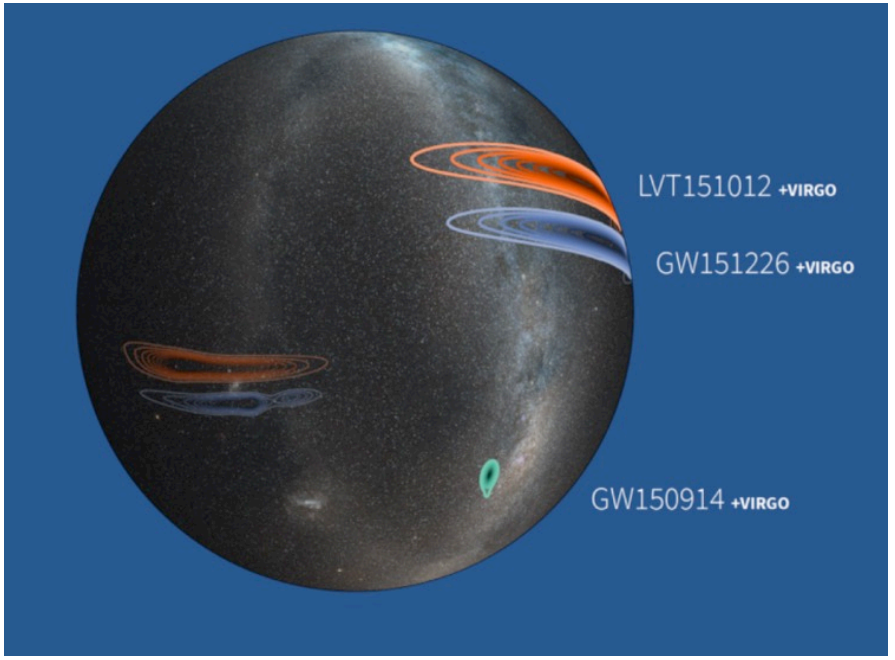

Simulation for 3rd detector at Virgo location with LIGO O1 sensitivity

GW detector network: 2015-2025

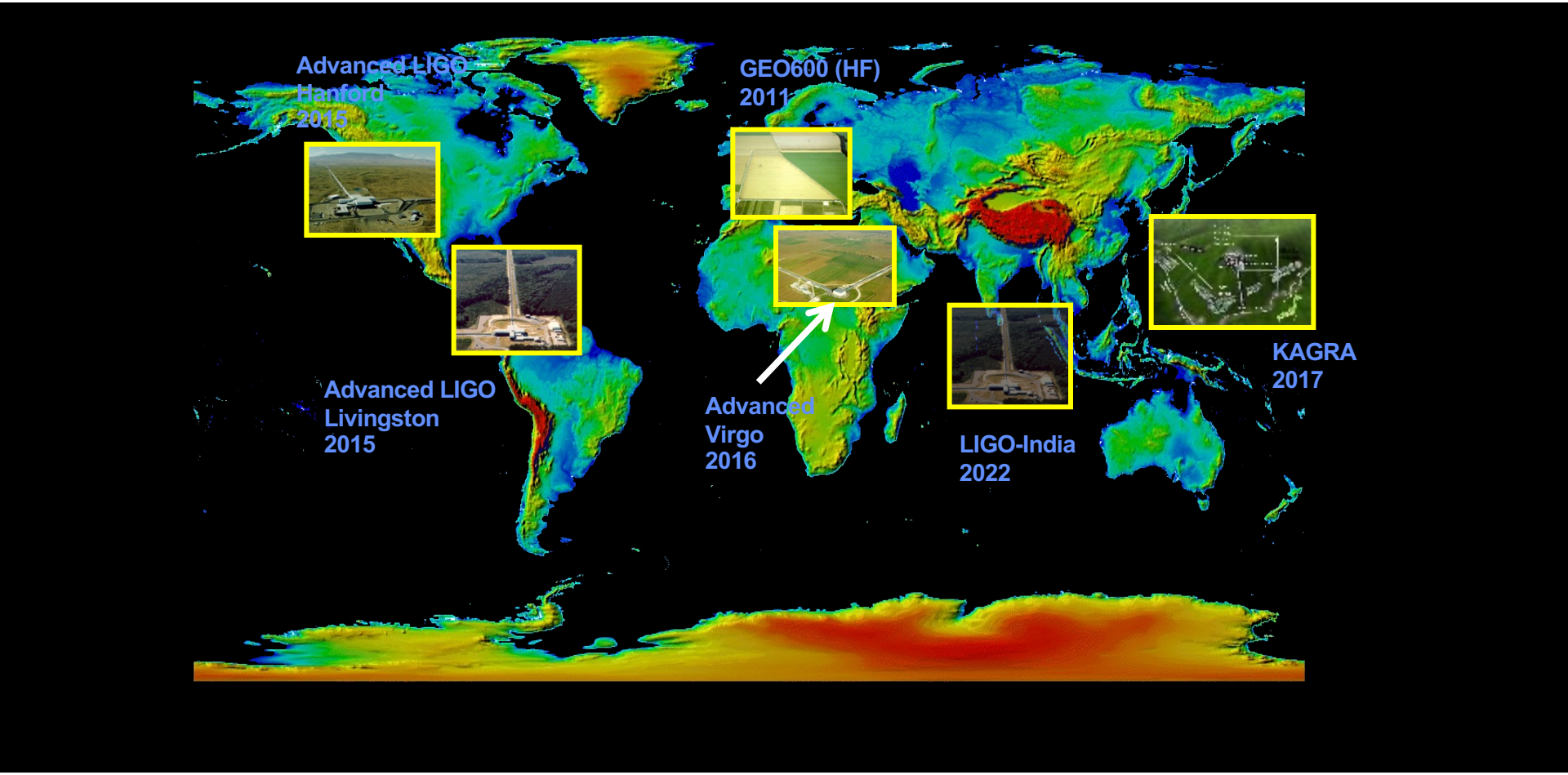

KAGRA

Kamioka Mine

- **Technologies crucial for next-generation detectors;**
- **KAGRA can be regarded as a 2.5-generation detector.**

Cryogenic Mirror

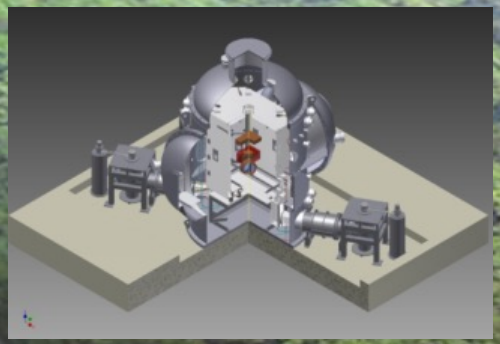

Underground

Third Generation Gravitational Wave Detectors

Einstein Telescope

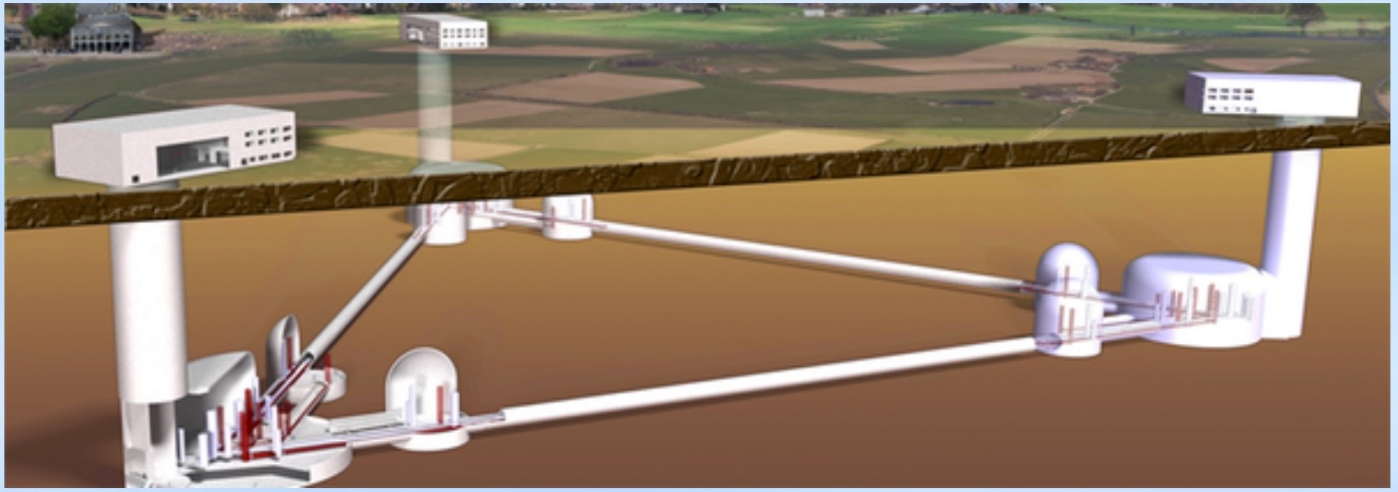

Underground to reduced seismic noise.
10 km arms
Cryogenic mirrors
Lower frequency limit – 1 Hz
10 x better sensitivity than 2nd generation detectors
Farther back in the universe

M. Punturo talk

Cosmic Explorer

Preliminary Concept

The Cosmic Explorer: x10 aLIGO

- Earth's Surface;
- 40 km arms
- Advanced LIGO Technology +
- Squeezed Light

arXiv:1607.08697v3 [astro-ph.IM] 11 Sep 2016

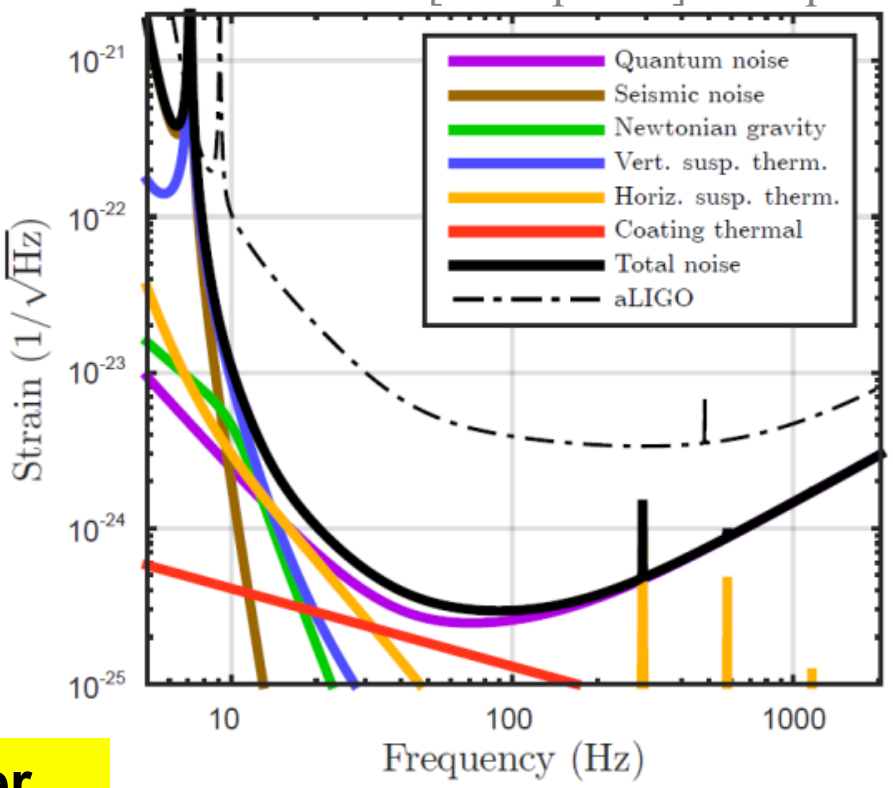

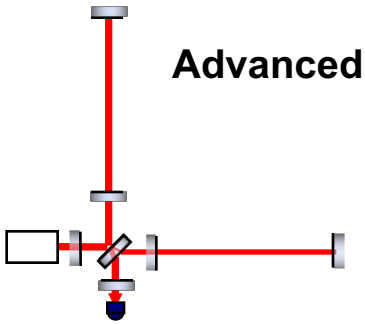

Advanced LIGO

Cosmic Explorer
40 km

Third Generation Gravitational Wave Detectors

With Einstein Telescope (European) or Cosmic Explorer (US) almost every stellar mass binary black hole merger in the observable universe will be detectable.

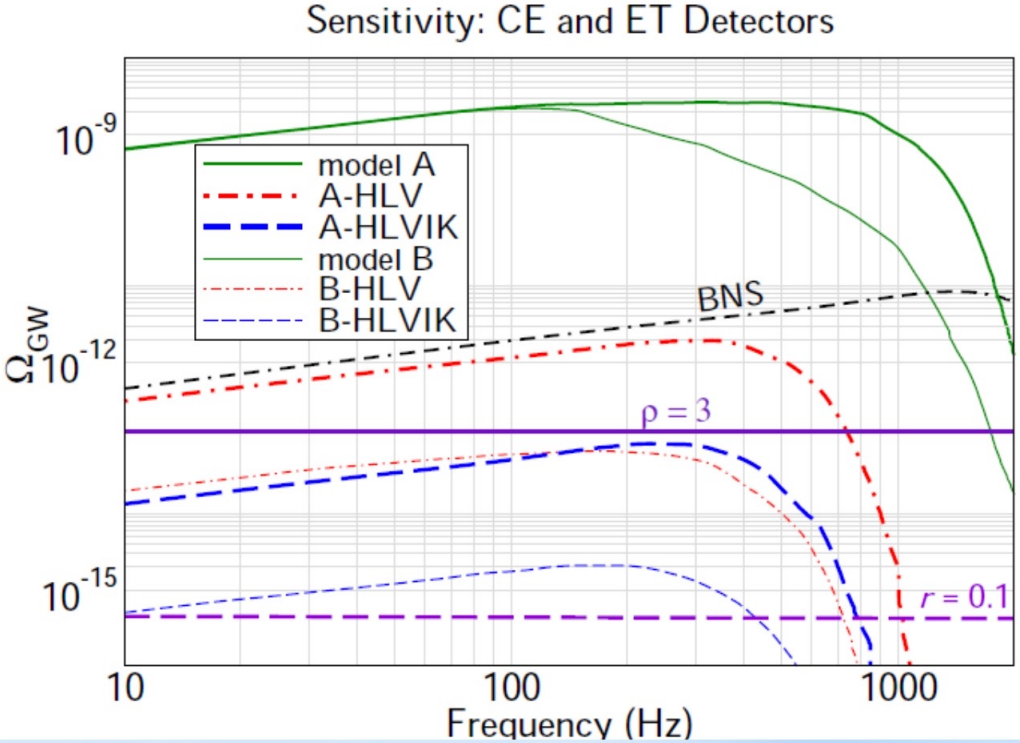

BBH confusion background can potentially be subtracted to observe the primordial background at the level of $\Omega_{GW} \sim 10^{-13}$ after five years of observation.

Arxiv:1611.08943

Space missions

Laser Interferometer Space Antenna - LISA

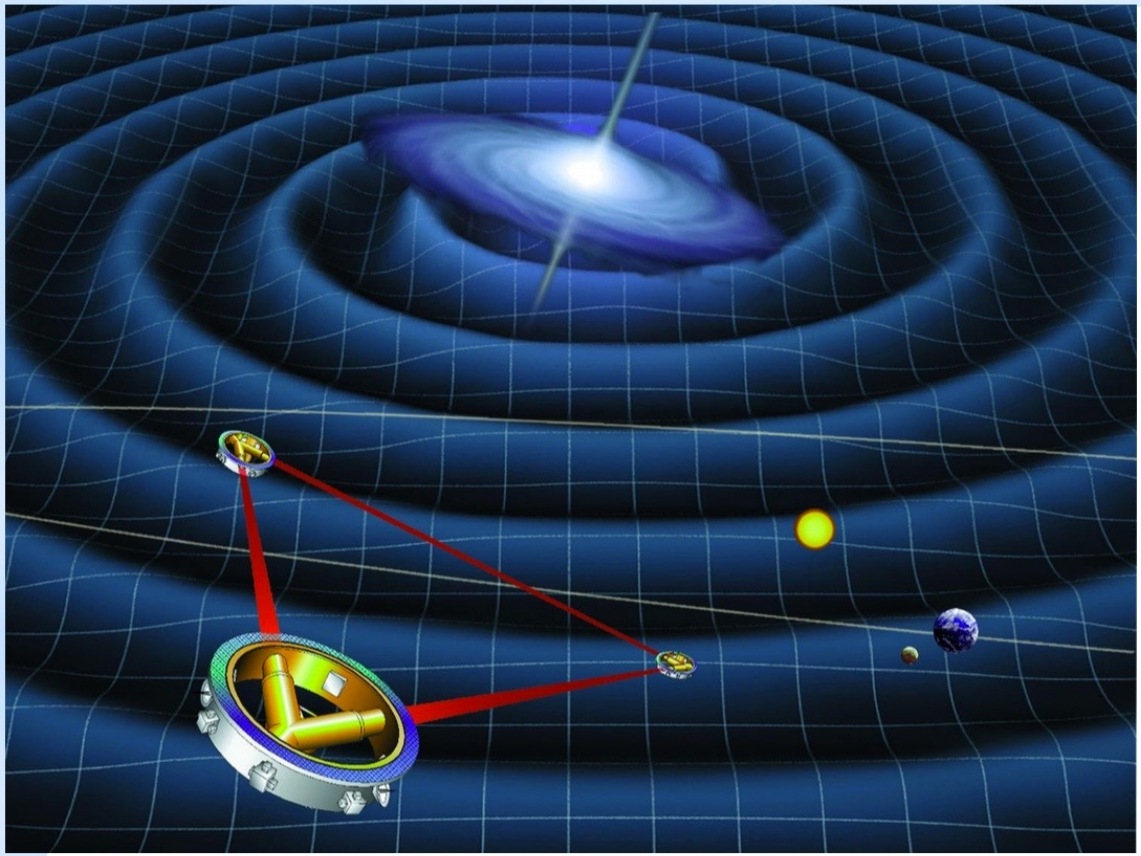

Present plan: 3 Interferometers
2.5×10^6 km arm lengths

ESA – All Systems GO!

Recent “Call” for mission

Acceptance - soon?

Planned launch 2034

NASA coming back

Earlier launch? 2028?

LIGO GW events and Lisa Pathfinder success have helped significantly

Tremendous activity at present

LISA in Orbit

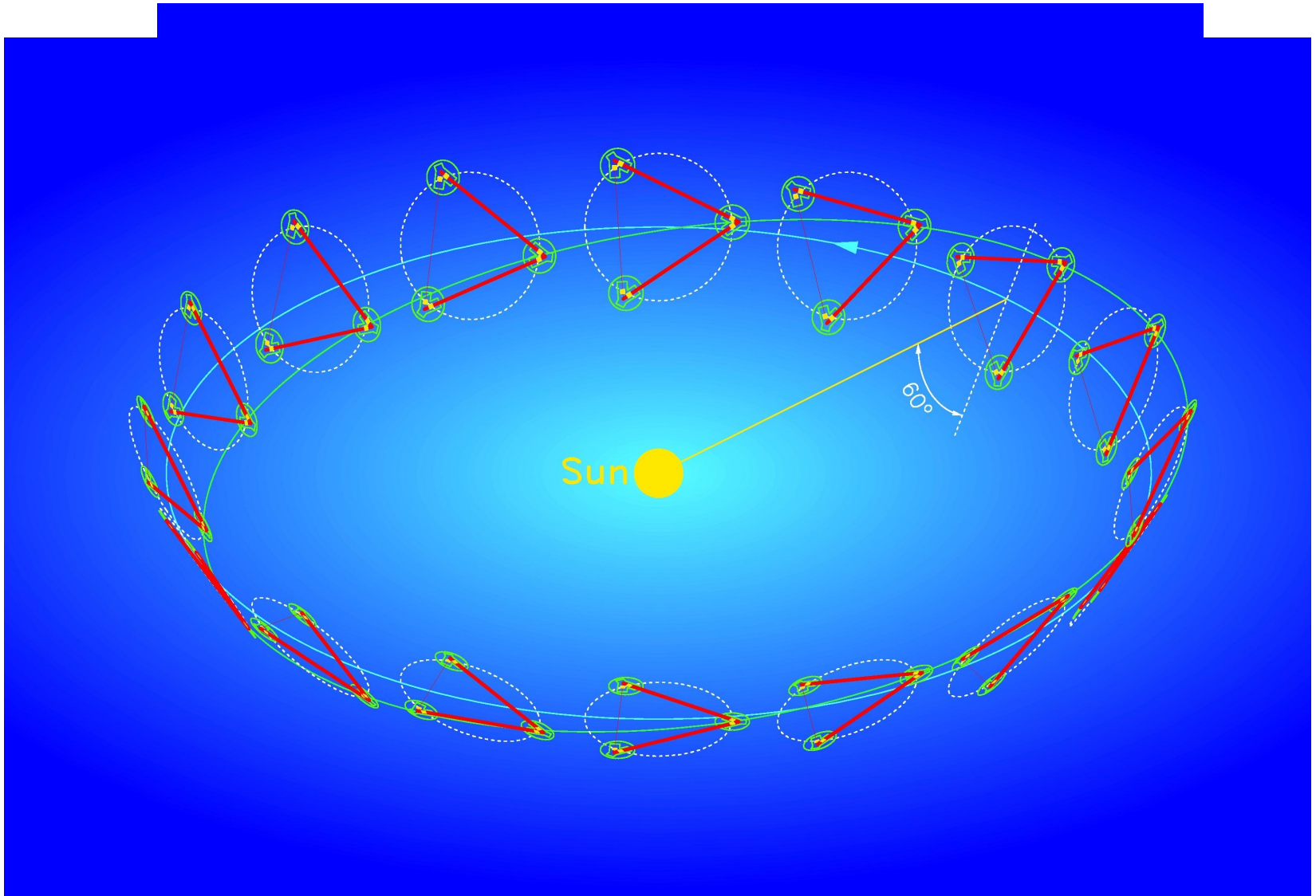

LISA physics

- the nature of gravity
- the fundamental nature of black holes
- black holes as sources of energy
- nonlinear structure formation
- dynamics of galactic nuclei
- formation and evolution of stellar binary systems
- the very early universe
- cosmography (specifically, the cosmic distance scale)

Gravitational Observatory Advisory Team – GOAT (ESA web site)

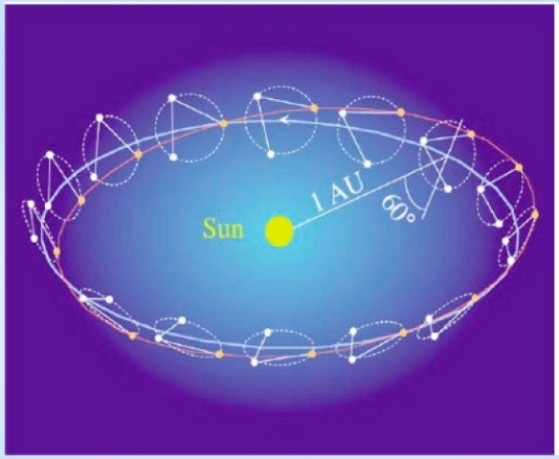

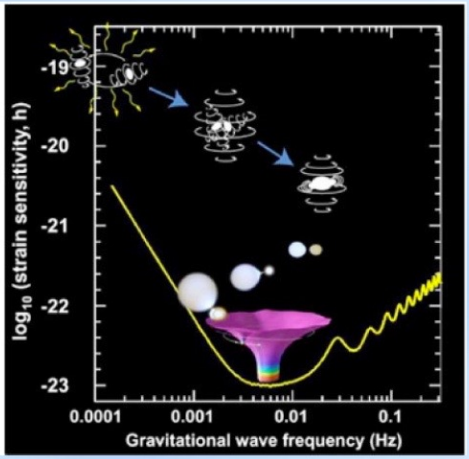

LISA Pathfinder – Demonstrating LISA Technology

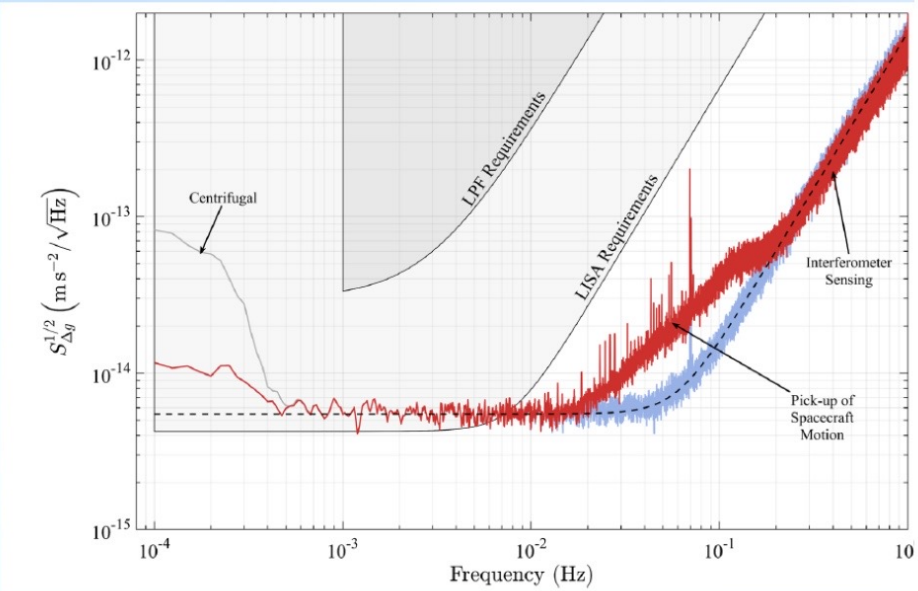

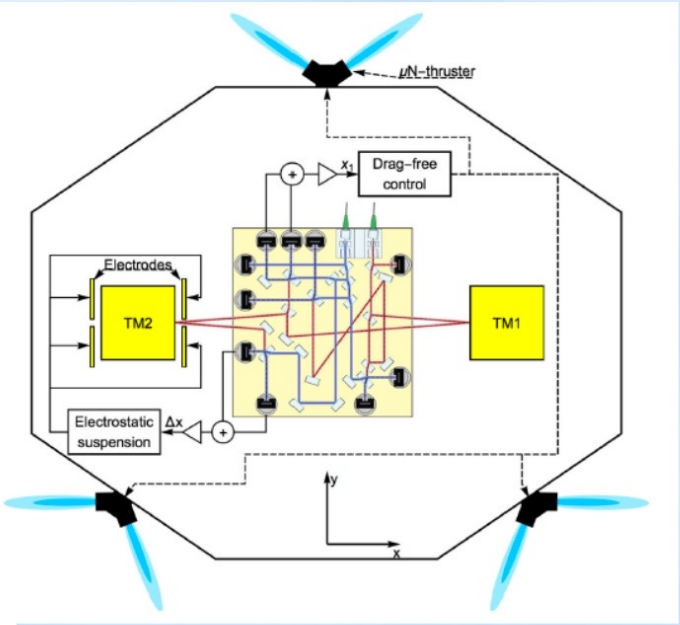

LISA Pathfinder worked! Exceeded requirements. Still, operation was not perfect, and there is lots of experimental work to do before LISA.

A set of cold gas micro-newton thrusters to ensure the spacecraft follows TM1. A second control loop forces TM2 to stay at a fixed distance from TM1 and thus centered in its own electrode housing.

PRL **116**, 231101 (2016)

LISA Proof Masses, Optical Bench, Interferometry and Telescopes

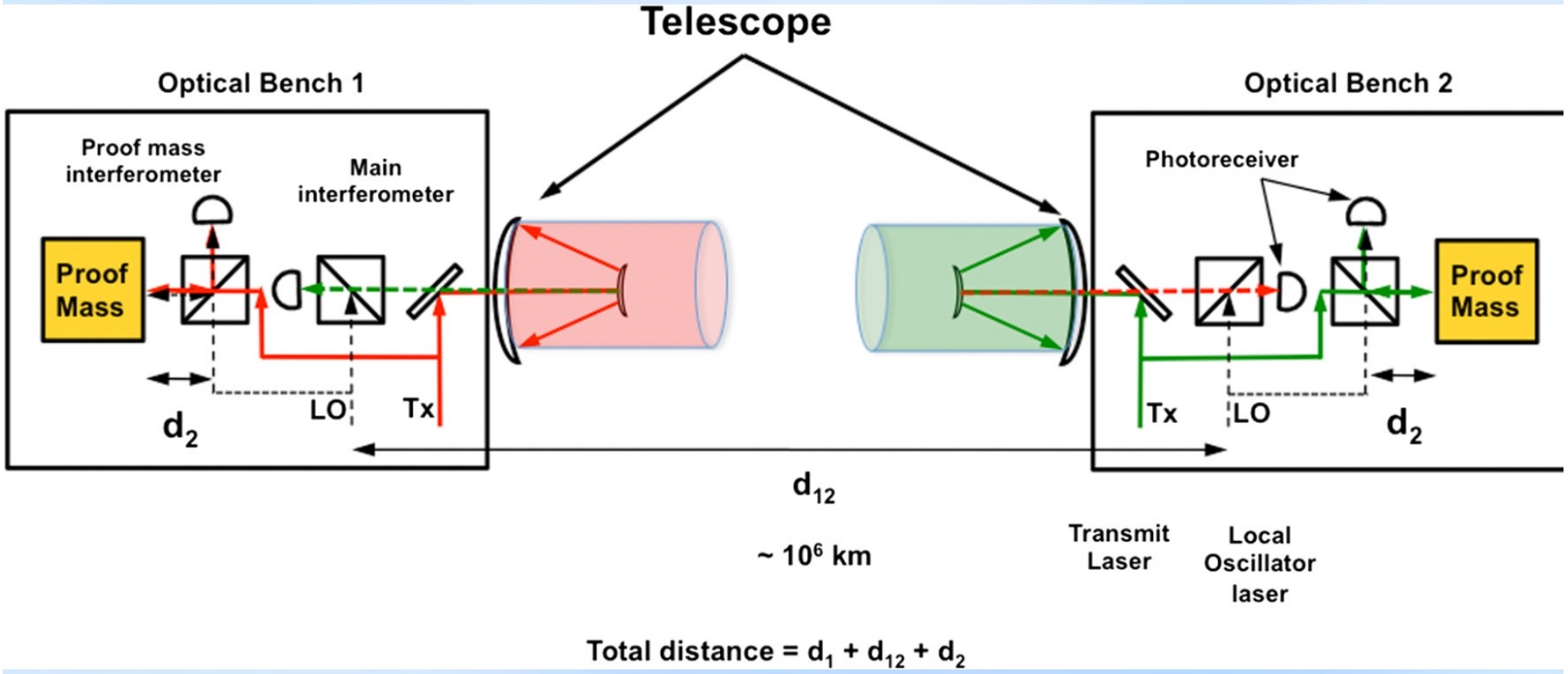

Livas et al, Opt. Eng. 52(9), 091811 (2013)

LISA Physics

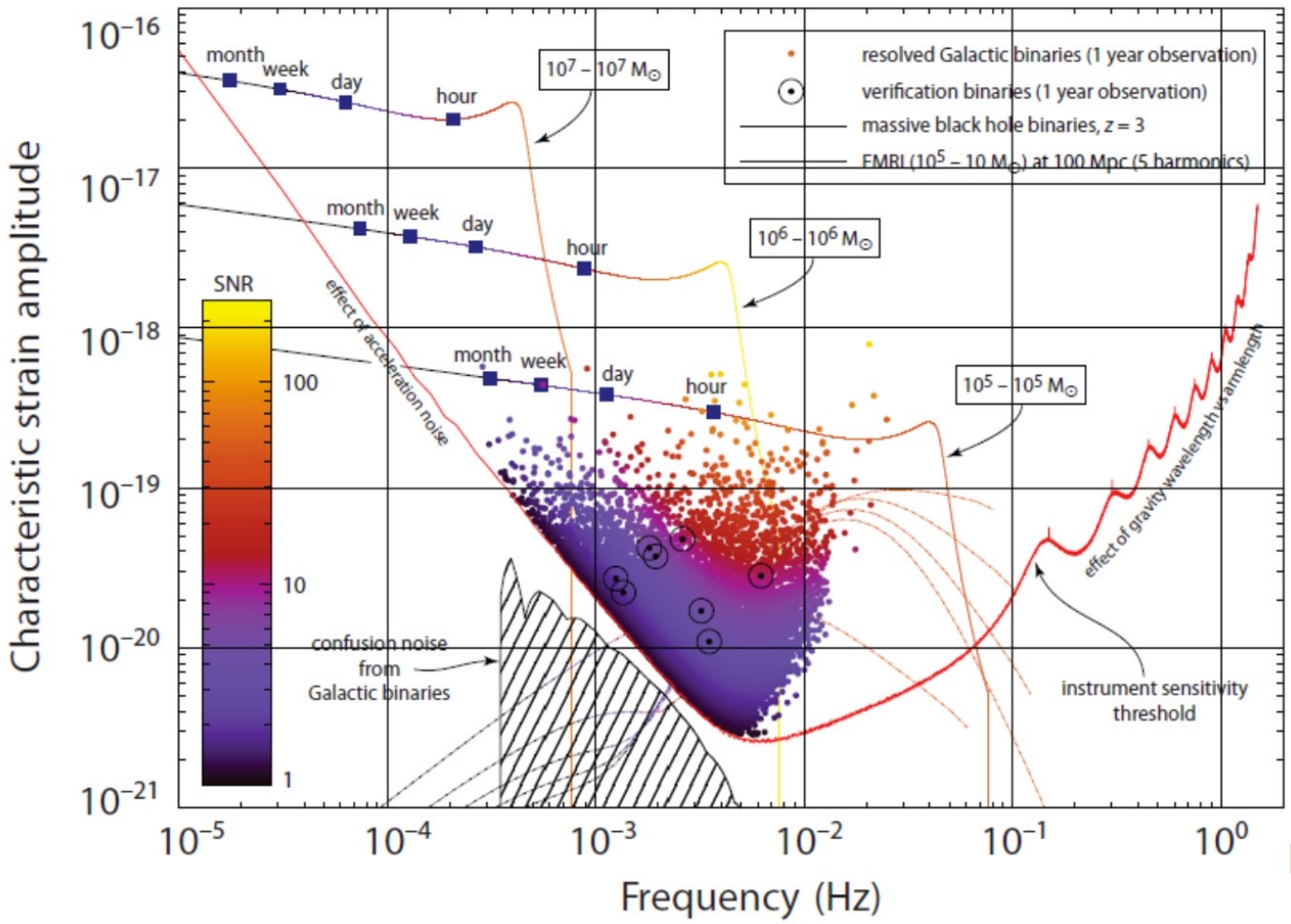

LISA GOAT

Characteristic strain amplitude versus frequency for a space-based laser interferometry mission (armlength 10^6 km, 1-yr observations). Objects expected to be strong gravitational wave sources over this frequency range.

Testing the Early Universe

- Inflation
- Electro-weak phase transition, or phase transitions related to new physics
- Cosmic strings (phase transitions, topological defects, cosmic superstrings)

Scientific topic	Source: ultra-compact binaries	Source: astrophysical black holes	Source: extreme mass-ratio inspirals	Source: background (astrophysical/cosmological)
nature of gravity				
fundamental nature of black holes				
black holes as sources of energy				
nonlinear structure formation				
dynamics of galactic nuclei				
formation/evolution of stellar binary systems				
very early Universe				
cosmography				

LISA GOAT

LISA Summary

The LISA project is presently moving forward rapidly.

ESA and NASA see this as a high priority.

A tremendous amount of R&D still needs to be done for LISA, and there is much experimental activity.

After the LHC, LISA may offer the best opportunity to observe the high energy physics that describes the universe.

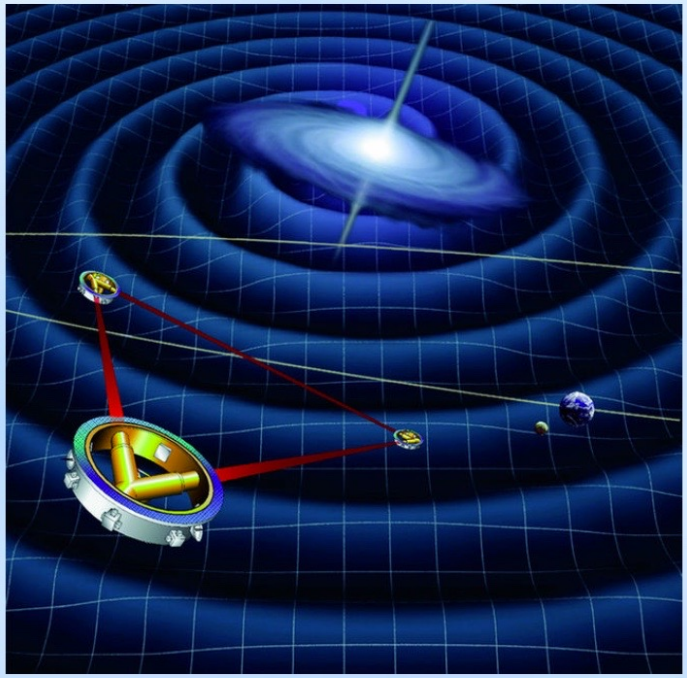

Pulsar Timing Arrays

Idea: use pulsars as clocks

1978SvA....22...36S

Opportunities for detecting ultralong gravitational waves

M. V. Sazhin

Shternberg Astronomical Institute, Moscow

(Submitted June 14, 1977)

Astron. Zh. **55**, 65–68 (January–February 1978)

The influence of ultralong gravitational waves on the propagation of electromagnetic pulses is examined. Conditions are set forth whereby it might be possible to detect gravitational waves arriving from binary stars. There are some prospects for detecting gravitational radiation from double superstars with masses $\mathfrak{M}_1 \approx \mathfrak{M}_2 \approx 10^{10}\,\mathfrak{M}_\odot$.

PACS numbers: 97.80.—d, 97.60.Gb, 95.30.Gv

Spin-Powered Pulsars: A Census

- Number of known pulsars: 1765
- Number of millisecond pulsars: 170
- Number of binary pulsars: 131
- Number of AXPs: 12
- Number of pulsars in globular clusters: 99*
- Number of extragalactic pulsars: 20

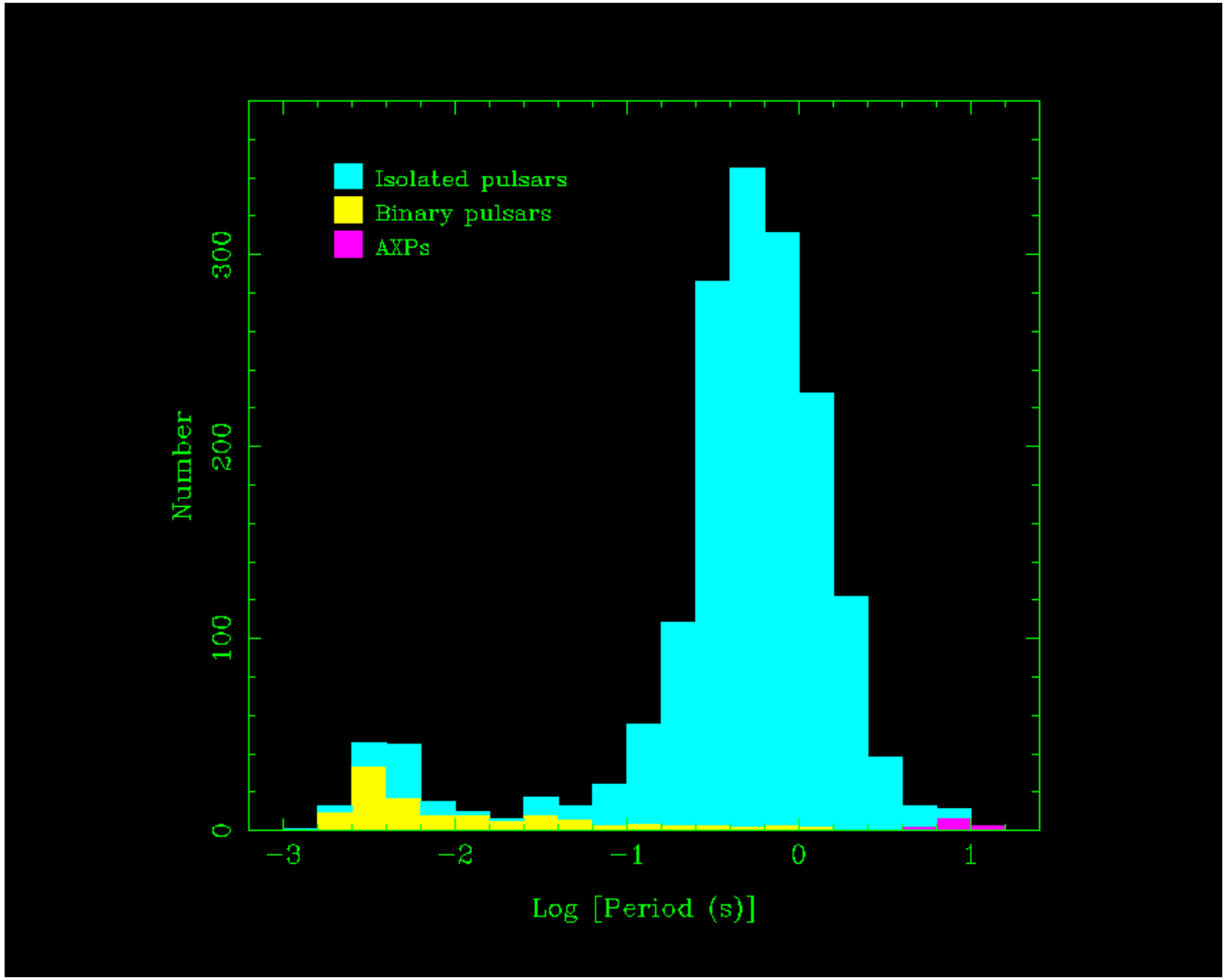

* Total known: 129 in 24 clusters (Paulo Freire's web page)

Data from ATNF Pulsar Catalogue, V1.25 (www.atnf.csiro.au/research/pulsar/psrcat; Manchester et al. 2005)

P - P Diagram

- Millisecond pulsars have very low P and are very old
- Most MSPs are binary
- MSPs are formed by 'recycling' an old pulsar in an evolving binary system
- 'Normal' pulsars have significant period irregularities, but MSP periods are very stable

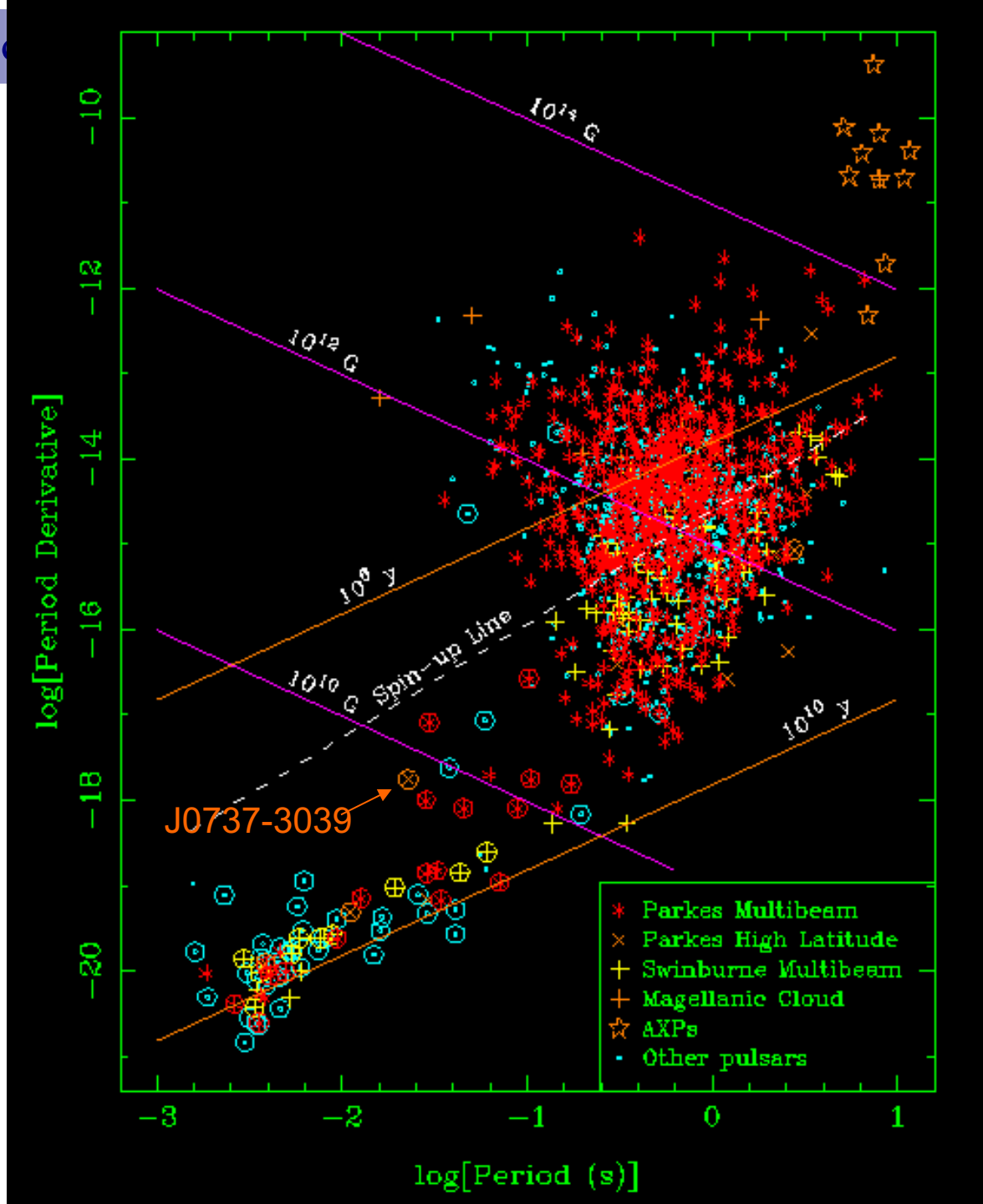

Pulsars and Gravitational Waves

Orbital decay in high-mass short-period binary systems accounted for by loss of energy to gravitational waves.

First observational evidence for gravitational waves!

Observed rates agree with the predictions of general relativity!

- PSR B1913+16: $\dot{P}_{b,obs}/\dot{P}_{b,pred} = 1.0013 \pm 0.0021$

Precision of GR test limited by uncertainty in correction for acceleration in gravitational field of the Galaxy (Weisberg & Taylor 2005)

- PSR B1534+12: $\dot{P}_{b,obs}/\dot{P}_{b,pred} = 0.91 \pm 0.05$

Limited by uncertainty in pulsar distance;assuming GR gives improved distance estimate (Stairs et al. 2002)

- PSR J1141-6545: $P_{b,obs}/P_{b,pred} = 1.05 \pm 0.25$

(NS-WD system) (Bailes et al. 2003)

- PSR J0737-3039A/B: $P_{b,obs}/P_{b,pred} = 1.004 \pm 0.014$

Expect 0.1% test in ~5 years!(Kramer et al. 2006)

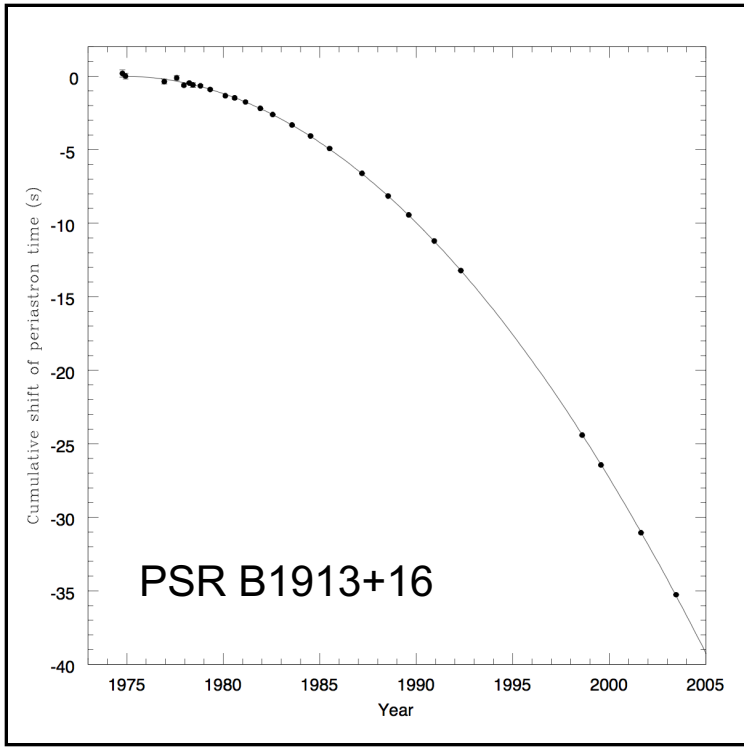

PSR J0737-3039A/B - the Double Pulsar

- Four times as relativistic as Hulse-Taylor binary pulsar
- Detection of both pulsars gives the mass ratio of the two stars

- Have measured five relativistic parameters in just two years!
- Four independent tests of general relativity
- Consistent at the 0.05% level!

R: Mass ratio

ω: periastron advance

γ: gravitational redshift

r & s: Shapiro delay

P_b: orbit decay

(Kramer et al. 2006)

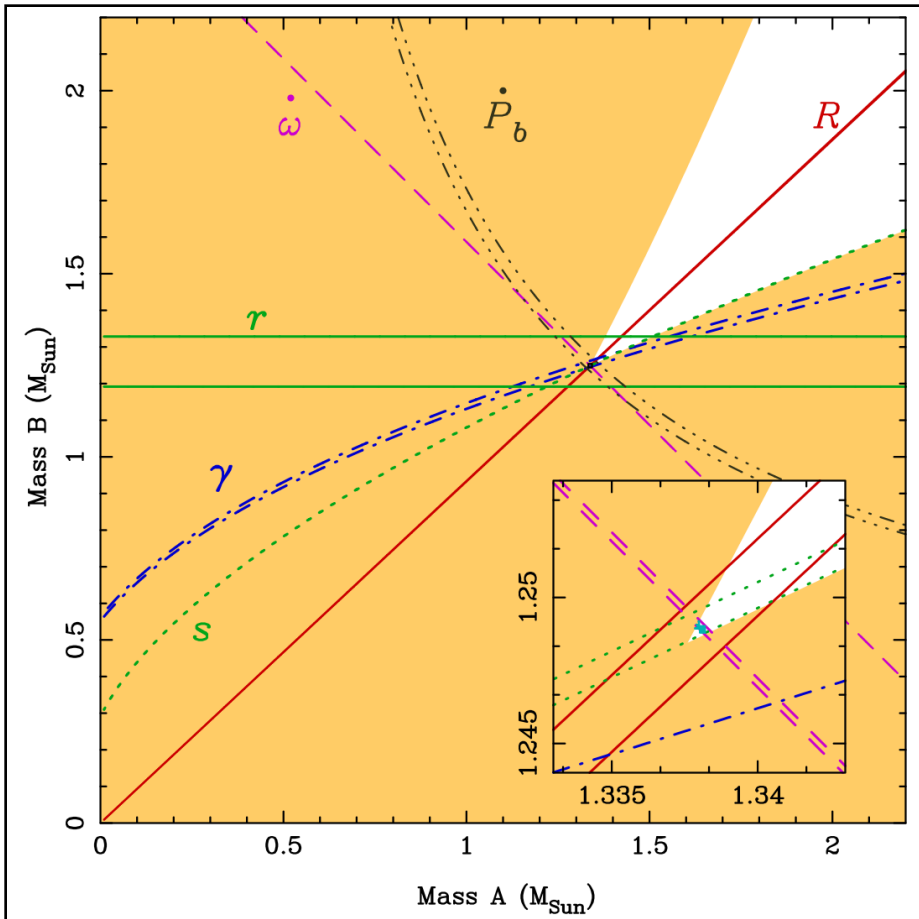

Pulsar limits on the GW Background

- Gravitational waves (GW) passing over the pulsar and the Earth perturb the apparent pulse period
- Results in additional 'noise' in pulse arrival times (TOAs) and hence increased scatter in timing residuals (differences between observed and predicted TOAs)
- If no signal detected, can set a limit on strength of GW background
- Best limits are obtained for GW frequencies ~ 1/T where T is length of data span
- Analysis of 8-year sequence of Arecibo observations of PSR B1855+09 gives $\Omega_{gw} = \rho_{gw}/\rho_c < 10^{-7}$ (Kaspi et al. 1994, McHugh et al.1996)
- Extended 17-year data set gives better limit, but non-uniformity makes quantitative analysis difficult (Lommen 2001)

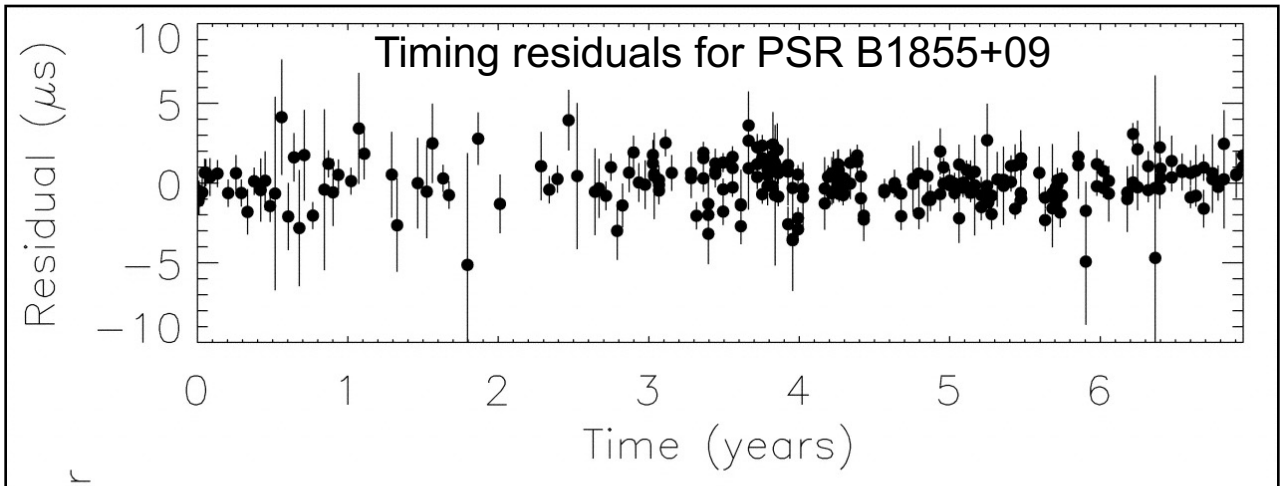

A Pulsar Timing Array

- With observations of many pulsars widely distributed on the sky can in principle ***detect*** a stochastic gravitational wave background
- Gravitational waves passing over Earth produce a ***correlated*** signal in the TOA residuals for all pulsars
- Gravitational waves passing over the pulsars are uncorrelated
- Requires observations of ~20 MSPs over 5 – 10 years;
- A timing array can detect instabilities in terrestrial time standards – establish a ***pulsar timescale***
- Can improve knowledge of Solar system properties, e.g. masses and orbits of outer planets and asteroids

Idea first discussed by Foster & Backer (1990)

- **Clock errors**

  All pulsars have the same TOA variations: monopole signature

- **Solar-System ephemeris errors**

  Dipole signature

- **Gravitational waves**

  Quadrupole signature

Can separate these effects provided there is a sufficient number of widely distributed pulsars

Detecting a Stochastic GW Background

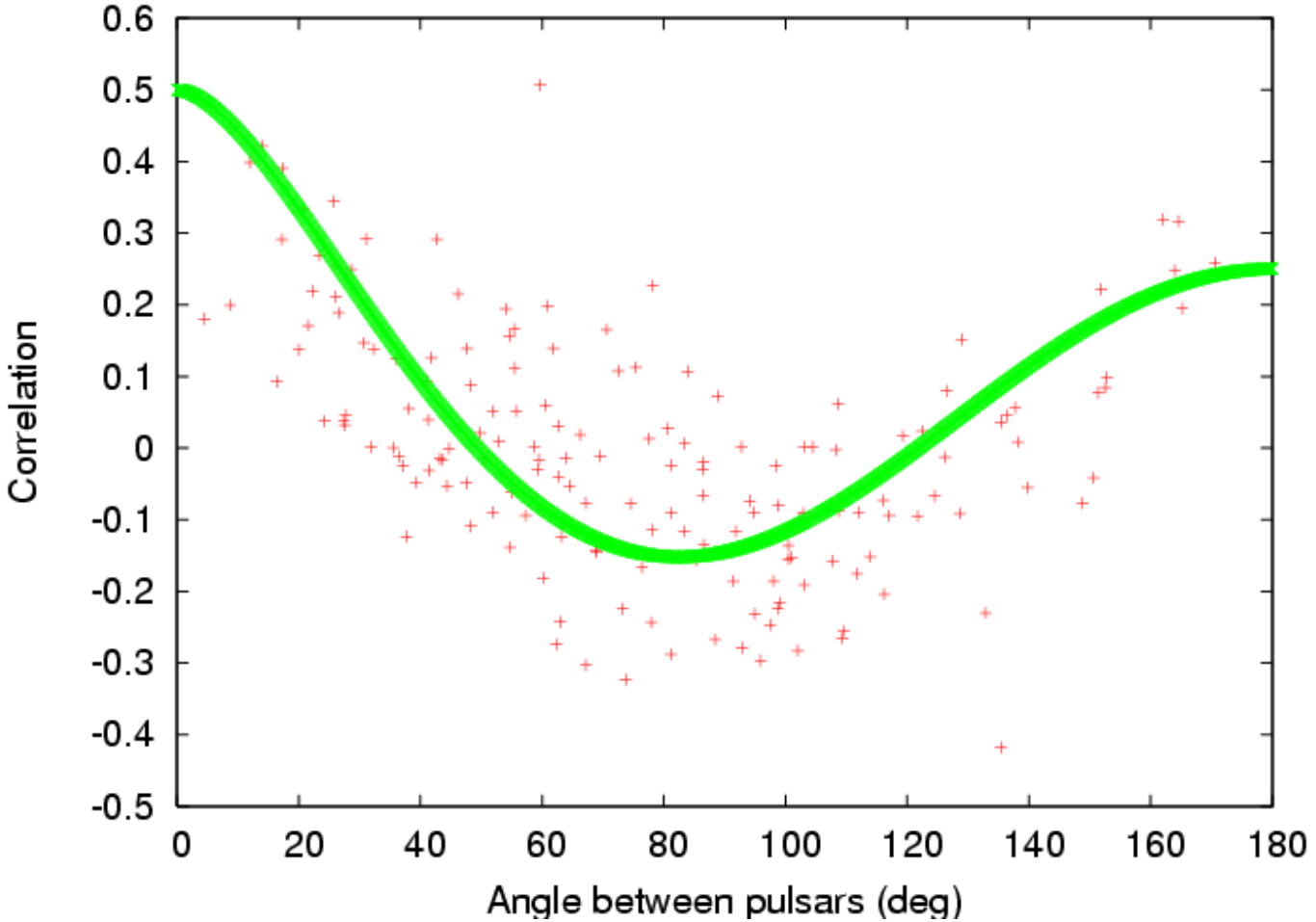

Simulation using Parkes Pulsar Timing Array (PPTA) pulsars with GW background from binary black holes in galaxies

(Rick Jenet, George Hobbs)

The Parkes Pulsar Timing Array Project

Collaborators:

- Australia Telescope National Facility, CSIRO
  - Dick Manchester, George Hobbs, Russell Edwards, John Sarkissian, John Reynolds, Mike Kesteven, Grant Hampson, Andrew Brown
- Swinburne University of Technology
  - Matthew Bailes, Ramesh Bhat, Joris Verbiest, Albert Teoh
- University of Texas, Brownsville
  - Rick Jenet, Willem van Straten
- University of Sydney
  - Steve Ord
- National Observatories of China, Beijing
  - Xiaopeng You
- Peking University, Beijing
  - Kejia Lee
- University of Tasmania
  - Aidan Hotan

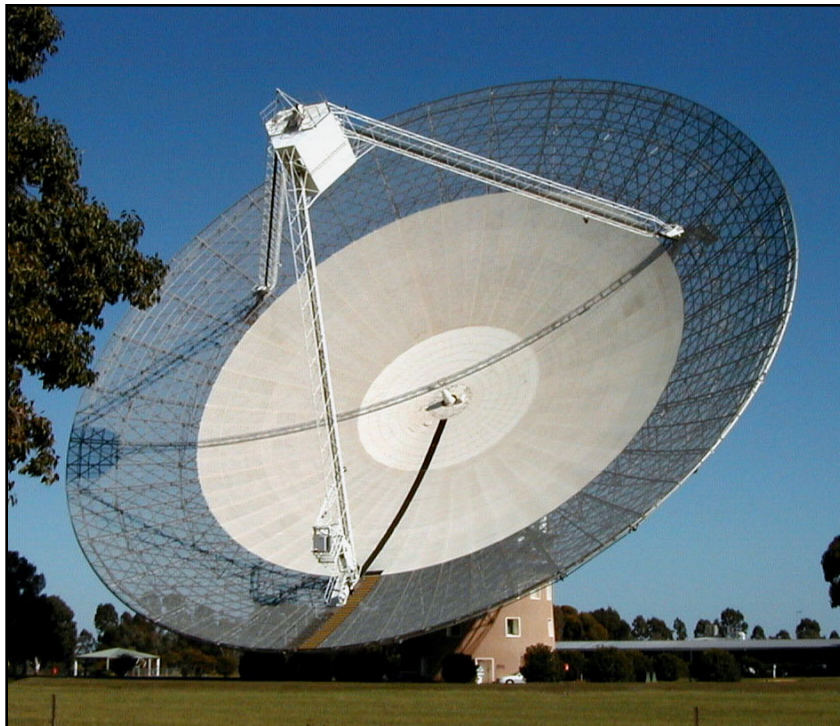

The PPTA Project: Goals

- To detect gravitational waves of astrophysical origin
- To establish a pulsar-based timescale and to investigate irregularities in terrestrial timescales
- To improve on the Solar System ephemeris used for barycentric correction
- Modelling and detection algorithms for GW signals
- Measurement and correction for interstellar and Solar System propagation effects
- Investigation and implementation of methods for real-time RFI mitigation

To achieve these goals we need ~weekly observations of ~20 MSPs over at least five years with TOA precisions of ~100 ns for ~10 pulsars and < 1 μs for rest

The PPTA Project: Methods

- Using the Parkes 64-m telescope at three frequencies (680, 1400 and 3100 MHz)
- Digital filterbank system, 256 MHz bandwidth (1 GHz early 2007), 8-bit sampling, polyphase filter
- CPSR2 baseband system 2 x 64 MHz bandwidth, 2-bit sampling, coherent de-dispersion
- Developing APSR with 512 MHz bandwidth and 8-bit sampling
- Implementing real-time RFI mitigation for 50-cm band
- TEMPO2: New timing analysis program, systematic errors in TOA corrections < 1 ns, graphical interfaces, predictions and simulations (Hobbs et al. 2006, Edwards et al. 2006)
- Observing 20 MSPs at 2 - 3 week intervals since mid-2004
- Looking to international co-operation to obtain improved data sampling including pulsars at northern declinations

Sky Distribution of Millisecond Pulsars

P < 20 ms and not in globular clusters

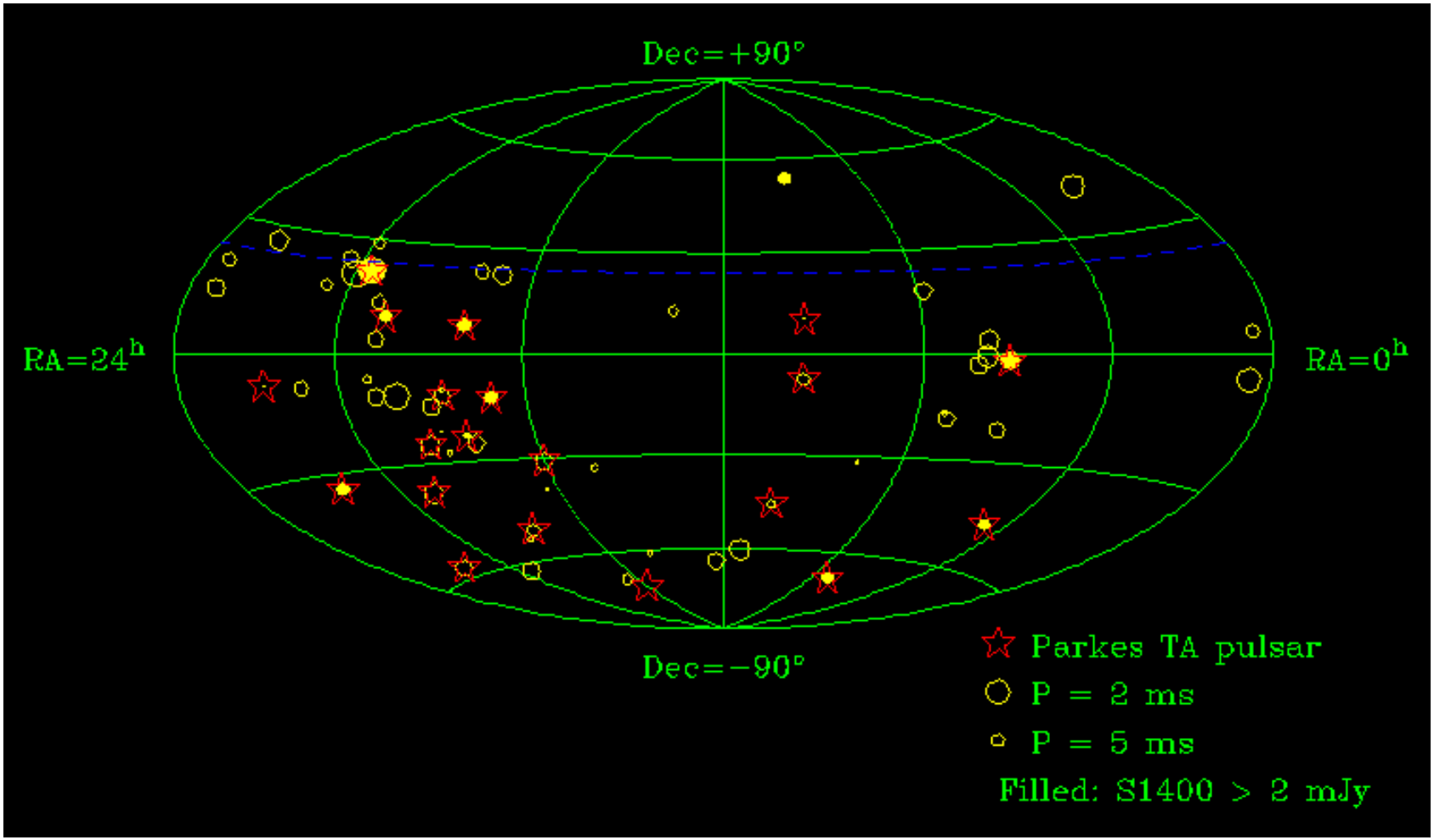

PPTA Pulsars

- 20 MSPs - all in Galactic disk except J1824-2452 (B1821-24) in M28
- Two years of timing data at 2 -3 week intervals and at three frequencies
- Uncorrected for DM variations and polarisation calibration
- Five pulsars with rms timing residuals < 500 ns, all < 2.5 μs
- Best results on J0437-4715 (120 ns) and B1937+21 (170 ns)

Still have a way to go!

Name	Period (ms)	DM (cm^{-3} pc)	Orbital period (d)	Rms Residual (μs)
J0437-4715	5.757	2.65	5.74	0.12
J0613-0200	3.062	38.78	1.20	0.83
J0711-6830	5.491	18.41	-	1.56
J1022+1001	16.453	10.25	7.81	1.11
J1024-0719	5.162	6.49	-	1.20
J1045-4509	7.474	58.15	4.08	1.44
J1600-3053	3.598	52.19	14.34	0.35
J1603-7202	14.842	38.05	6.31	1.34
J1643-1224	4.622	62.41	147.02	2.10
J1713+0747	4.570	15.99	67.83	0.19
J1730-2304	8.123	9.61	-	1.82
J1732-5049	5.313	56.84	5.26	2.40
J1744-1134	4.075	3.14	-	0.65
J1824-2452	3.054	119.86	-	0.88
J1857+0943	5.362	13.31	12.33	2.09
J1909-3744	2.947	10.39	1.53	0.22
J1939+2134	1.558	71.04	-	0.17
J2124-3358	4.931	4.62	-	2.00
J2129-5721	3.726	31.85	6.63	0.91
J2145-0750	16.052	9.00	6.84	1.44

Dispersion Measure Variations

- ΔDM from 10/50cm or 20/50cm observation pairs
- Variations observed in most of PPTA pulsars
- ΔDM typically a few x 10^{-3} cm^{-3} pc
- Weak correlation of d(DM)/dt with DM, closer to linear rather than $DM^{1/2}$
- Effect of Solar wind observed in pulsars with low ecliptic latitude

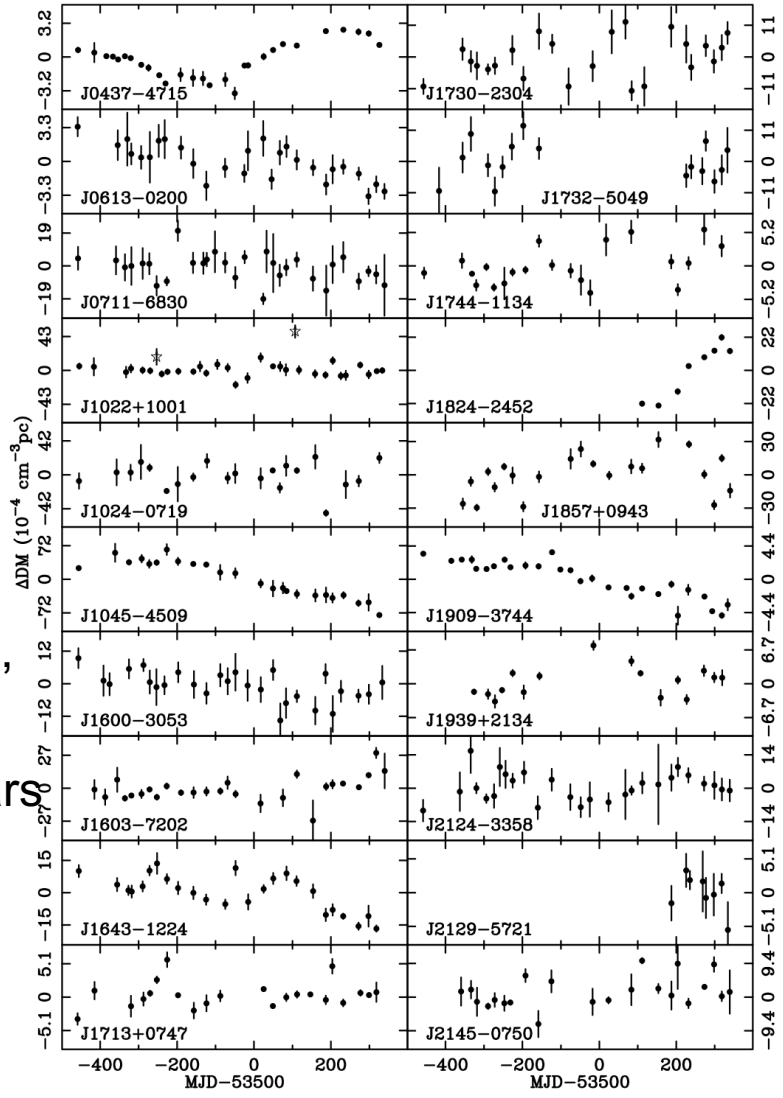

(You et al.,)

The Gravitational Wave Spectrum

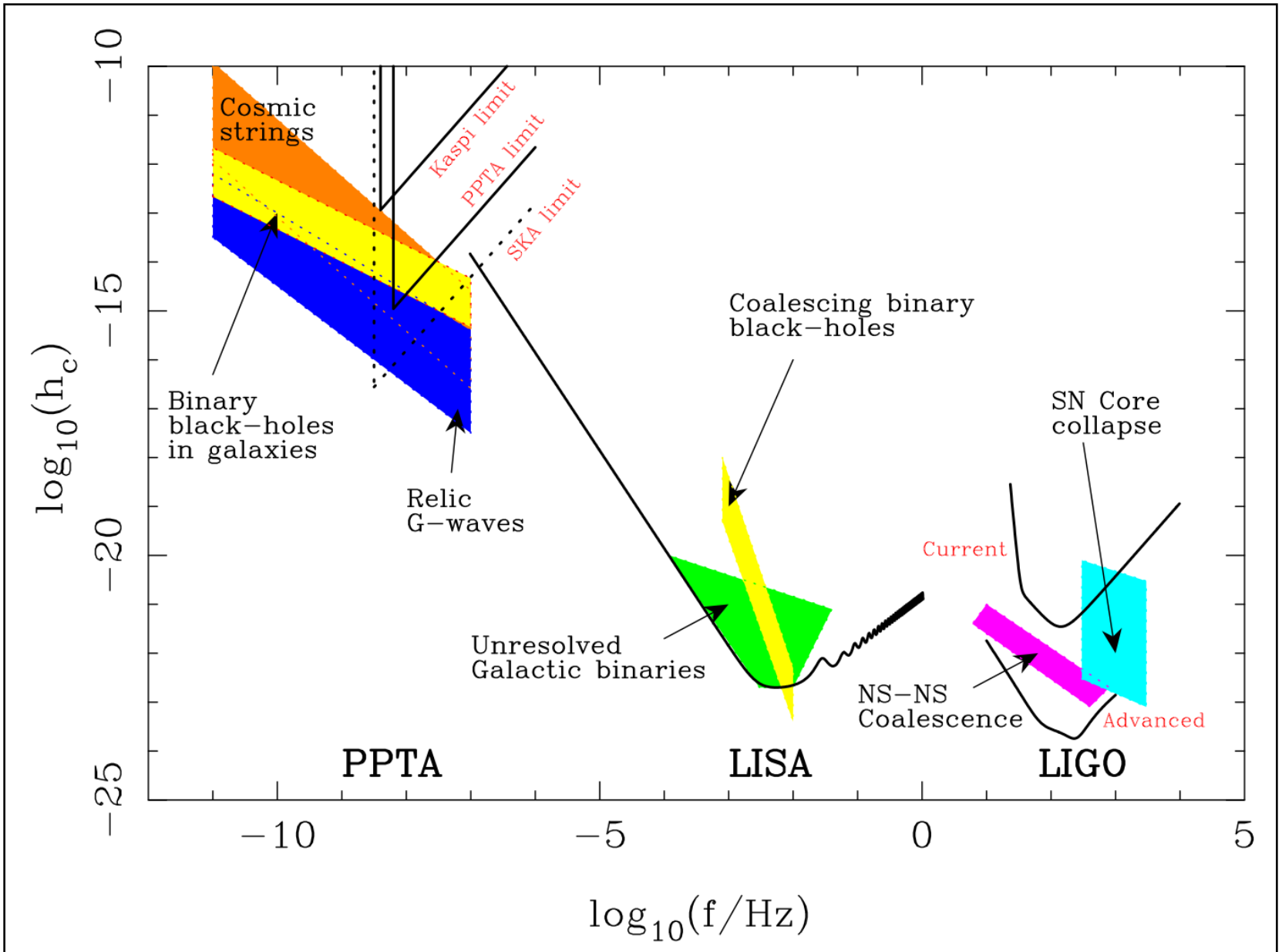

Current and Future Limits on the Stochastic GW Background

- Arecibo data for PSR B1855+09 (Kaspi et al. 1994) combined with subset of recent PPTA data
- Monte Carlo methods used to determine detection limit for stochastic background described by $h_c = A(f/1\text{yr})^{\alpha}$ (where α = -2/3 for SMBH, ~ -1 for relic radiation, ~ -7/6 for cosmic strings)
- ➢ Current limit: $\Omega_{gw}(1/8\ \text{yr}) \sim 2 \times 10^{-8}$
- ➢ For full PPTA (100ns, 5 yr): ~ 10^{-10}
- Currently consistent with all SMBH evolutionary models
- If no detection with full PPTA, all current models ruled out
- Already limiting EOS of matter in epoch of inflation and tension in cosmic strings

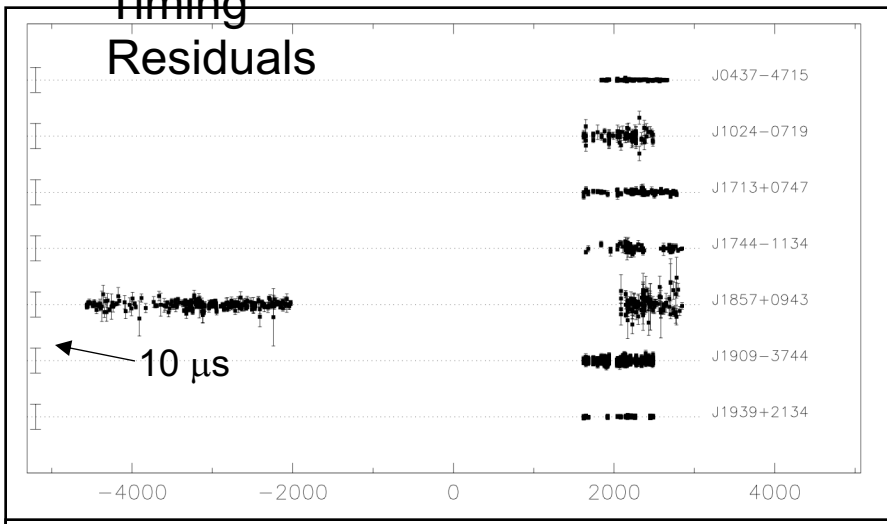

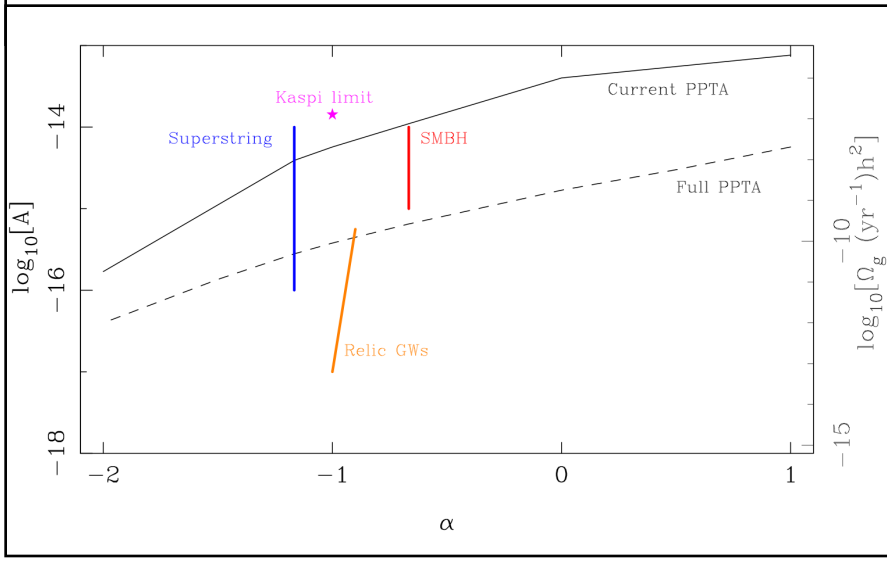

(Jenet et al. 2006)

NANOGrav

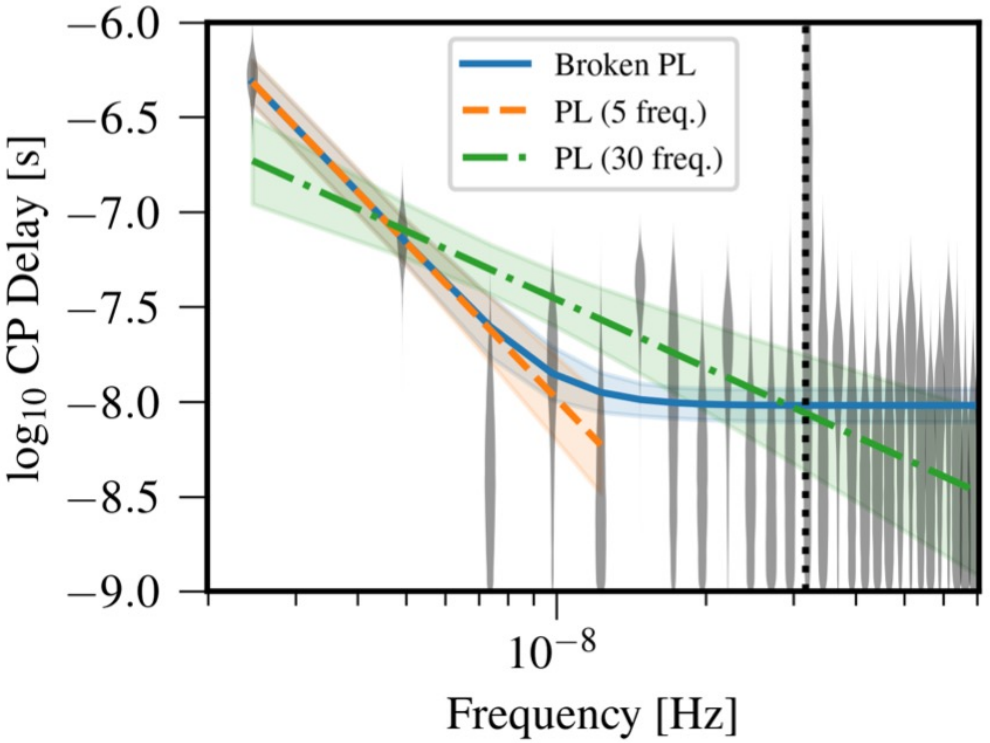

$$S(f) = \frac{A_{\rm CP}^2}{12\pi^2}\left(\frac{f}{f_{\rm yr}}\right)^{-\gamma} f_{\rm yr}^{-3},$$

$$S(f) = \frac{A_{\rm CP}^2}{12\pi^2}\left(\frac{f}{f_{\rm yr}}\right)^{-\gamma}\left(1+\left(\frac{f}{f_{\rm bend}}\right)^{1/\kappa}\right)^{\kappa(\gamma-\delta)} f_{\rm yr}^{-3},$$

NANOGrav Collaboration, 2009.04496

NANOGrav

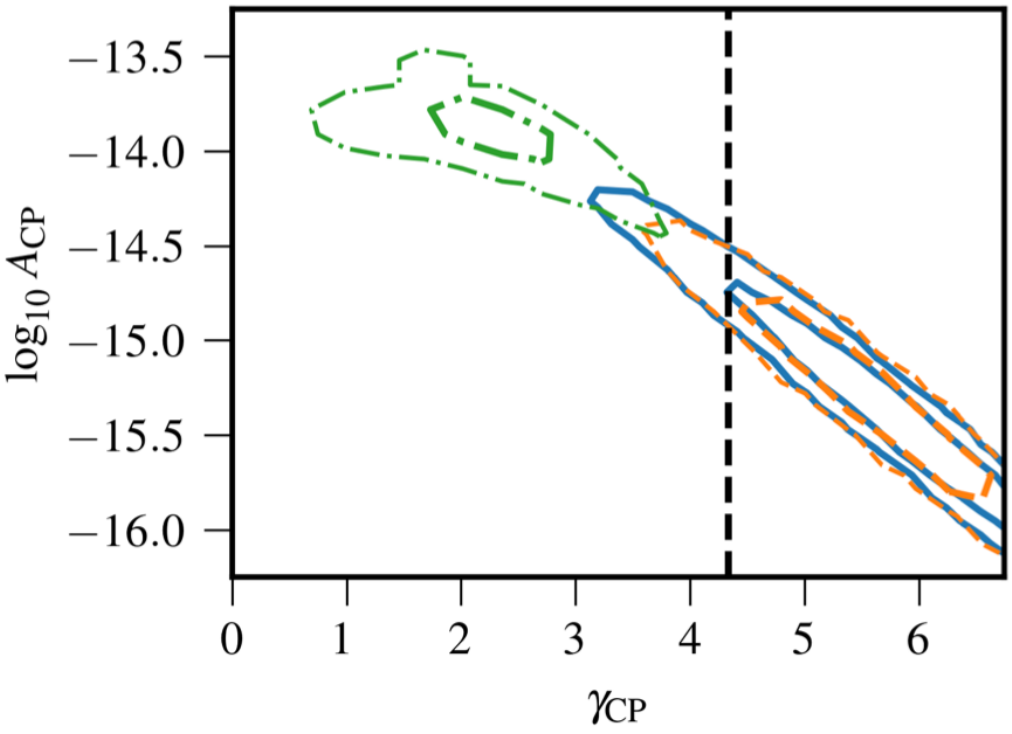

NANOGrav Collaboration, 2009.04496

NANOGrav

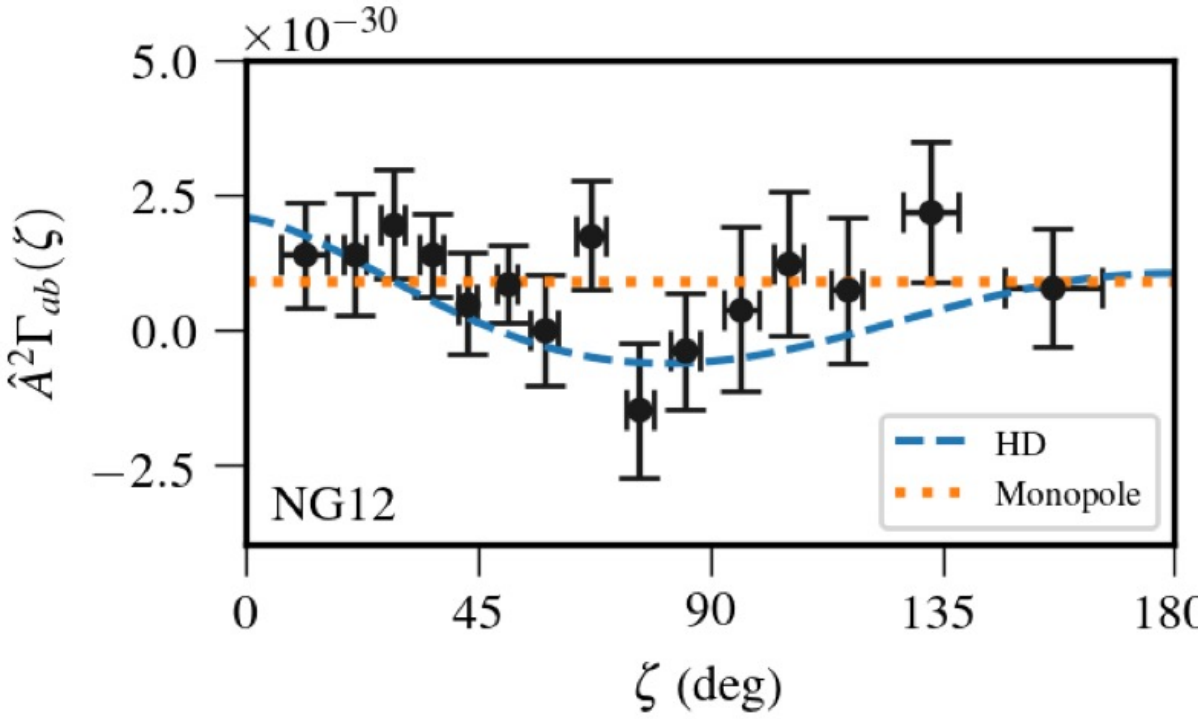

NANOGrav Collaboration, 2009.04496

Summary pulsars

- Direct detection of gravitational waves (GW) is a major goal of current astrophysics - it will open a new window on the Universe
- A pulsar timing array can ***detect*** GW from astrophysical sources
- Pulsars are sensitive to GW at nHz frequencies - complementary to ground-based and space-based laser-interferometer systems
- Parkes Pulsar Timing Array (PPTA) timing 20 MSPs since mid-2004. Goal is ~100 ns time residuals on at least half of sample, currently have five with rms residuals < 500 ns
- Current data improve the limit on the stochastic GW background by a factor of five. Full PPTA should detect the predicted background
- Expect pulsar-based timescale to have better long-term stability than current best terrestrial timescales
- SKA will herald a new era in the study of gravitational waves!

GW from Primordial Magnetic Field at QCD phase transition

Pulsar timing arrays

$$S(f) = \frac{A_{\rm CP}^2}{12\pi^2}\left(\frac{f}{f_{\rm yr}}\right)^{-\gamma} f_{\rm yr}^{-3},$$

$$h_{\rm c}(f) = \sqrt{12\pi^2 S(f) f^3} = A_{\rm CP}\left(\frac{f}{f_{\rm yr}}\right)^{\frac{3-\gamma}{2}}$$

$$\Omega_{\rm GW}^0(f) = \Omega_{\rm yr}\left(\frac{f}{f_{\rm yr}}\right)^{\beta},$$

$$\Omega_{\rm yr} = \frac{2\pi^2}{3H_0^2} f_{\rm yr}^2 A_{\rm CP}^2, \quad \beta = 5 - \gamma.$$

A. Roper Pol et al., 2201.05630

Pulsar timing arrays

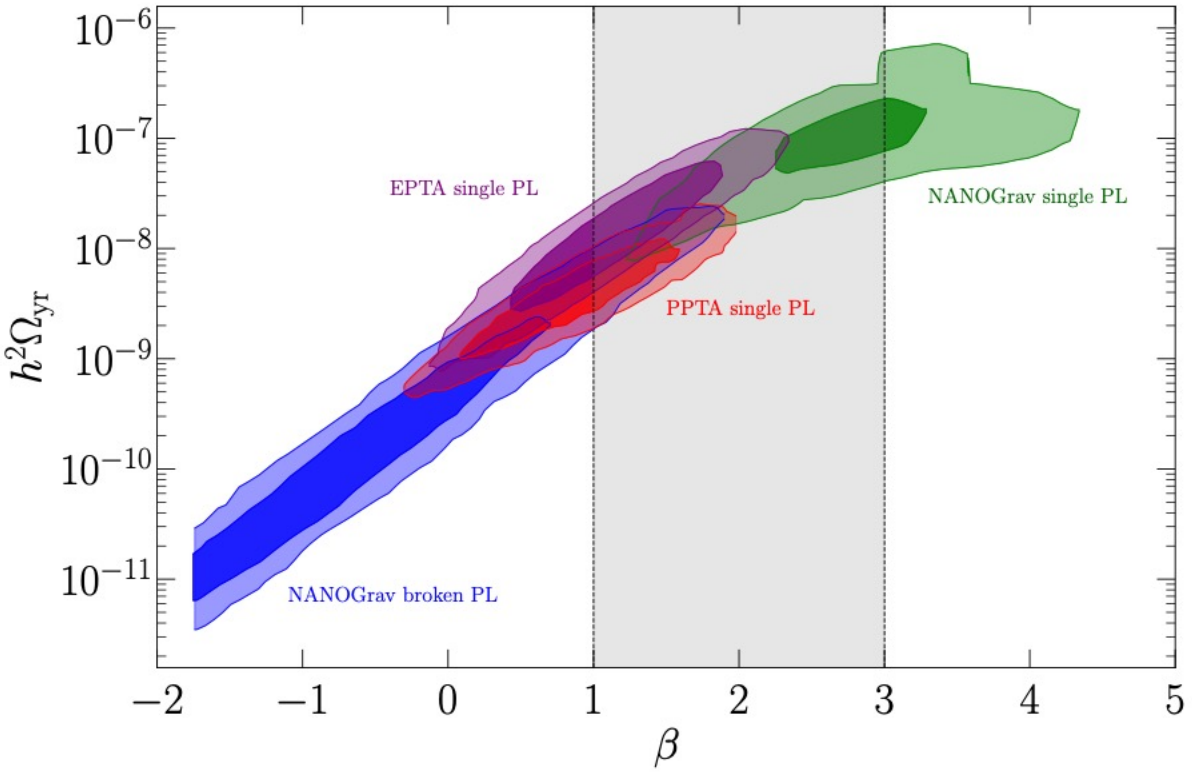

A. Roper Pol et al., 2201.05630

Pulsar timing arrays

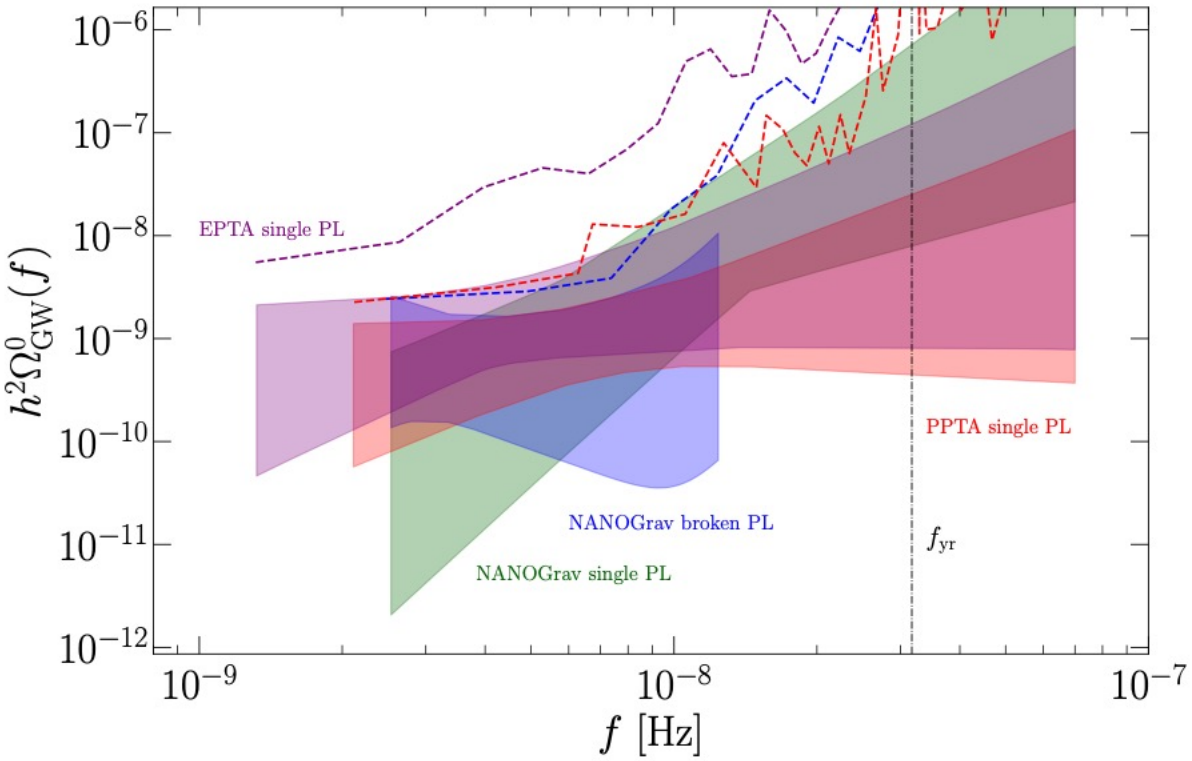

A. Roper Pol et al., 2201.05630

Gravitational signal from primordial magnetic field

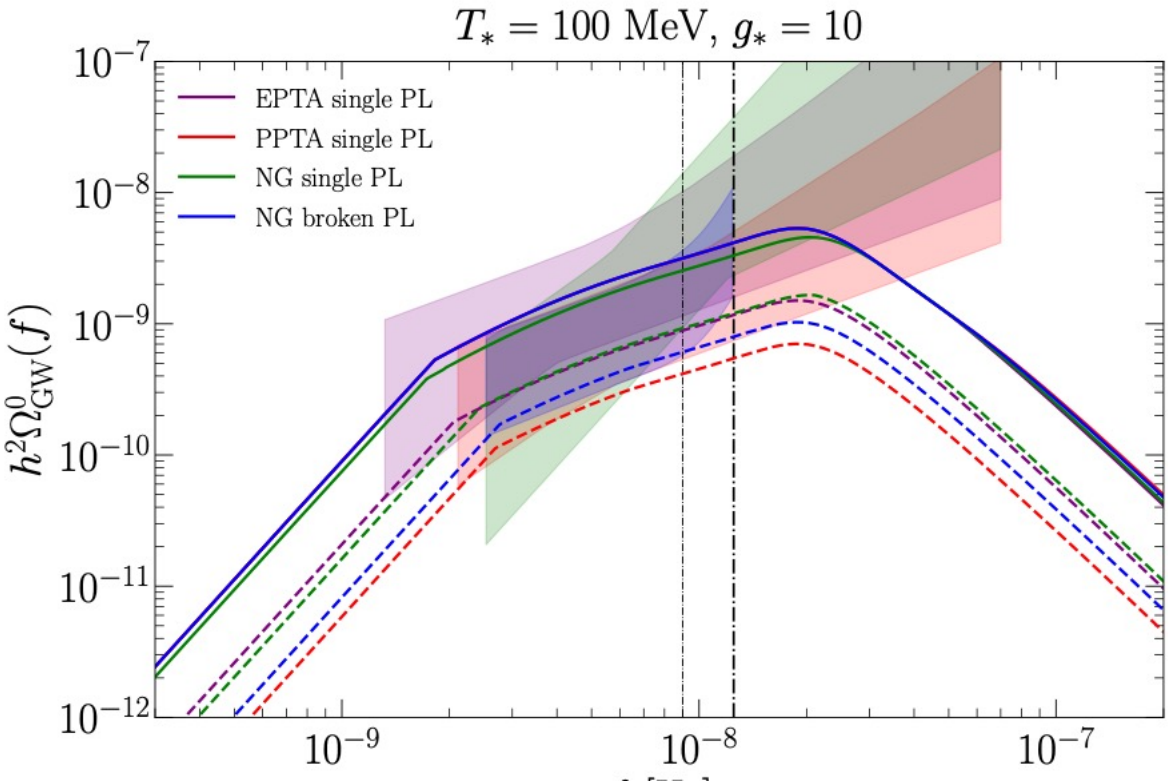

A. Roper Pol et al., 2201.05630

Primordiam magnetic field and SGWB

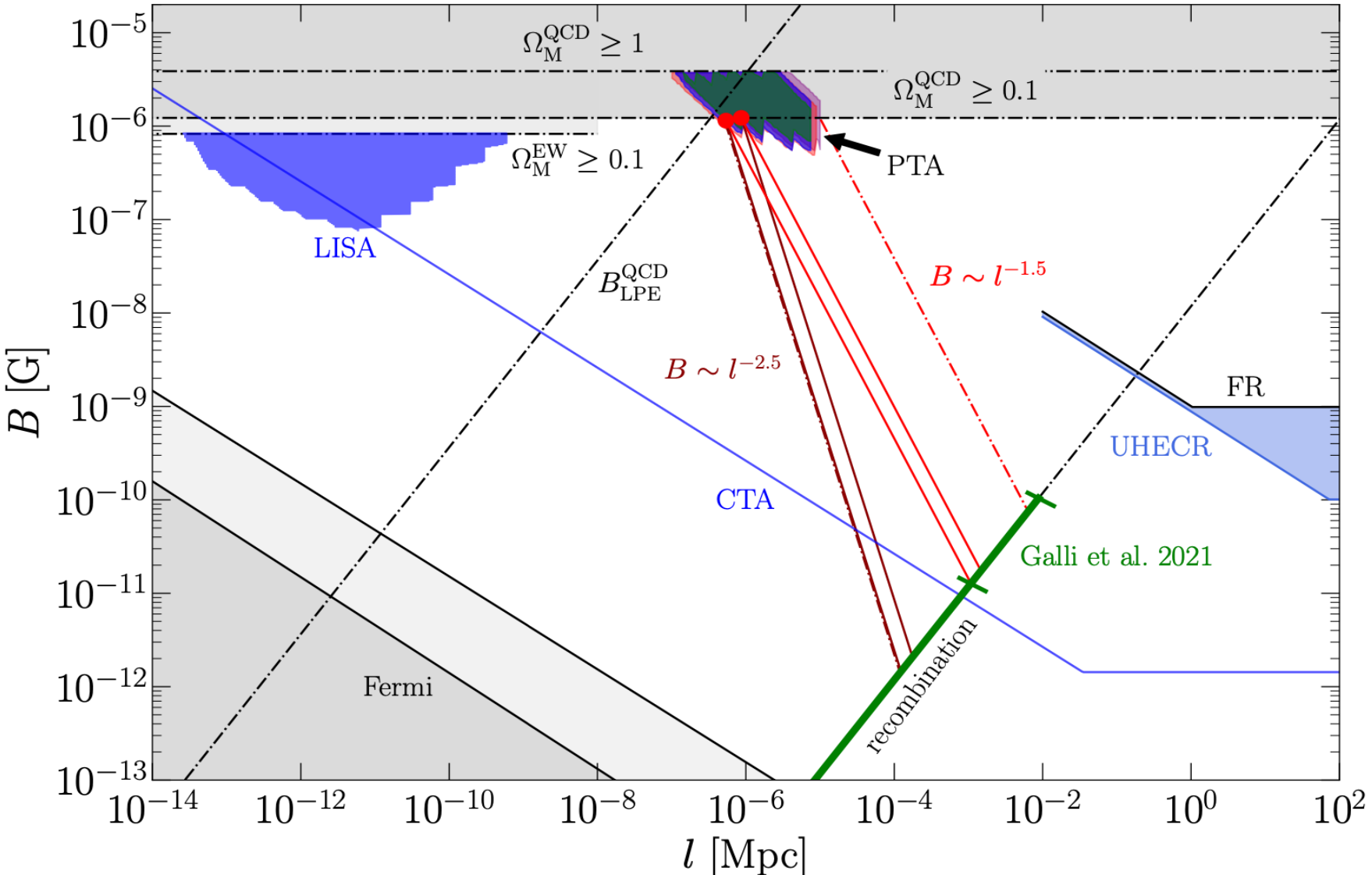

SGWB from SMBH binaries

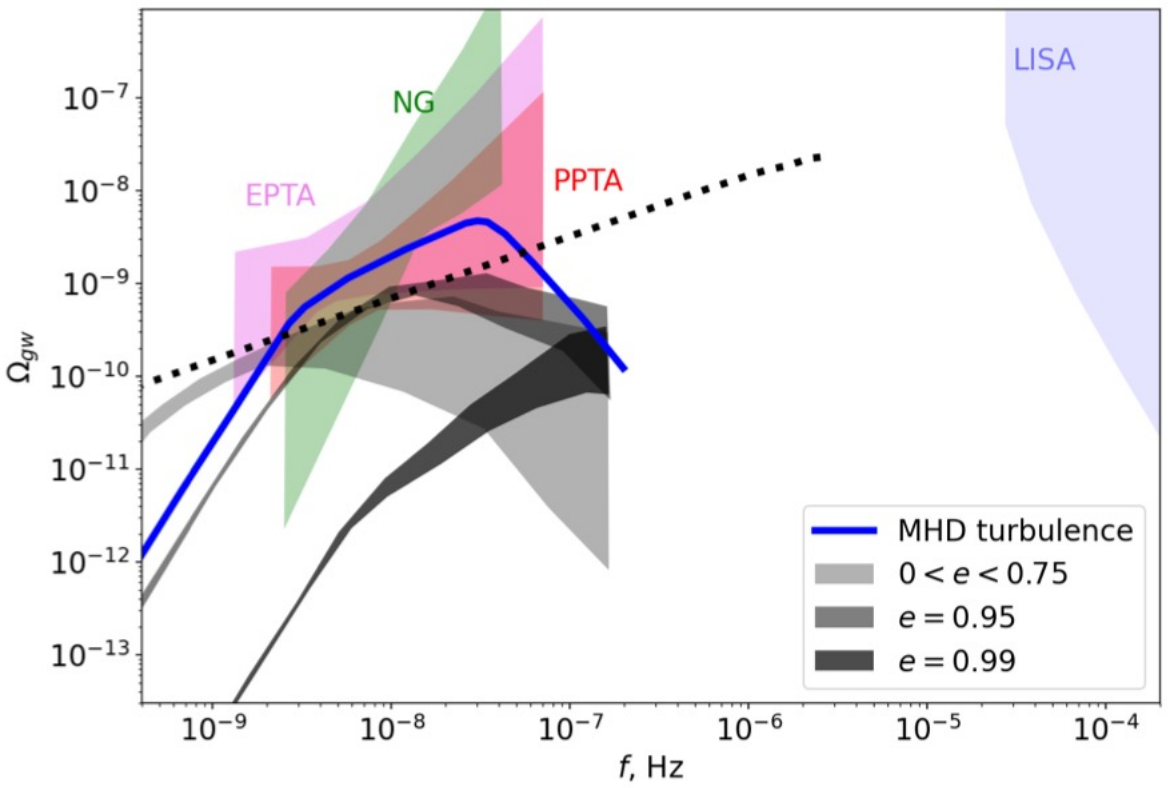

A. Roper Pol et al., 2201.05630

Inter-Galactic Magnetic Field detection with gamma-rays

Primordial magnetic field and cosmological model

Produced spectrum of PMF

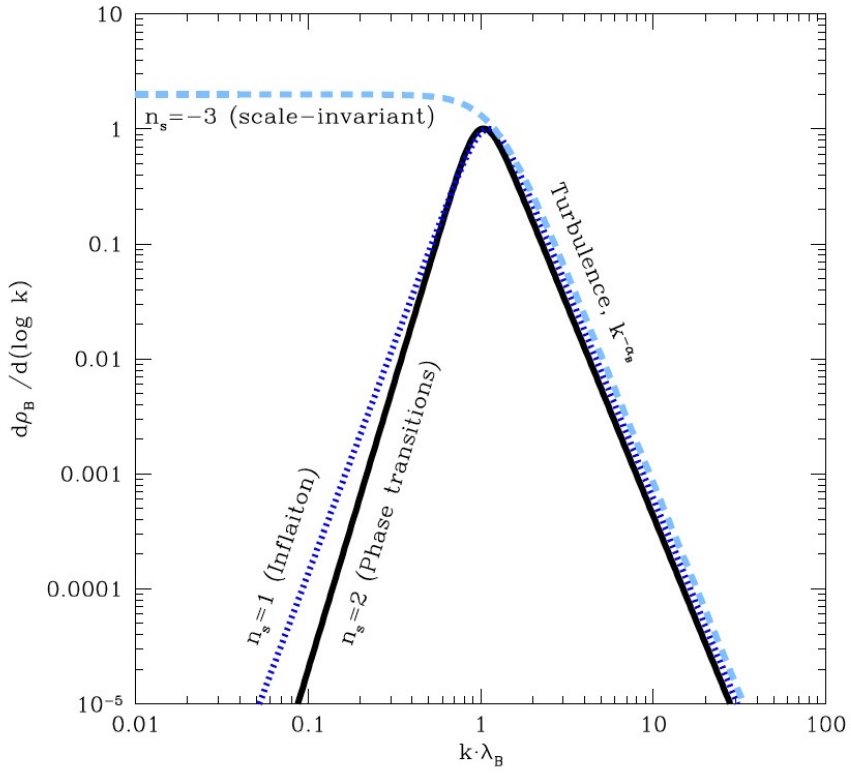

From R.Durrer and A.Neronov, A&A Rev. 21 62, [1303.7121].

Early Universe evolution of spectrum of PMF

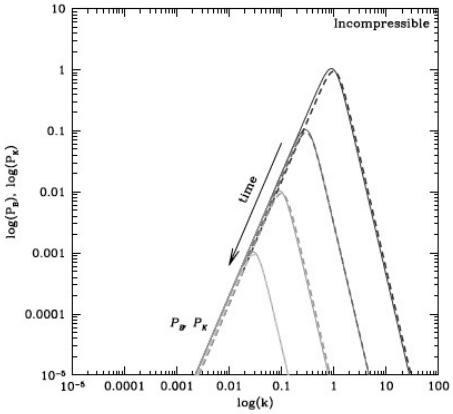

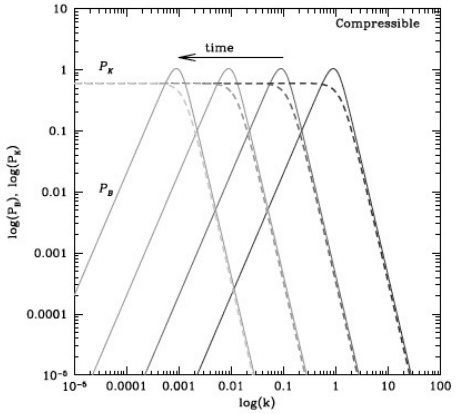

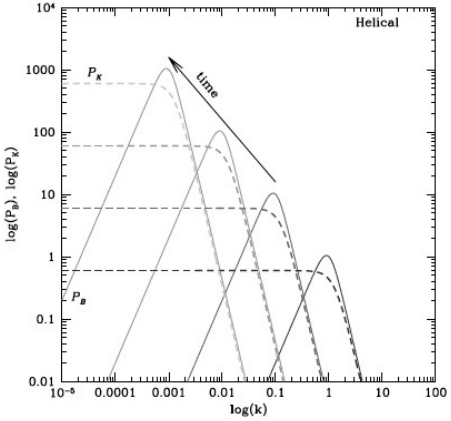

$$H = \int \mathbf{A} \cdot \mathbf{B}\, d^3\mathbf{r}$$

R.Durrer and A.Neronov, A&A Rev. 21 62, [1303.7121].

PMF from inflation and phase transitions

$$\mathcal{P}_B(\tau_0, k) \lesssim (10^{-15}\,\mathrm{G})^2 \left(\frac{k}{a_0}\,\mathrm{Mpc}\right)^2 \left(\frac{H_{\mathrm{reh}}}{H_{\mathrm{inf}}}\right)^{1/3} \frac{10^{-14}\,\mathrm{GeV}}{H_{\mathrm{inf}}}. \tag{3.20}$$

For classical scenarios we obtained the bound (3.20), which requires an extremely low scale inflation of $H_{\mathrm{inf}} \lesssim 10^{-19}\,\mathrm{GeV}$ (3.22) in order for magnetic fields of $10^{-15}\,\mathrm{G}$ to be produced on Mpc scales or larger without spoiling the cosmological perturbations. Thus unless reheating and baryogenesis happen within a very narrow temperature window of $5\,\mathrm{MeV} \lesssim T_{\mathrm{reh}} \lesssim 10^2\,\mathrm{MeV}$, classical scenarios cannot produce the intergalactic magnetic fields suggested by gamma ray observations.

Quantum mechanical scenarios were found to be even more restricted; in cases where the quantum vector fluctuations smoothly convert into classical fluctuations, our result (4.15) shows that the produced magnetic fields cannot exceed $10^{-43}\,\mathrm{G}$ on Mpc or larger scales, independently of the inflation scale. Even with non-smooth quantum to classical transitions (such as in resonant production), as long as the condition (4.23) is satisfied, the constraints on quantum mechanically produced magnetic fields are at least as strong as the constraint for classical scenarios.

D.Green, T.Kobayashi 1511.08793

MF before EW phase transition

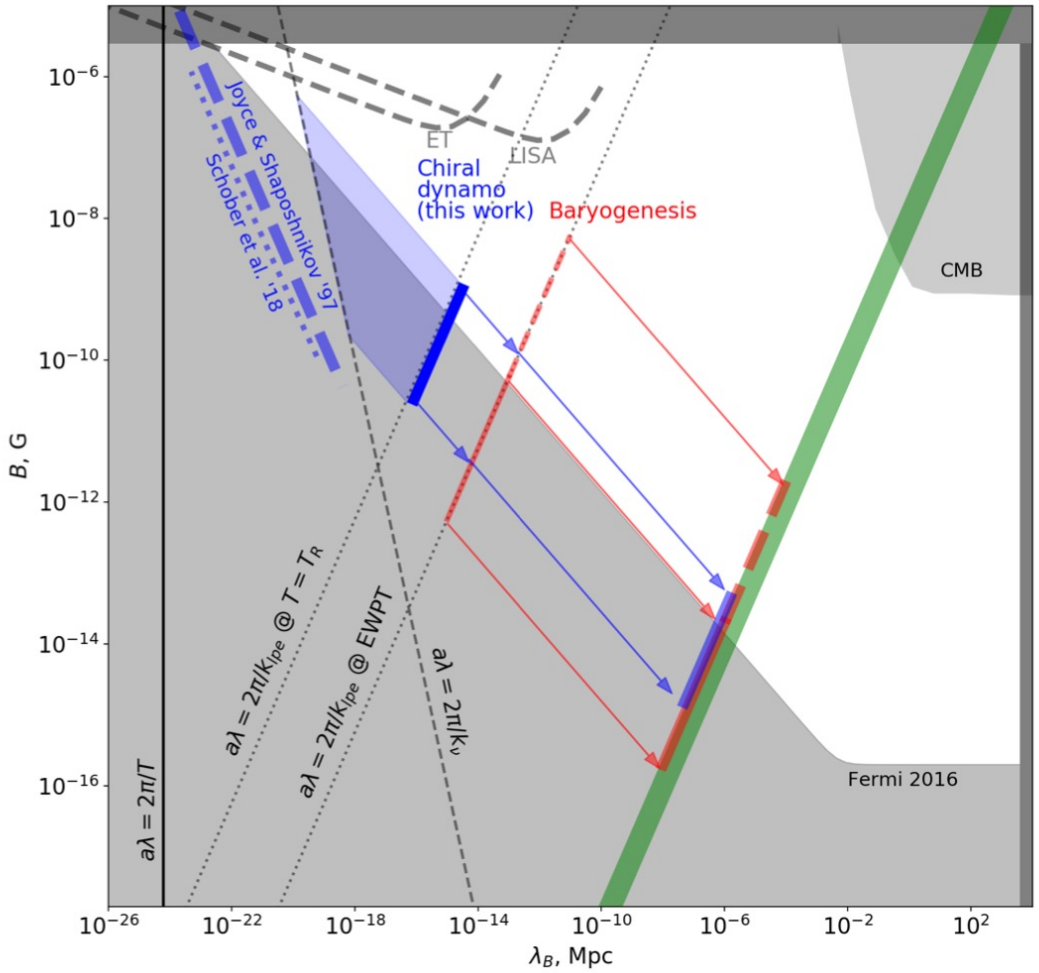

A. Neronov and D.S., 2010.13571

PMF from phase transitions

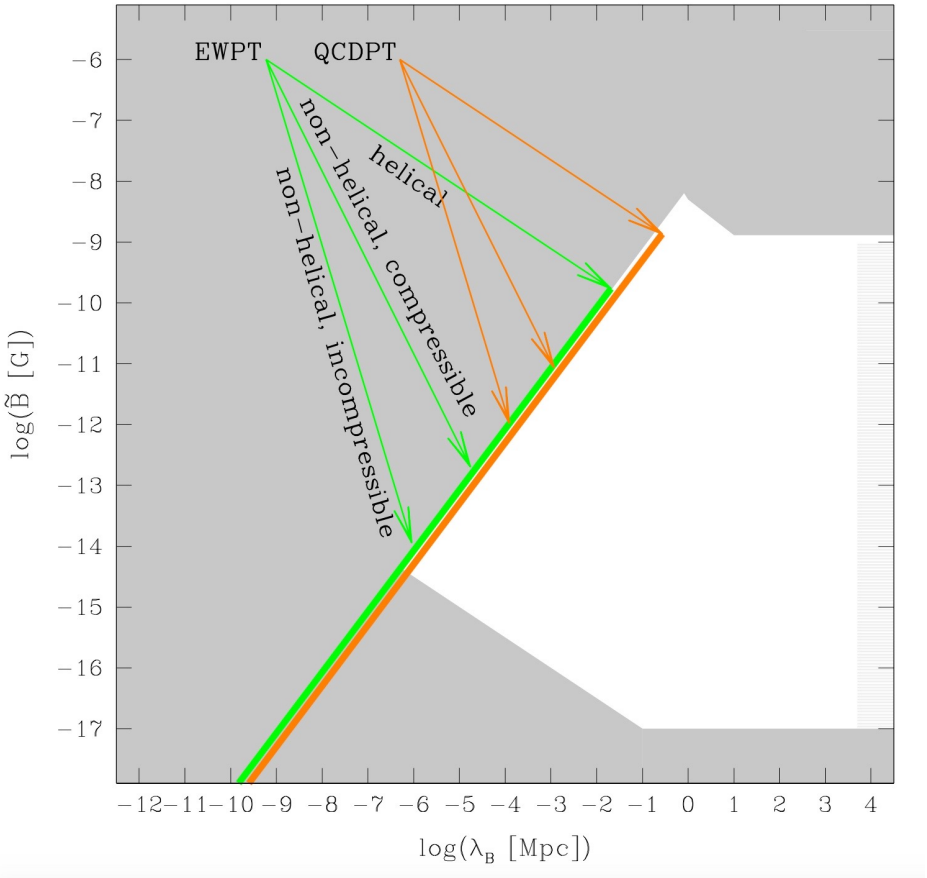

R.Durrer and A.Neronov, A&A Rev. 21 62, [1303.7121].

PMF limit from CMB

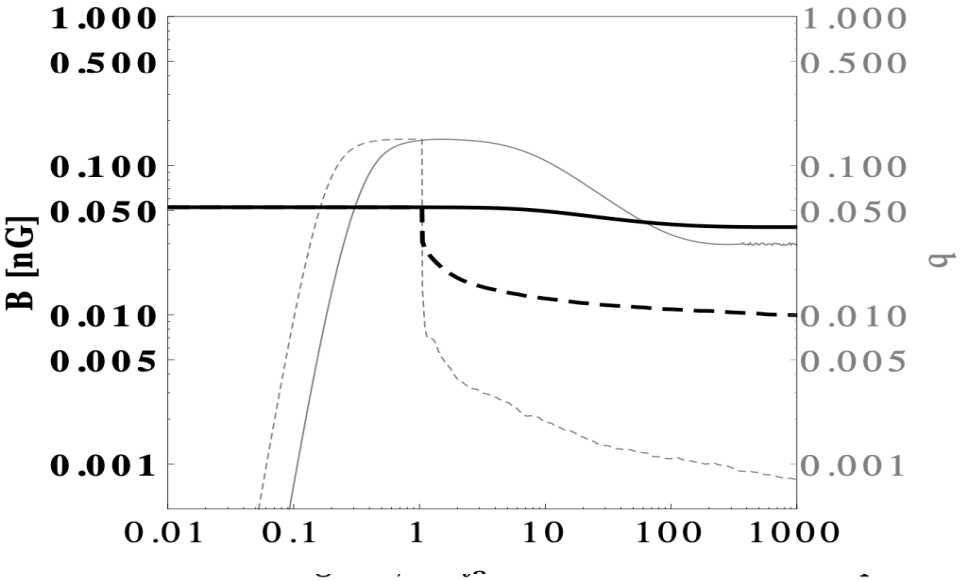

limit on PMFs from inhomogeneous recombination. Note that the PMF scenarios that are shown in Fig. 1 produce a maximum clumping of $b = 0.15$ and are therefore excluded somewhat beyond the 95% confidence level. The 95% confidence level excluded PMFs are given by

$$B < 47\,\mathrm{pG} \qquad \text{scale} - \text{invariant spectra } n = 0\,,$$
$$B < 8.9\,\mathrm{pG} \qquad \text{Batchelor spectrum } n = 5\,.$$

L.Jedamzik, A.Saveliev, PRL, [1804.06115].

PMF and CMB models

	Planck ΛCDM	Planck+H3 ΛCDM	Planck+H3 M1	Planck+H3 M2
$\Omega_b h^2$	0.02237 ± 0.00015	0.02263 ± 0.00014	$0.02270^{+0.00014}_{-0.00016}$	0.02280 ± 0.00016
$\Omega_c h^2$	0.1200 ± 0.0012	0.1172 ± 0.0011	0.1216 ± 0.0014	0.1191 ± 0.0012
τ	0.0546 ± 0.0075	$0.0629^{+0.0075}_{-0.0087}$	0.0555 ± 0.0073	$0.0607^{+0.0071}_{-0.0085}$
n_s	0.9651 ± 0.0041	0.9721 ± 0.0040	0.9628 ± 0.0040	0.9734 ± 0.0042
$b^{(a)}$	-	-	$0.61^{+0.16(0.35)(0.57)}_{-0.20(0.33)(0.42)}$	$0.30 \pm 0.11(0.22)(0.34)$
H_0	67.37 ± 0.54	68.70 ± 0.50	71.03 ± 0.74	69.81 ± 0.62
Ω_m	0.3151 ± 0.0074	0.2977 ± 0.0064	0.2873 ± 0.0064	0.2926 ± 0.0064
σ_8	0.8113 ± 0.0060	0.8080 ± 0.0064	0.8265 ± 0.0079	0.8192 ± 0.0075
S_8	0.831 ± 0.013	0.805 ± 0.012	0.809 ± 0.012	0.809 ± 0.012
z_*	1089.91 ± 0.26	1089.35 ± 0.24	$1107.9^{+4.2}_{-3.6}$	$1096.8^{+2.6}_{-2.0}$
r_*	144.44 ± 0.27	144.96 ± 0.25	142.22 ± 0.65	143.69 ± 0.48
$z_{\rm drag}$	1059.94 ± 0.30	1060.33 ± 0.29	$1076.9^{+3.8}_{-3.4}$	$1067.4^{+2.4}_{-2.0}$
$r_{\rm drag}$	147.10 ± 0.27	147.55 ± 0.25	144.89 ± 0.64	146.28 ± 0.49
$r_{\rm drag}h$	99.11 ± 0.93	101.36 ± 0.87	102.91 ± 0.92	102.11 ± 0.89
$\chi^2_{\rm lensing}$	9.23 ± 0.70 (8.73)	9.6 ± 1.2 (8.74)	9.20 ± 0.66 (8.91)	9.33 ± 0.80 (9.39)
$\chi^2_{\rm plik}$	2359.5 ± 6.2 (2347.6)	2364.0 ± 6.6 (2350.93)	2366.2 ± 6.7 (2355.6)	2367.4 ± 7.1 (2359.2)
$\chi^2_{\rm lowl}$	23.40 ± 0.86 (23.18)	22.36 ± 0.72 (22.76)	24.30 ± 0.97 (24.0)	22.37 ± 0.72 (21.9)
$\chi^2_{\rm simall}$	397.0 ± 1.8 (396.0)	399.0 ± 3.3 (397.2)	397.0 ± 1.7 (395.6)	398.2 ± 2.7 (396.3)
$\chi^2_{\rm prior}$	11.6 ± 4.6 (4.46)	11.6 ± 4.6 (4.38)	11.6 ± 4.5 (4.21)	11.9 ± 4.6 (3.42)
$\chi^2_{\rm CMB}$	2789.1 ± 6.4 (2775.5)	2794.9 ± 7.2 (2779.7)	2796.8 ± 6.9 (2784.2)	2797.3 ± 7.3 (2786.8)
$\chi^2_{\rm H3}$	-	22 ± 4 (24.92)	6.1 ± 3.4 (5.74)	12.9 ± 4.2 (9.62)
$\chi^{2(\rm tot)}_{\rm bestfit}$	2779.9	2809.0	2794.1	2799.9

L.Jedamzik, A.Pogosyan, PRL, [2004.09487] H3=3 local H0 measurements.

PMF and CMB models

	Global ΛCDM	Global M1	Global M2
$\Omega_b h^2$	0.02266 ± 0.00013	0.02266 ± 0.00014	0.02278 ± 0.00015
$\Omega_c h^2$	0.11680 ± 0.00079	0.1210 ± 0.0015	0.1187 ± 0.0010
τ	$0.0622^{+0.0070}_{-0.0083}$	0.0541 ± 0.0074	$0.0587^{+0.0069}_{-0.0077}$
n_s	0.9725 ± 0.0036	0.9624 ± 0.0038	0.9725 ± 0.0037
$b^{(a)}$	-	$0.48^{+0.16}_{-0.18}$	$0.246^{+0.097}_{-0.11}$
H_0	68.86 ± 0.37	70.57 ± 0.61	69.69 ± 0.47
Ω_m	0.2955 ± 0.0046	0.2898 ± 0.0046	0.2927 ± 0.0045
σ_8	0.8056 ± 0.0061	0.8208 ± 0.0078	0.8148 ± 0.0070
S_8	0.7995 ± 0.0088	0.8067 ± 0.0094	0.8048 ± 0.0090
z_*	1089.28 ± 0.19	$1105.0^{+4.6}_{-3.8}$	$1095.8^{+2.5}_{-2.1}$
r_*	145.04 ± 0.20	$142.65^{+0.65}_{-0.76}$	143.89 ± 0.46
$z_{\rm drag}$	1060.37 ± 0.29	$1074.3^{+4.1}_{-3.5}$	$1066.5^{+2.3}_{-2.0}$
$r_{\rm drag}$	147.62 ± 0.21	$145.31^{+0.65}_{-0.75}$	146.48 ± 0.47
$r_{\rm drag} h$	101.66 ± 0.62	102.54 ± 0.66	102.08 ± 0.63
$\chi^2_{\rm lensing}$	$9.9 \pm 1.3(9.1)$	$9.17 \pm 0.67(8.6)$	$9.48 \pm 0.94(8.7)$
$\chi^2_{\rm plik}$	$2365.4 \pm 6.4(2354.8)$	$2364.6 \pm 6.2(2353.5)$	$2366.8 \pm 6.5(2352.9)$
$\chi^2_{\rm lowl}$	$22.27 \pm 0.66(22.6)$	$24.26 \pm 0.96(25.1)$	$22.43 \pm 0.69(22.5)$
$\chi^2_{\rm simall}$	$398.6 \pm 2.9(398.3)$	$396.8 \pm 1.6(395.7)$	$397.6 \pm 2.2(399.2)$
$\chi^2_{\rm H3}$	$20.0 \pm 3.1(23.1)$	$8.3 \pm 3.3(6.92)$	$13.6 \pm 3.3(13.5)$
$\chi^2_{\rm SN}$	$1034.80 \pm 0.09(1034.73)$	$1034.96 \pm 0.19(1034.92)$	$1034.86 \pm 0.14(1034.8)$
$\chi^2_{\rm 6DF}$	$0.073 \pm 0.067(0.013)$	$0.20 \pm 0.12(0.18)$	$0.123 \pm 0.089(0.09)$
$\chi^2_{\rm MGS}$	$2.51 \pm 0.43(2.11)$	$3.14 \pm 0.48(3.18)$	$2.81 \pm 0.45(2.76)$
$\chi^2_{\rm DR14LYA}$	$4.00 \pm 0.21(4.15)$	$3.81 \pm 0.21(3.79)$	$3.90 \pm 0.21(3.93)$
$\chi^2_{\rm DR12BAO}$	$3.99 \pm 0.71(3.42)$	$5.4 \pm 1.5(5.16)$	$4.5 \pm 1.0(4.11)$
$\chi^2_{\rm DES}$	$516.4 \pm 4.4(512.1)$	$516.8 \pm 4.6(512.9)$	$517.1 \pm 4.6(511.1)$
$\chi^2_{\rm prior}$	$24 \pm 7(10.1)$	$24 \pm 7(13.4)$	$24 \pm 7(12.0)$
$\chi^2_{\rm CMB}$	$2796.2 \pm 6.9(2784.9)$	$2794.9 \pm 6.4(2782.89)$	$2796.3 \pm 6.6(2783.2)$
$\chi^2_{\rm BAO}$	$10.58 \pm 0.98(9.7)$	$12.6 \pm 1.9(12.3)$	$11.3 \pm 1.4(10.9)$
$\chi^{2({\rm tot})}_{\rm bestfit}$	4374.6	4363.3	4365.6

TABLE II. Same as in Table I but for the global fit to a combination of Planck, BAO, SN, DES and H3.

L.Jedamzik, A.Pogosyan, PRL, [2004.09487].

PMF and CMB models

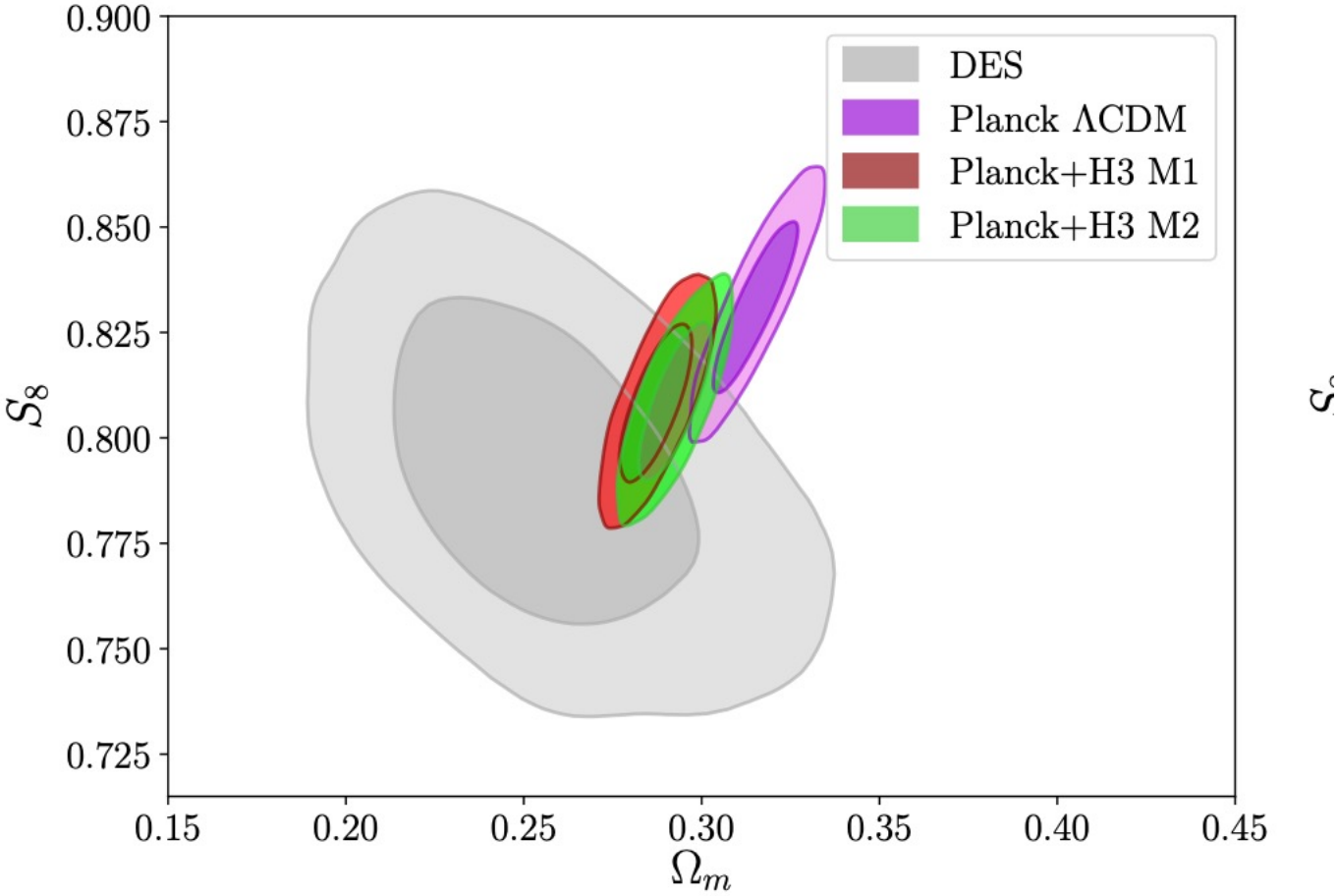

L.Jedamzik, A.Pogosyan, PRL, [2004.09487].

PMF and CMB models

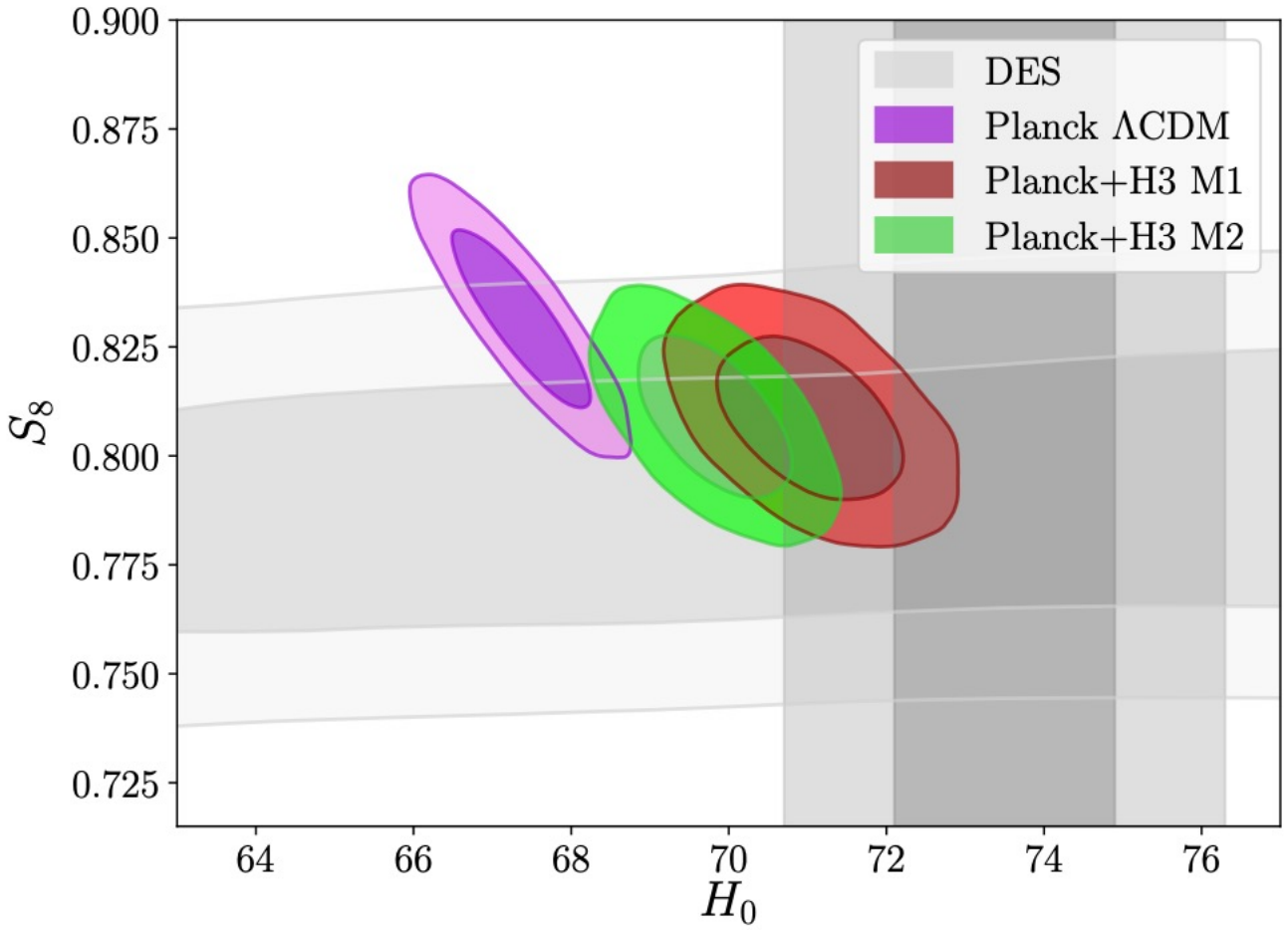

L.Jedamzik, A.Pogosyan, PRL, [2004.09487].

Production of GW with MF in EW phase transition

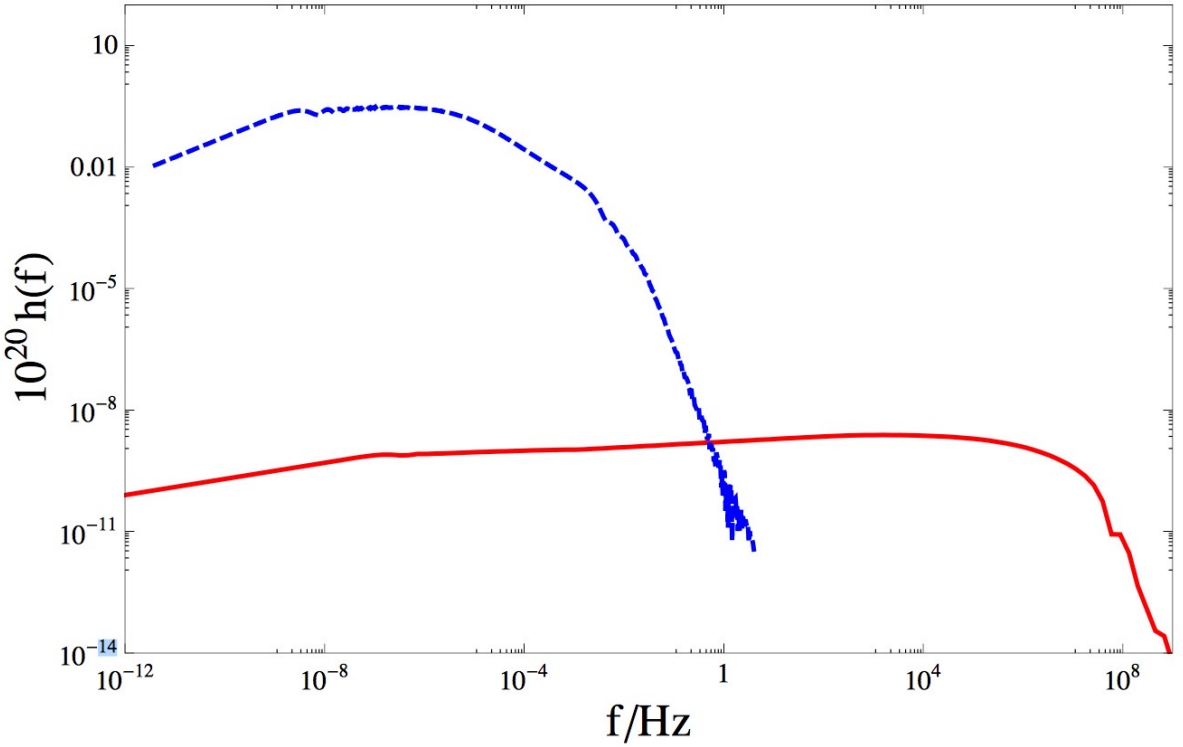

C. Caprini et al., JCAP 0911 (2009) 001

Nanograv measurement

NANOGrav measurement

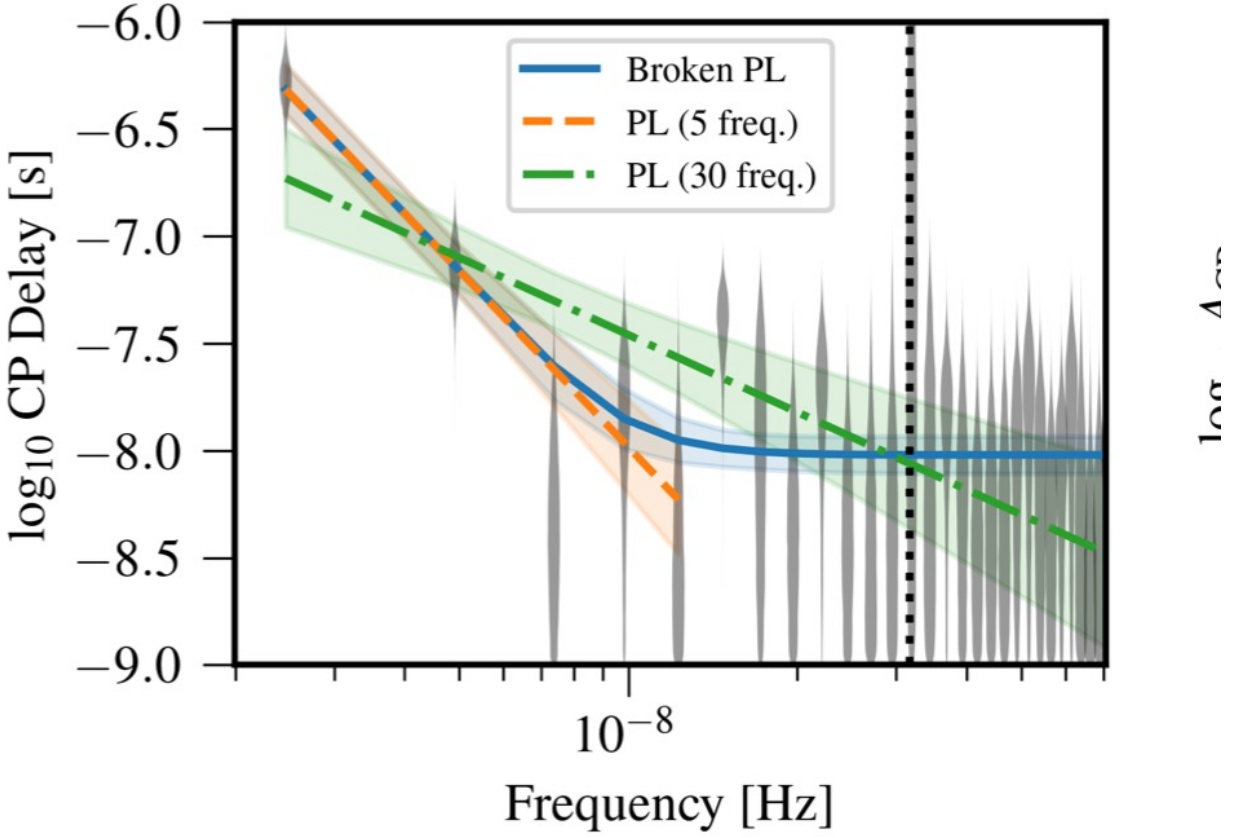

Z. Arzoumanian et al., 2009.04496

NANOGrav measurement

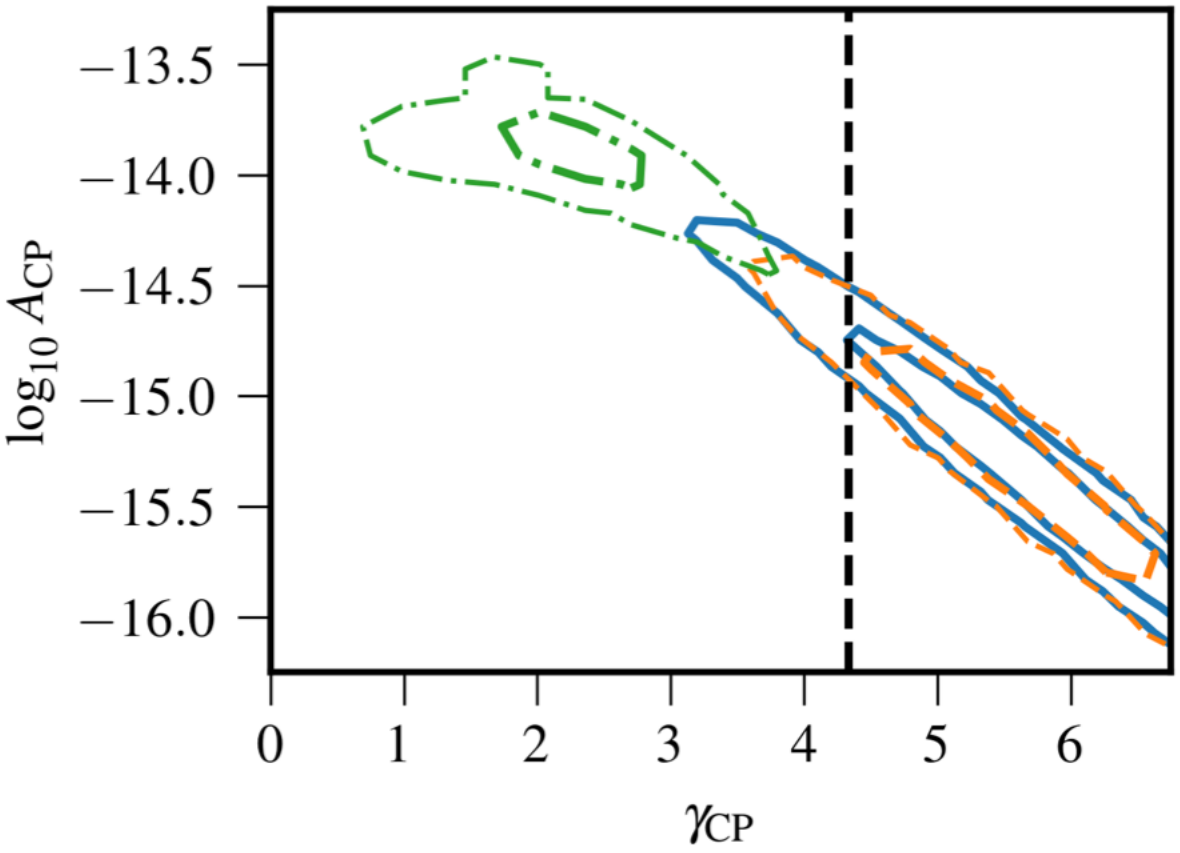

Z. Arzoumanian et al., 2009.04496

NANOGrav measurement

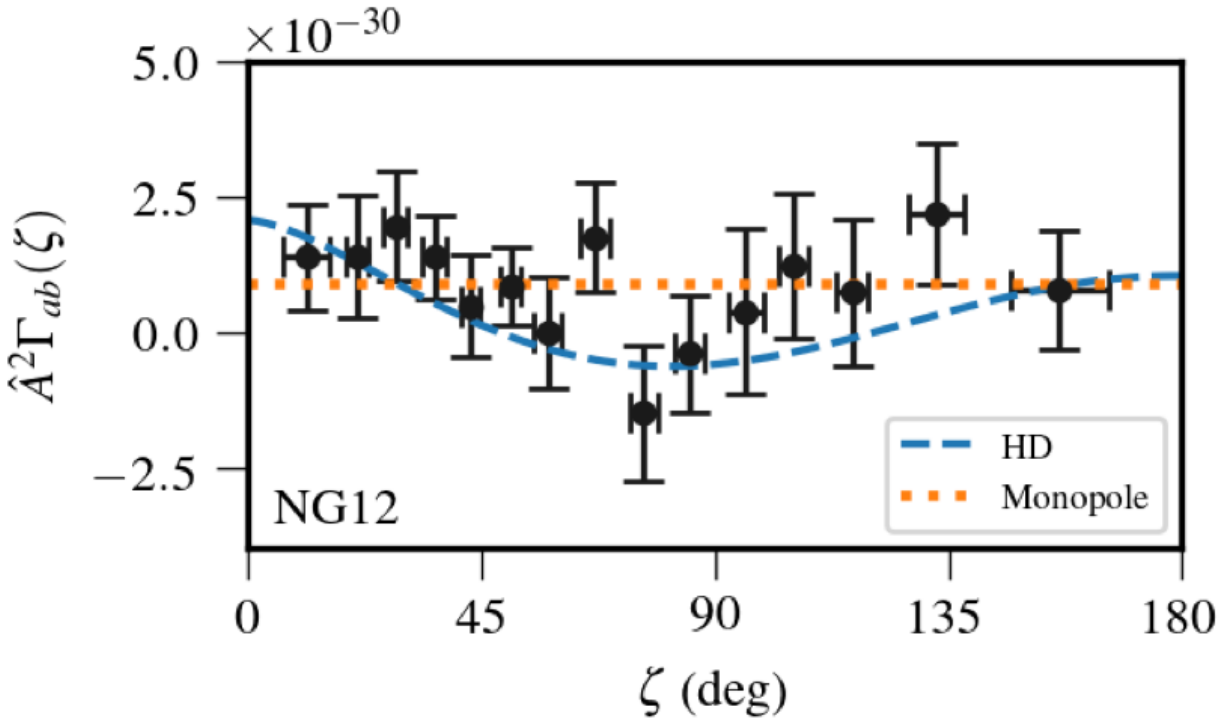

Z. Arzoumanian et al., 2009.04496

GW from QCD phase transition

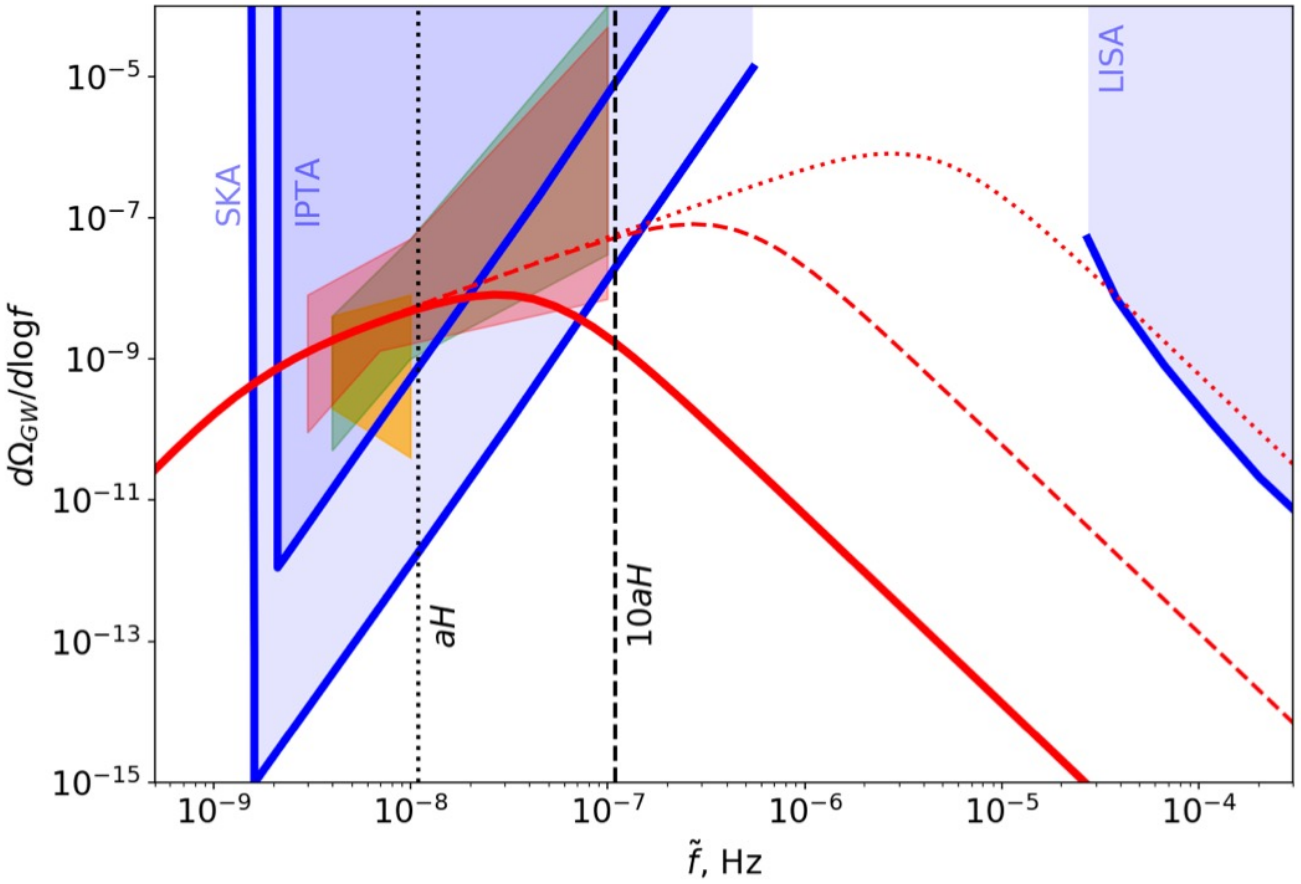

A. Neronov et al., 2009.14174

IGMF from QCD phase transition

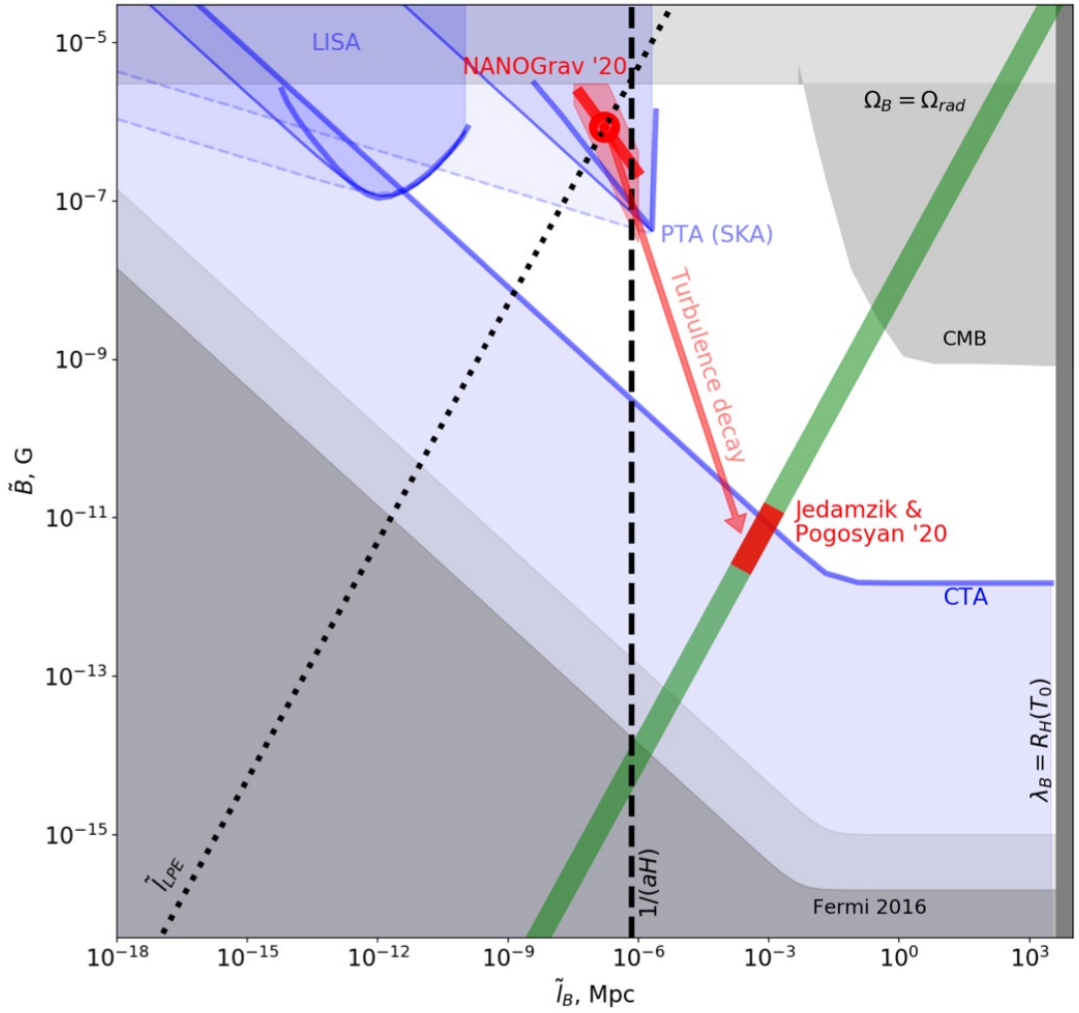

A. Neronov et al., 2009.14174

Multi-messenger observation of binary neutron star collision

First multi-messenger observation: SN1987A

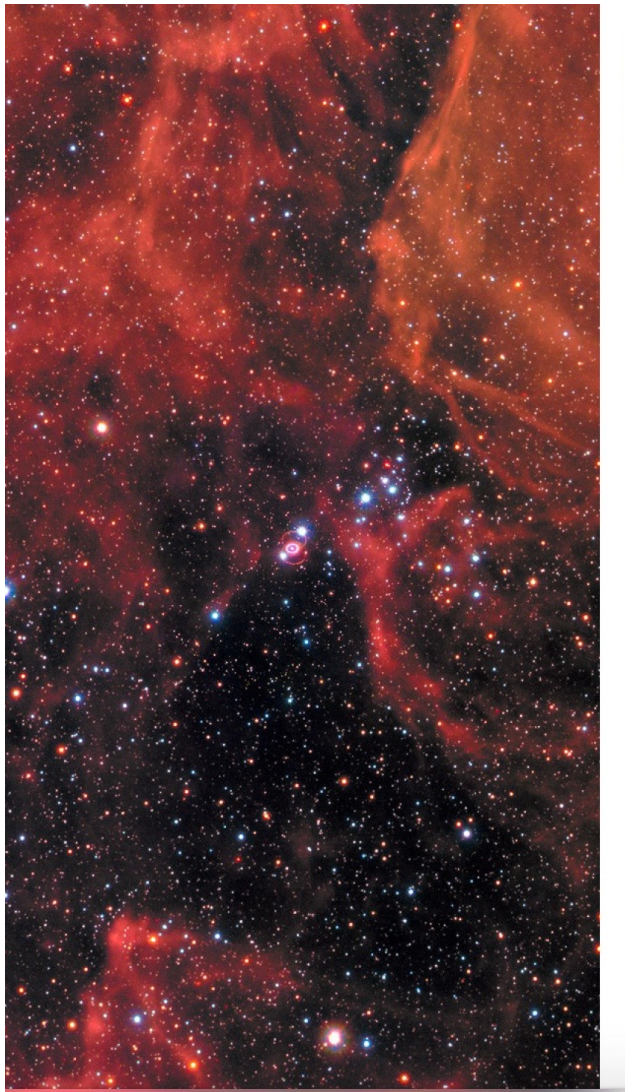

Annu. Rev. Astron. Astrophys. 1989. 27:629–700

SUPERNOVA 1987A

W. David Arnett

Departments of Physics and Astronomy, University of Arizona, Tucson, Arizona 85721

John N. Bahcall

Institute for Advanced Study, Princeton, New Jersey 08540, and Space Telescope Science Institute, Baltimore, Maryland 21208

Robert P. Kirshner

Harvard-Smithsonian Center for Astrophysics, MS-19, 60 Garden Street, Cambridge, Massachusetts 02138

Stanford E. Woosley

Board of Studies in Astronomy and Astrophysics, University of California, Santa Cruz, California 95064, and General Studies Group, Lawrence Livermore National Laboratory, Livermore, California 94550

1. INTRODUCTION

On February 23.316 UT, 1987, light and neutrinos from the brightest supernova in 383 years arrived at Earth, shocking astrophysicists into a frenzied state of activity. Since that time Supernova 1987A (SN 1987A) has taken its place [illegible] astronomy, but also as one of the most thoroughly studied objects outside the solar system. Detected by instruments on the ground, below the ground, in space, and from [illegible] from all continents, including Antarctica. Studied at all wavelengths from radio through gamma rays, SN 1987A is the only object besides the Sun to have been detected in neutrinos. From these extensive observations has emerged

"Multimessenger"

Neutrinos and photons

1300 papers on SN1987A

Binary neutron stars

Network for multi-messenger observations with GW

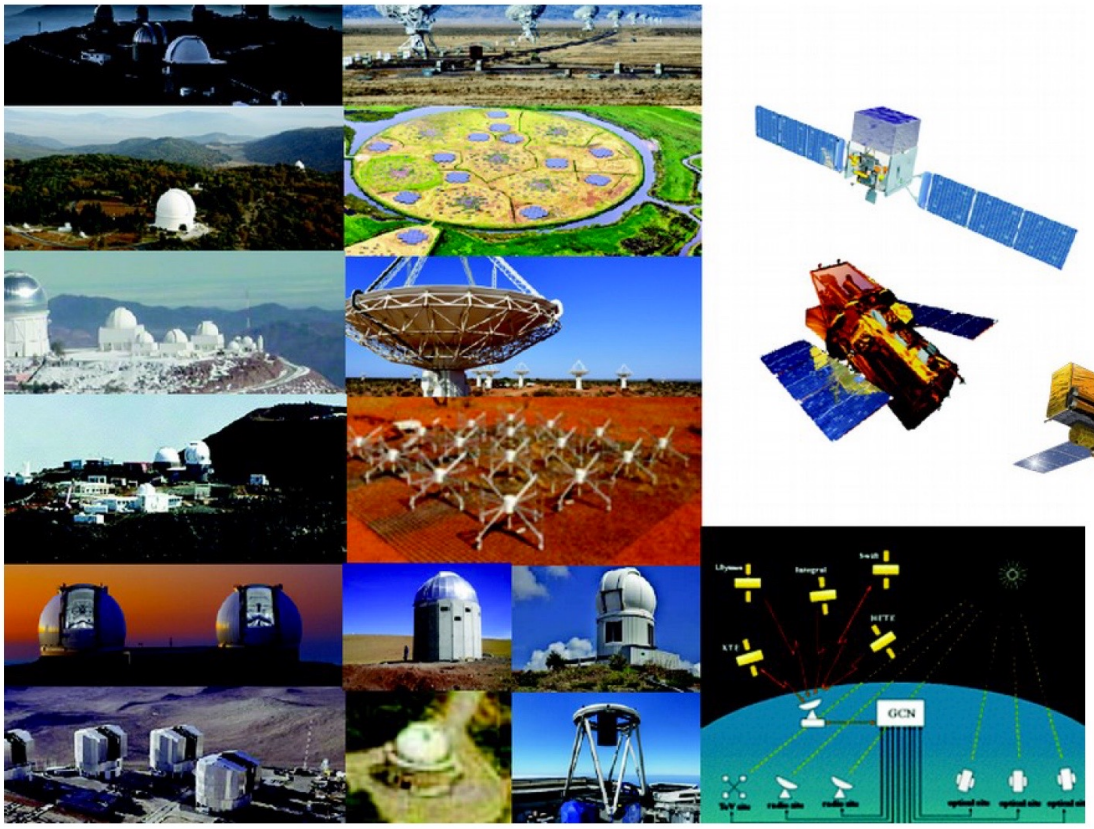

2009 – Prototype demonstration of online analysis and alert testing
2013 – Initiate global discussion about GW-EM follow-up program
2017 – Memoranda of Understanding signed with **90+ groups around the globe**

Observation of binary neutron star merger

The Astrophysical Journal Letters, 848:L12 (59pp), 2017 October 20 https://doi.org/10.3847/2041-8213/aa91c9

OPEN ACCESS

Multi-messenger Observations of a Binary Neutron Star Merger

LIGO Scientific Collaboration and Virgo Collaboration, Fermi GBM, INTEGRAL, IceCube Collaboration, AstroSat Cadmium Zinc Telluride Imager Team, IPN Collaboration, The Insight-Hxmt Collaboration, ANTARES Collaboration, The Swift Collaboration, AGILE Team, The 1M2H Team, The Dark Energy Camera GW-EM Collaboration and the DES Collaboration, The DLT40 Collaboration, GRAWITA: GRAvitational Wave Inaf TeAm, The Fermi Large Area Telescope Collaboration, ATCA: Australia Telescope Compact Array, ASKAP: Australian SKA Pathfinder, Las Cumbres Observatory Group, OzGrav, DWF (Deeper, Wider, Faster Program), AST3, and CAASTRO Collaborations, The VINROUGE Collaboration, MASTER Collaboration, J-GEM, GROWTH, JAGWAR, Caltech-NRAO, TTU-NRAO, and NuSTAR Collaborations, Pan-STARRS, The MAXI Team, TZAC Consortium, KU Collaboration, Nordic Optical Telescope, ePESSTO, GROND, Texas Tech University, SALT Group, TOROS: Transient Robotic Observatory of the South Collaboration, The BOOTES Collaboration, MWA: Murchison Widefield Array, The CALET Collaboration, IKI-GW Follow-up Collaboration, H.E.S.S. Collaboration, LOFAR Collaboration, LWA: Long Wavelength Array, HAWC Collaboration, The Pierre Auger Collaboration, ALMA Collaboration, Euro VLBI Team, Pi of the Sky Collaboration, The Chandra Team at McGill University, DFN: Desert Fireball Network, ATLAS, High Time Resolution Universe Survey, RIMAS and RATIR, and SKA South Africa/MeerKAT
(See the end matter for the full list of authors.)

Received 2017 October 3; revised 2017 October 6; accepted 2017 October 6; published 2017 October 16

Abstract

On 2017 August 17 a binary neutron star coalescence candidate (later designated GW170817) with merger time 12:41:04 UTC was observed through gravitational waves by the Advanced LIGO and Advanced Virgo detectors. The *Fermi* Gamma-ray Burst Monitor independently detected a gamma-ray burst (GRB 170817A) with a time delay of $\sim$1.7 s with respect to the merger time. From the gravitational-wave signal, the source was initially localized to a sky region of 31 deg^2 at a luminosity distance of 40^{+8}_{-8} Mpc and with component masses consistent with neutron stars. The component masses were later measured to be in the range 0.86 to 2.26 $M_{\odot}$. An extensive observing campaign was launched across the electromagnetic spectrum leading to the discovery of a bright optical transient (SSS17a, now with the IAU identification of AT 2017gfo) in NGC 4993 (at $\sim$40 Mpc) less than 11 hours after the merger by the One-Meter, Two Hemisphere (1M2H) team using the 1 m Swope Telescope. The optical transient was independently detected by multiple teams within an hour. Subsequent observations targeted the object and its environment. Early ultraviolet observations revealed a blue transient that faded within 48 hours. Optical and infrared observations showed a redward evolution over $\sim$10 days. Following early non-detections, X-ray and radio emission were discovered at the transient's position $\sim$9 and $\sim$16 days, respectively, after the merger. Both the X-ray and radio emission likely arise from a physical process that is distinct from the one that generates the UV/optical/near-infrared emission. No ultra-high-energy gamma-rays and no neutrino candidates consistent with the source were found in follow-up searches. These observations support the hypothesis that GW170817 was produced by the merger of two neutron stars in NGC 4993 followed by a short gamma-ray burst (GRB 170817A) and a kilonova/macronova powered by the radioactive decay of *r*-process nuclei synthesized in the ejecta.

Key words: gravitational waves – stars: neutron

1. Introduction

Over 80 years ago Baade & Zwicky (1934) proposed the idea of neutron stars, and soon after, Oppenheimer & Volkoff (1939) carried out the first calculations of neutron star models. Neutron stars entered the realm of observational astronomy in the 1960s by providing a physical interpretation of X-ray emission from Heuvel 1975; Massevitch et al. 1976; Clark 1979; Clark et al. 1979; Dewey & Cordes 1987; Lipunov et al. 1987; for reviews see Kalogera et al. 2007; Postnov & Yungelson 2014). The Hulse-Taylor pulsar provided the first firm evidence (Taylor & Weisberg 1982) of the existence of gravitational waves (Einstein 1916, 1918) and sparked a renaissance of observational tests of general relativity (Damour & Taylor 1991, 1992;

56 teams and collaborations

3600 co-authors, 900 institutes

What is the sequence of observations?

First hints of interpretation

« The big picture »

- A guide to the jungle of 80+ articles
- An exhaustive record for the 192 ! GCN Notices exchanged about GW170817

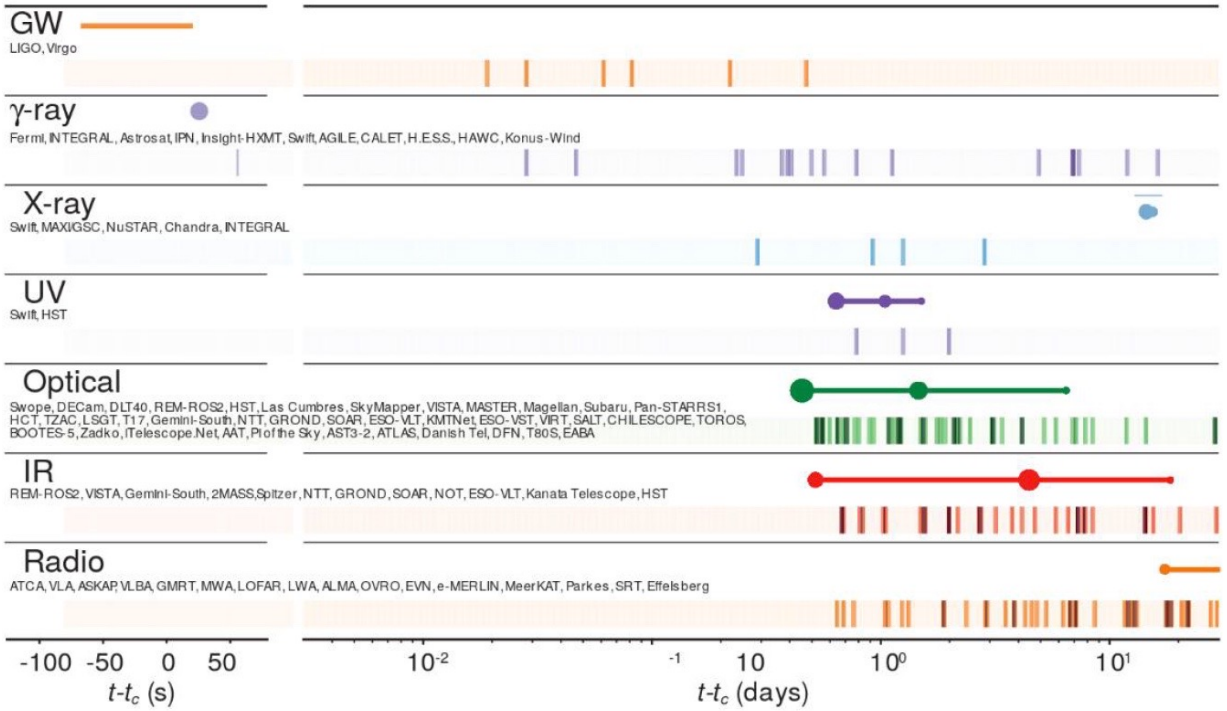

Main discoveries

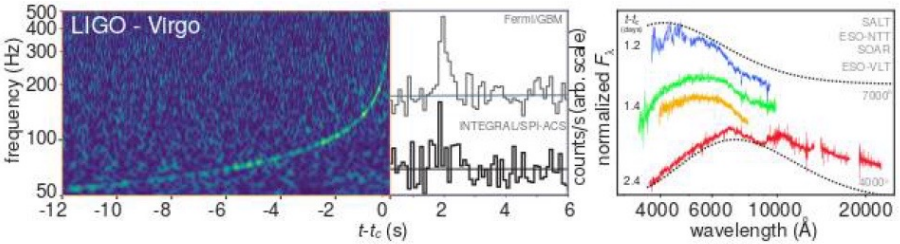

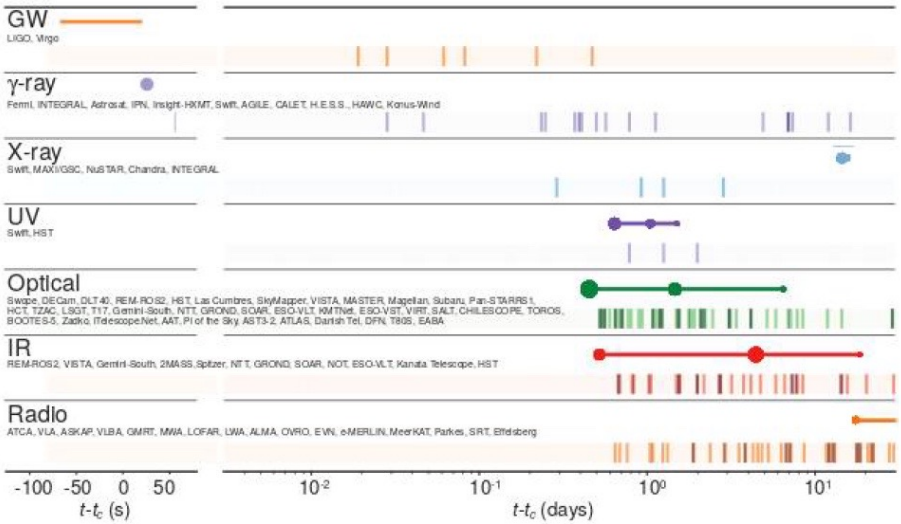

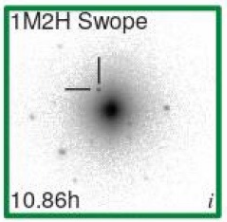

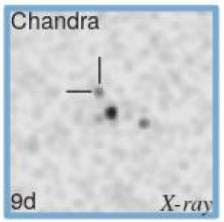

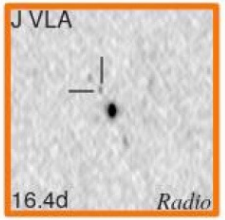

Main discoveries (1)

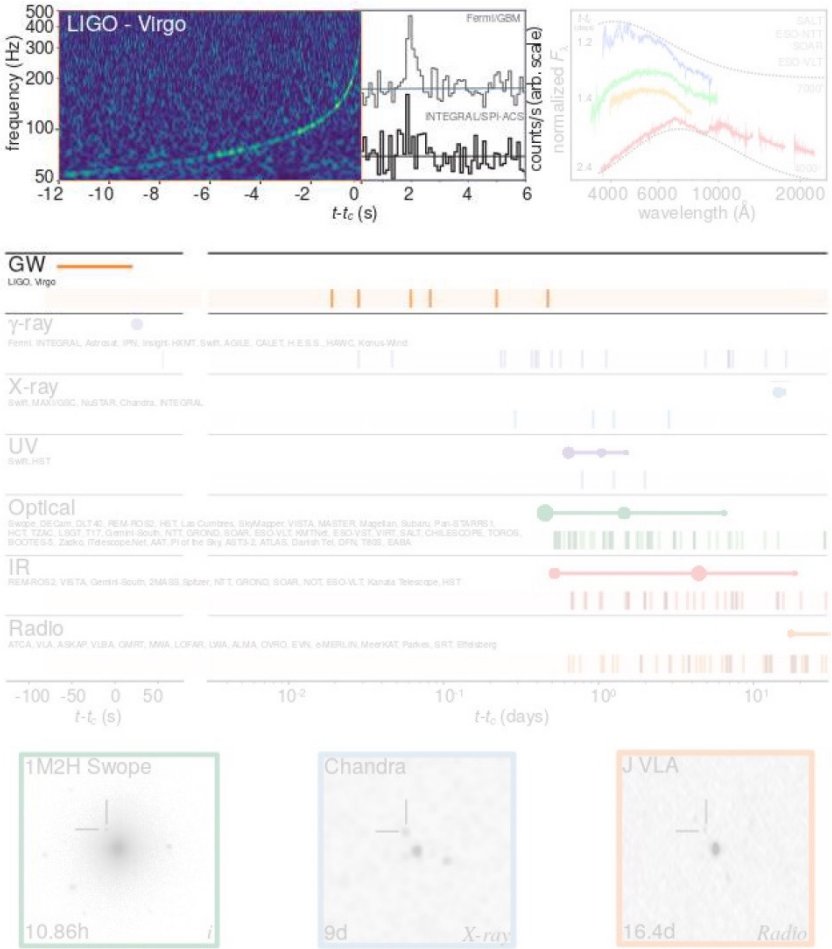

Short gamma-ray burst – GRB170817A

"Fireball model"

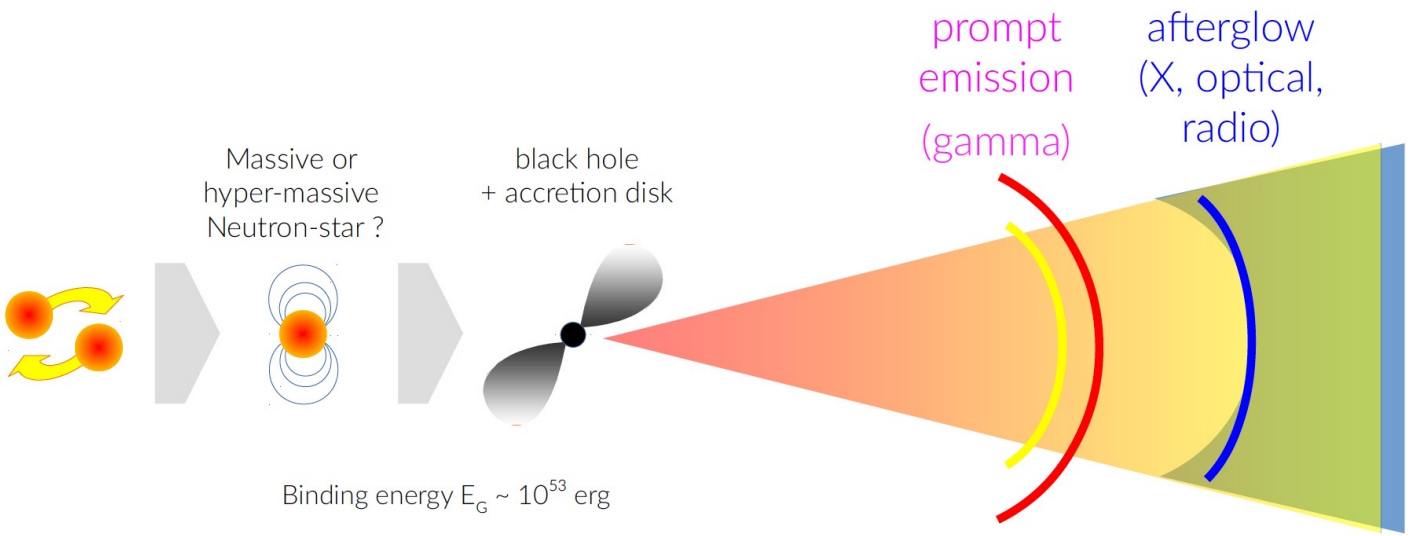

- E_{iso} ~ 5 x 10^{46} erg, 10,000 x less than usual
  - This is **not a standard "on-axis"** short GRB – Off-axis ?
- 1.7 s after the merger
  - Favors hyper massive neutron star (life time ~ seconds)

H.E.S.S. Observatory

- Array of four 12m telescopes + one 28m telescope
- Low energy threshold ~30 GeV
- HESS II FoV 3.5 deg
- 28m telescope design allows fast slewing

HESS phase I	HESS phase II
4 x 12m telescopes	4 x 12m + 1 x 28 m telescopes
FoV: 5°	FoV: 5° / 3.5°
Energy threshold ~100 GeV	Energy threshold ~30 GeV
Angular resolution < 0.1°	Angular resolution < 0.1- 0.4°

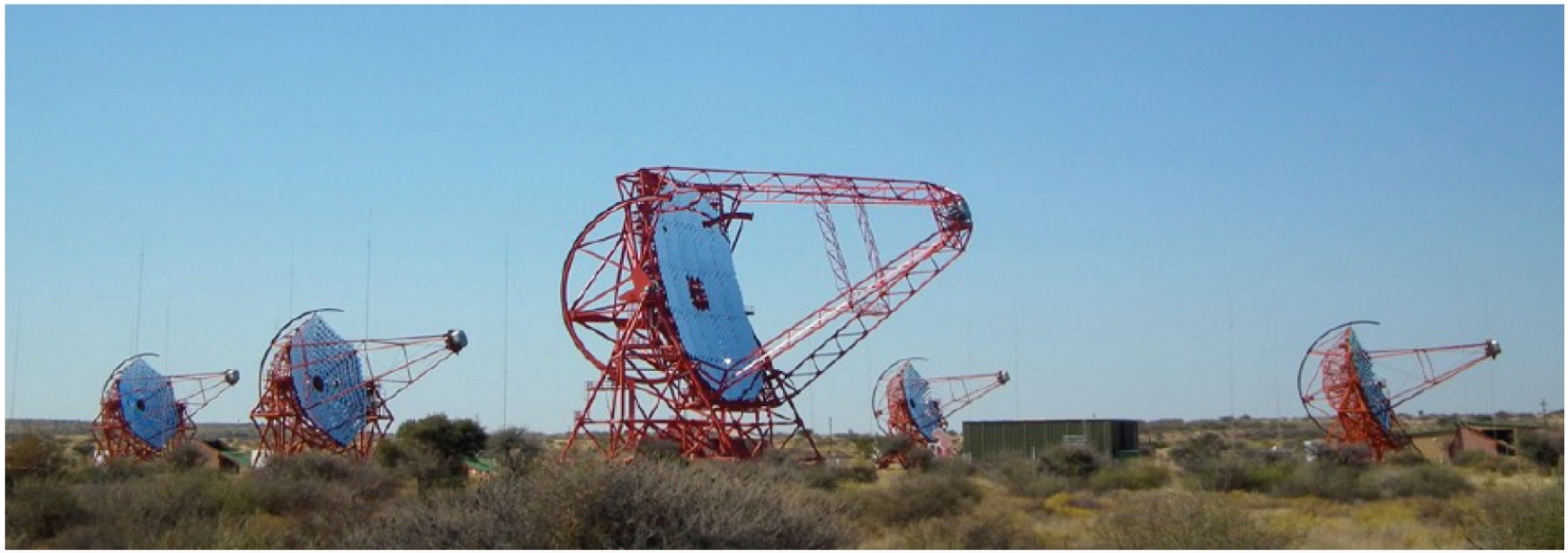

H.E.S.S. first observations of GW170817

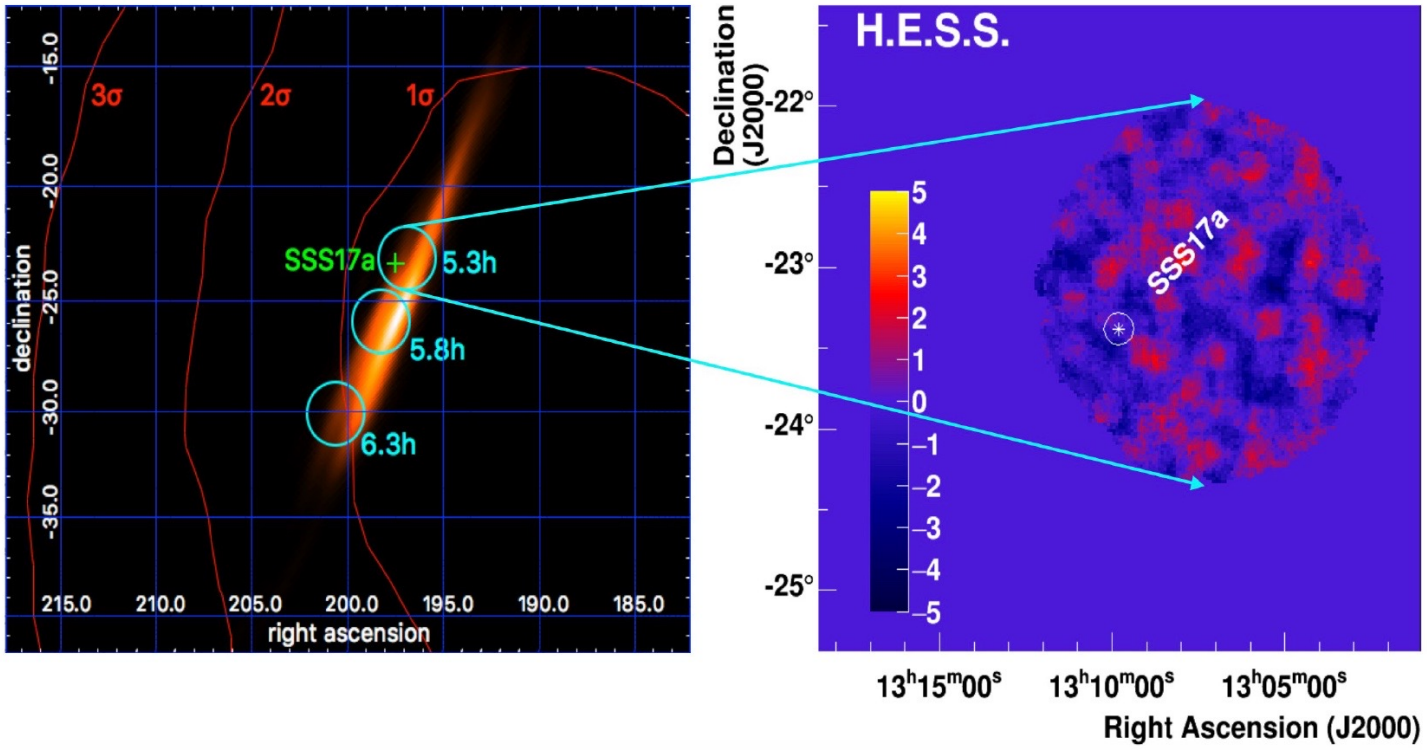

H.E.S.S. observations of GW170817

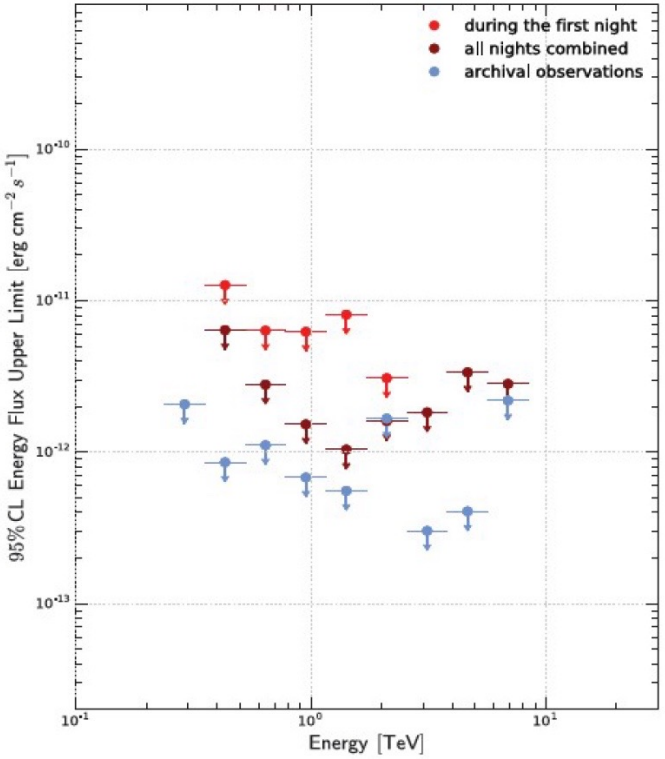

(a) SSS17a: H.E.S.S. limits

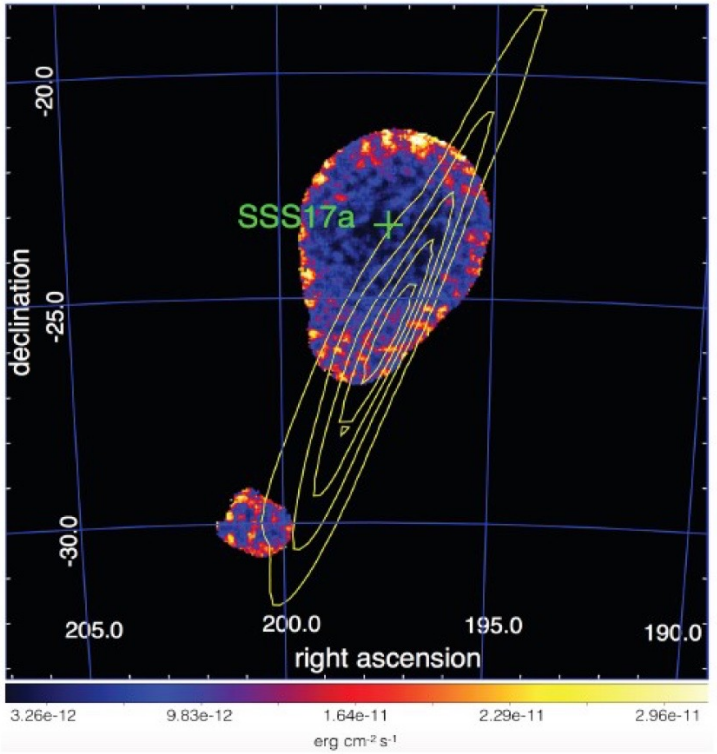

(b) GW170817: H.E.S.S. flux limit map

Gamma-ray follow-up observations of GW170817

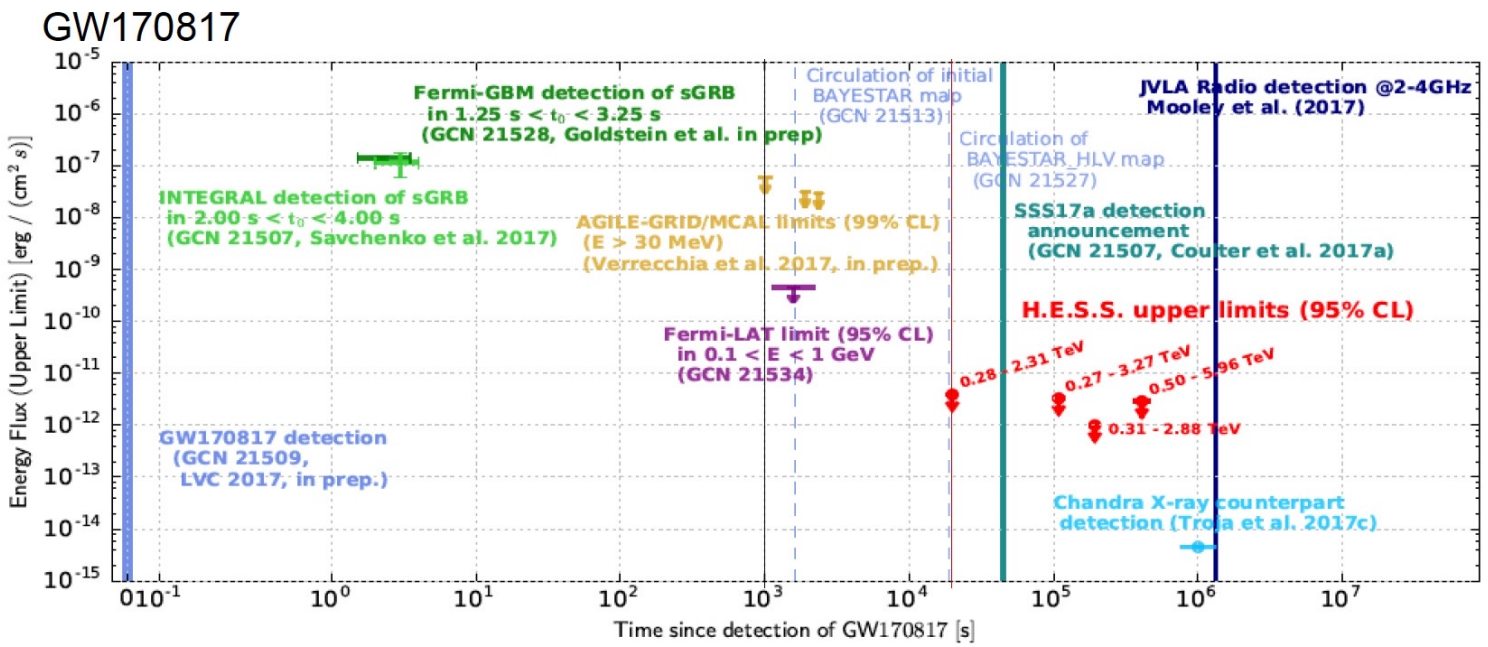

- 27 min after GW170817 : First GW map : uncertainty covering 24,200 deg^2 at 90% containment : not suitable for scheduling follow-up observations with H.E.S.S.

- 5h later (LIGO+VIRGO map) : uncertainty covering 31 deg^2 at 90% containment
  → HESS follow-up observations first night : only 35 min to derive pointing strategy before visibility window.
  3 observations of 28 min each (with CT5)
  → Shortest time delay by any ground based pointing instrument participating in the follow-up of GW170817

Main discoveries (2)

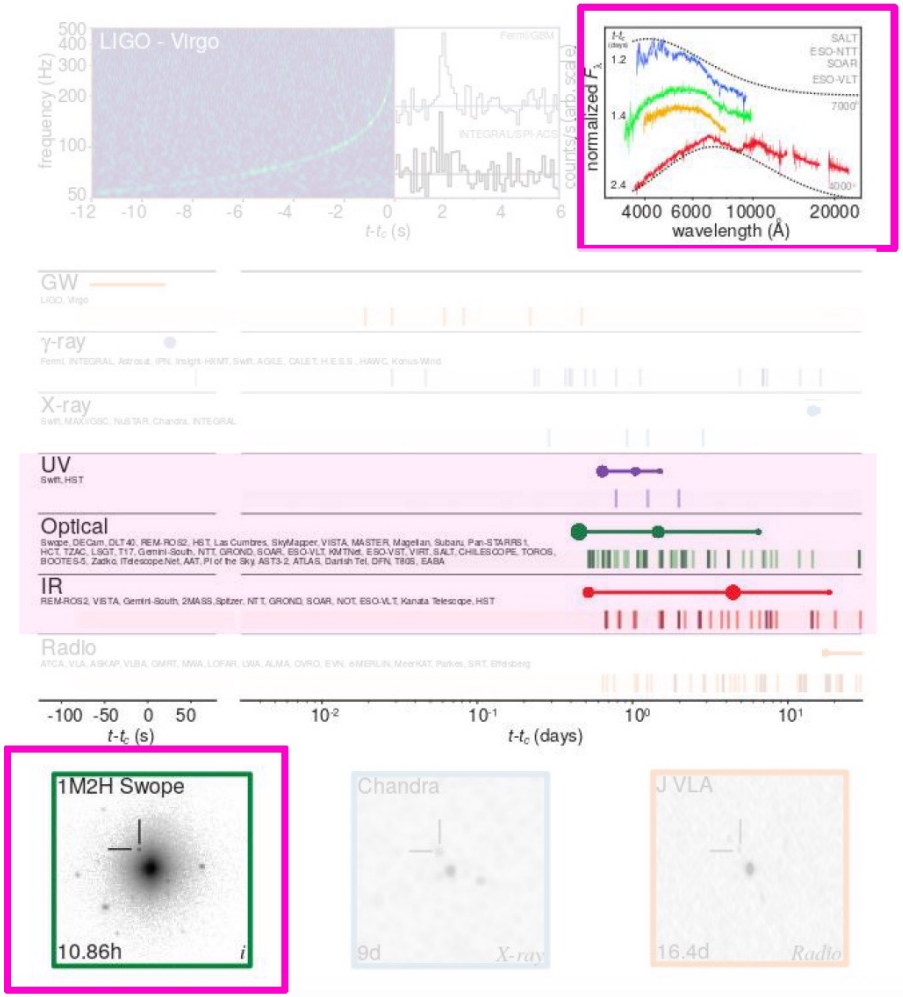

The race to 1st optical detection

t_c + 40 min: 1st LV announcement
candidate BNS associated with GRB

t_c + 1h05 : Fermi report
preliminary localization = 1100 deg^2

t_c + 1h30 min: LV update
H1-only loc. and distance = 37 ± 12 Mpc

t_c + 5h : LIGO Virgo loc. = 30 deg^2
distance = 40 ± 8 Mpc
Too late for Australia and South Africa

t_c + 11h : Swope detects SSS17a and its host galaxy NGC4993
9th field taken at 20:33 LT, Las Campanas Obs
180 galaxies at ~40 Mpc in the error box

+ 5 more independent detections in the following hour

t_c + 13h: Swope announcement
GCN Circular #21529

t_c + 17h: 1st report on spectroscopic obs.
(GCN Circular #21547)

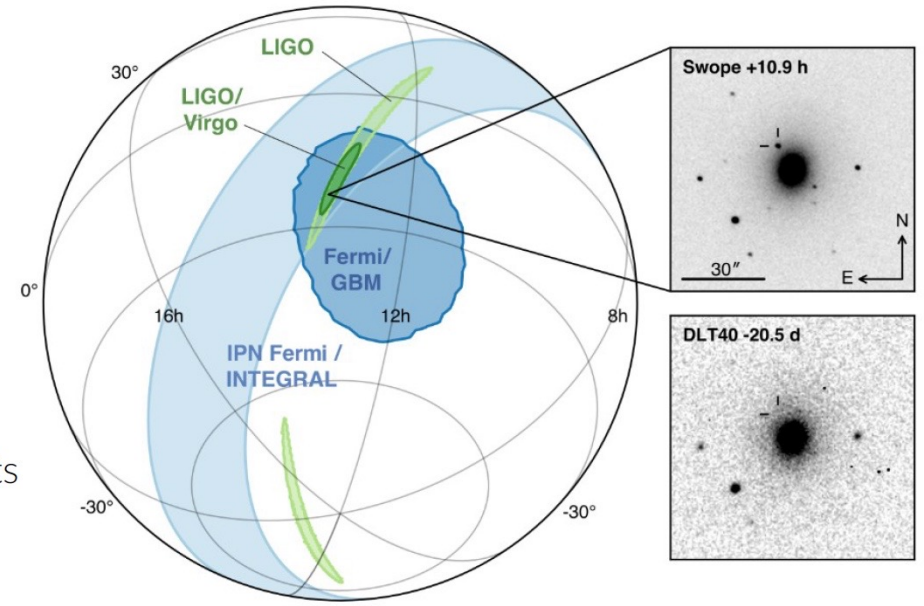

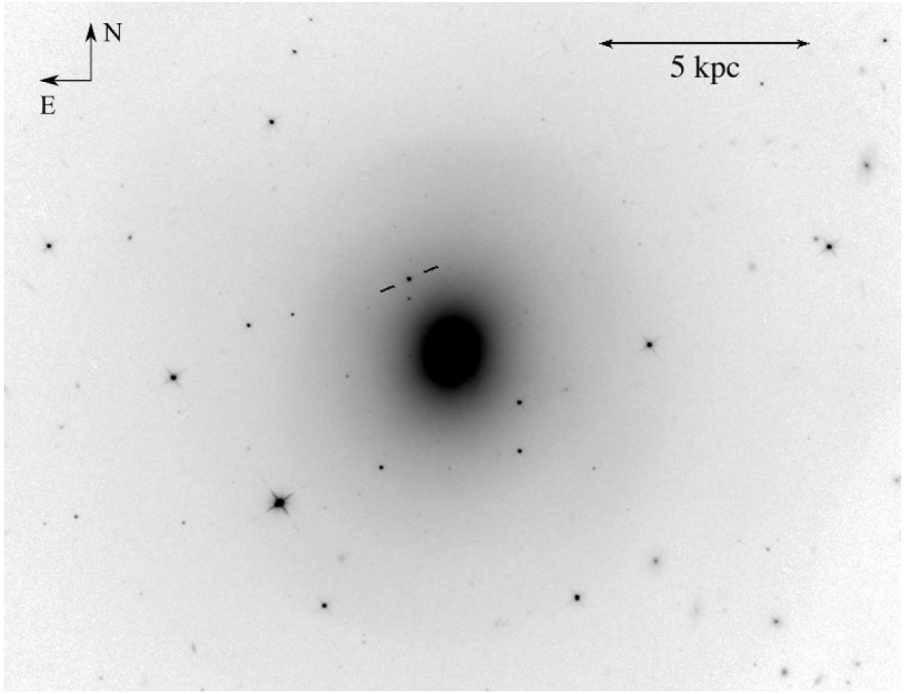

HST/WFC3-IR F110W t_c+4.79d Tanvir et al, ApJL 848:L27 2017

Photometry

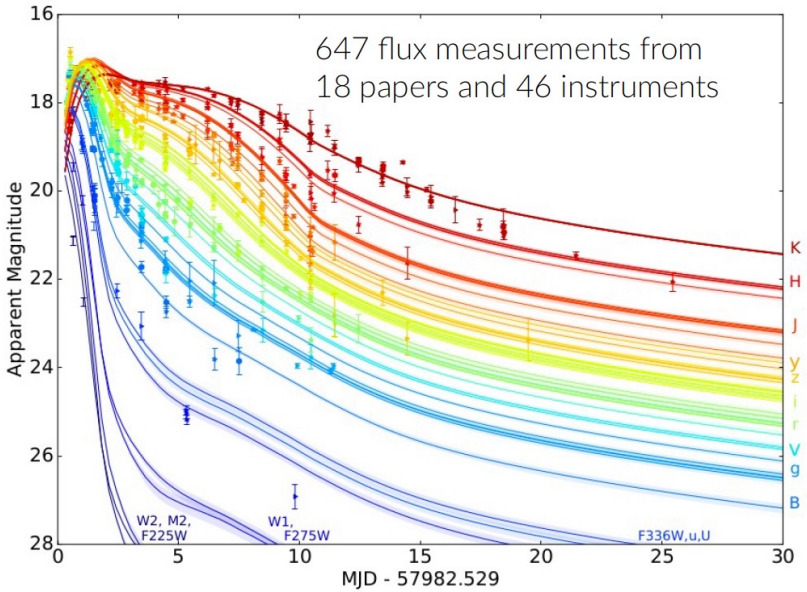

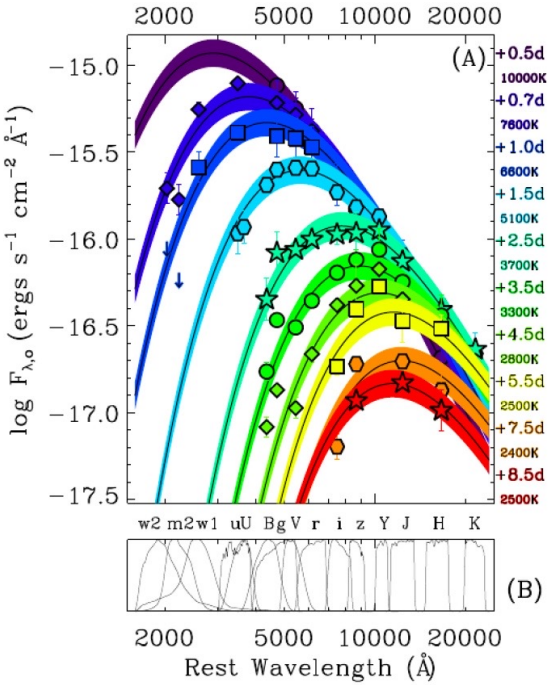

Discovery: 17.48 mag (*i* band)
Rapidly rise and fading after ~1 day
Decline faster in the blue band, 1.5 mag/day
SED shifts from near-UV to near-IR in 8 days – **hot ejecta and rapid cooling**

V. Ashley Villar et al, arXiv:1710.11576

Drout et al, Science, 2017

Kilonova model (r-process)

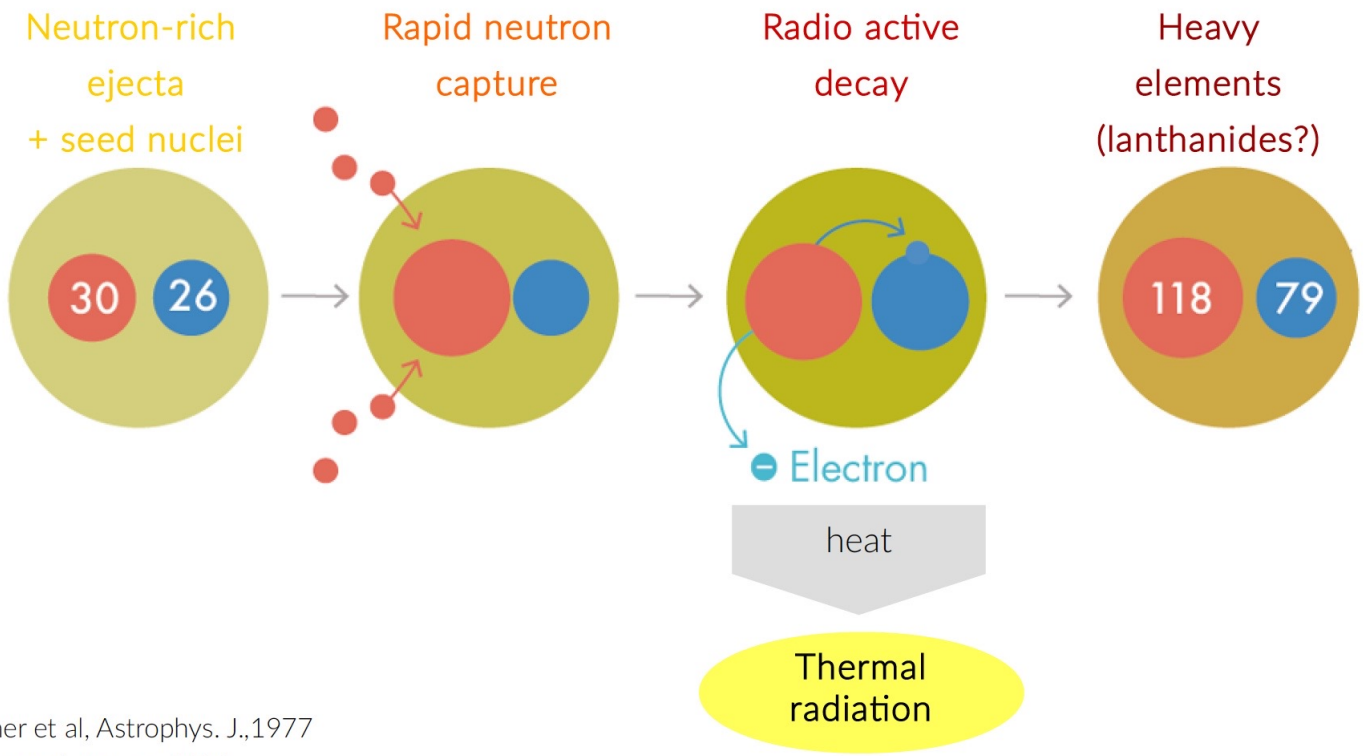

Lattimer et al, Astrophys. J.,1977
Eichler et al, Nature 1989
Li & Paczynsky, Astrophys. J. 1998

Inferring the kilonova model

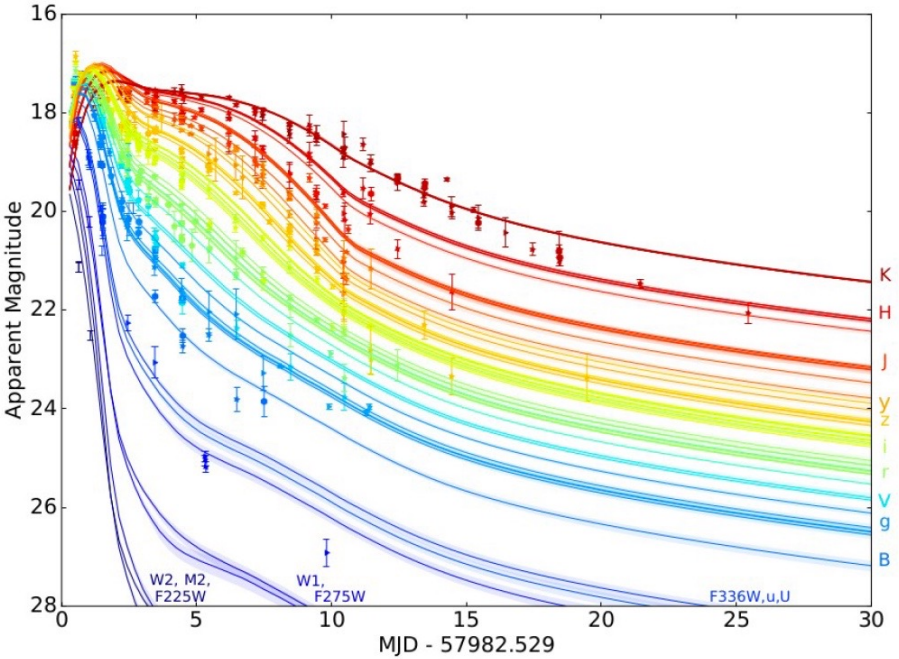

$$M_{ej} \sim 0.02 M_\odot$$
$$v_{ej} \sim 0.26\, c$$

$$M_{ej} \sim 0.04 M_\odot$$
$$v_{ej} \sim 0.15\, c$$

$$M_{ej} \sim 0.01 M_\odot$$
$$v_{ej} \sim 0.14\, c$$

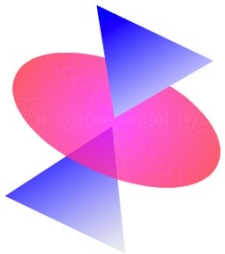

Proton-rich polar ejecta

Tidal tails or delayed outflow from accretion disk

- Best fit has three components
  - Lanthanide-poor (blue, 0.5 cm^2/g), intermediate (magenta, 3 cm^2/g) and lanthanide-rich (red, , 10 cm^2/g)
- Good fit provides **evidence for heavy-element nucleosynthesis and ejection**
  - Supernova models (^{56}Ni decay, Fe opacity) do not fit

V. Ashley Villar et al, arXiv:1710.11576

Spectrometry

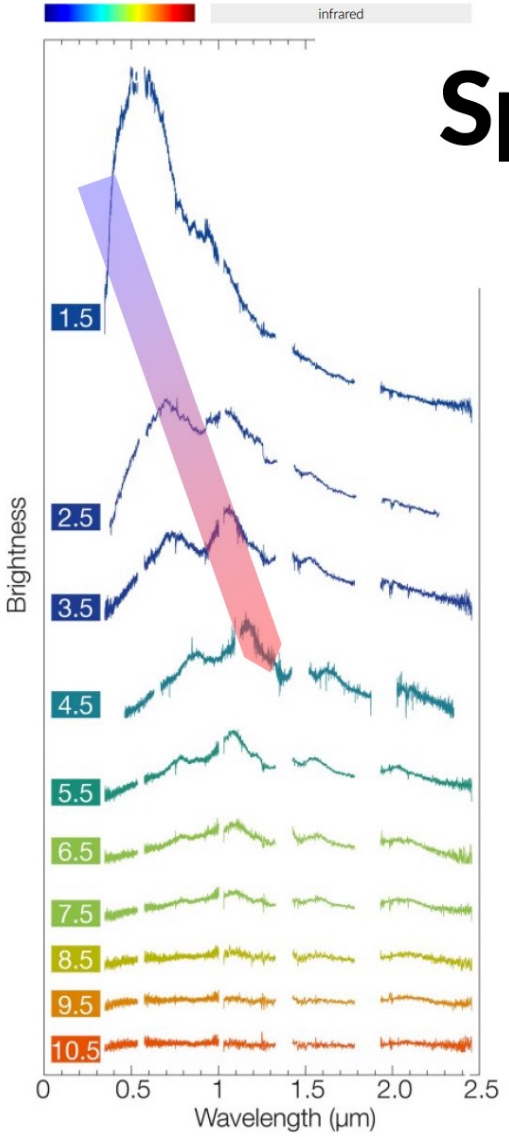

Pian et al, Nature, 2017

ESO VLT – X-shooter

Absorption lines consistent with Cesium and Tellurium

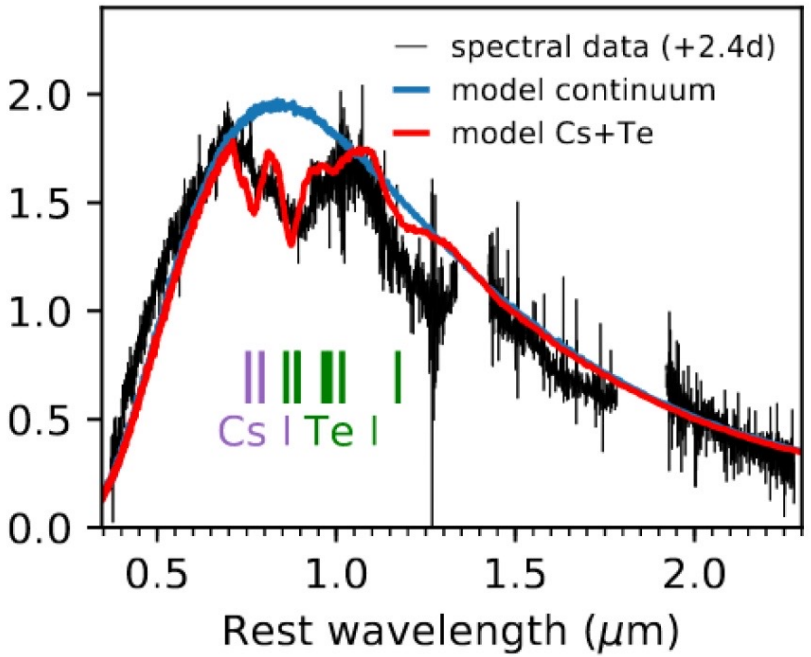

Smartt et al, Nature, 2017

ESO VLT – X-shooter

Kilonova –Nucleosynthesis (1)

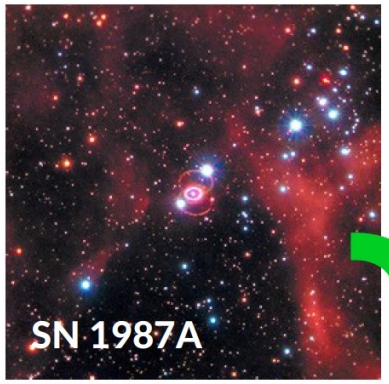

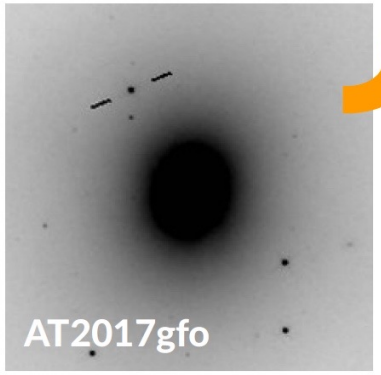

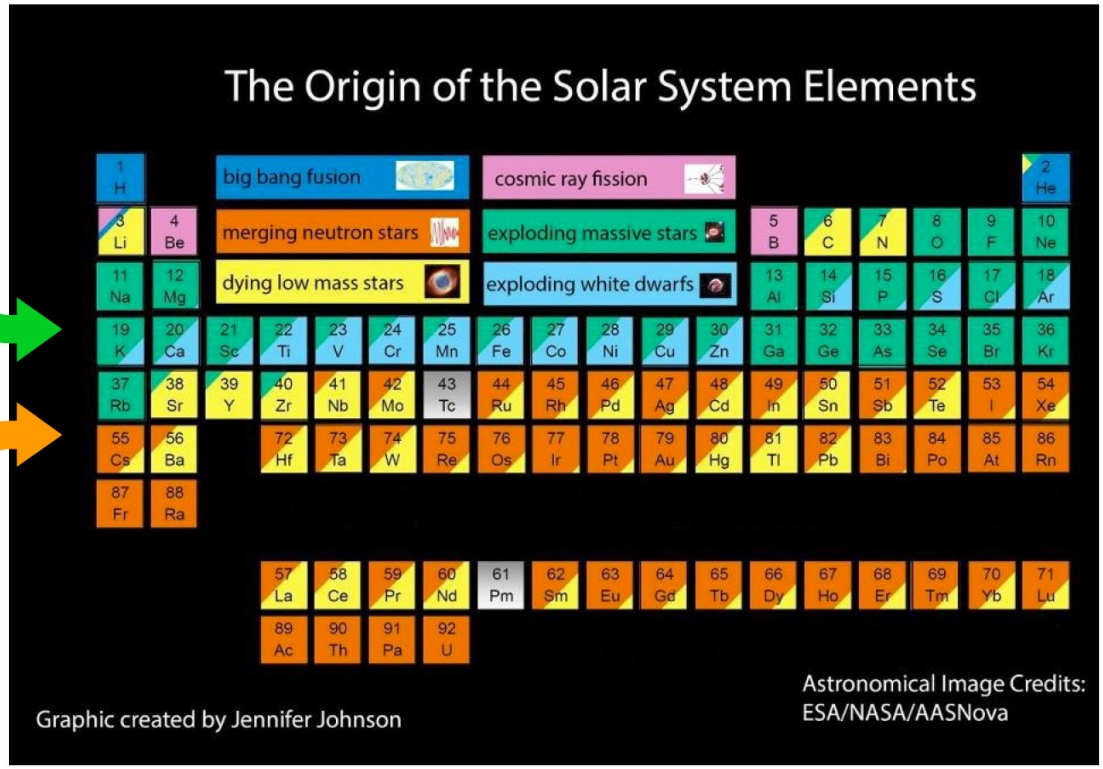

Kilonova –Nucleosynthesis (2)

$16\,000\ \mathrm{M}_\oplus$
of heavy elements

$10\ \mathrm{M}_\oplus$
in gold and platinum

(according to Edo Berger)

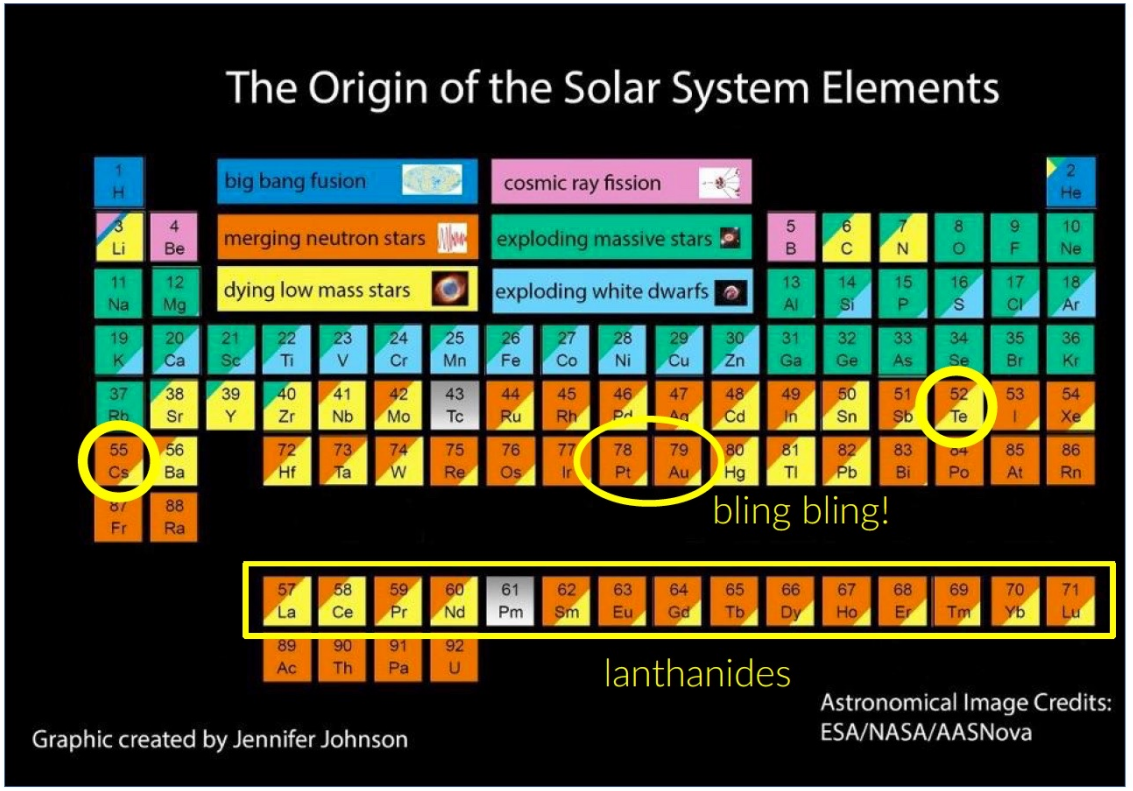

Main discoveries (3)

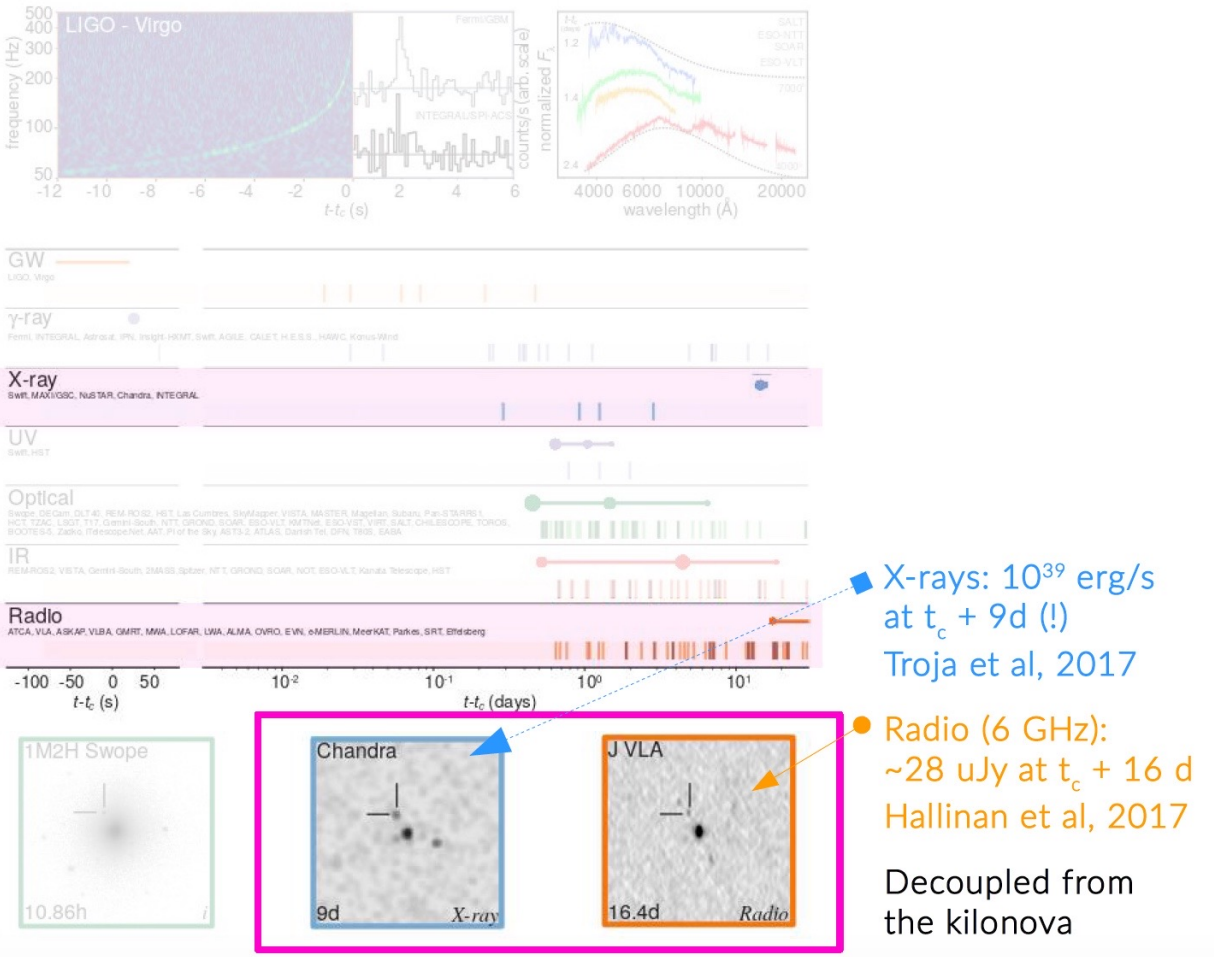

So far, no convincing global model

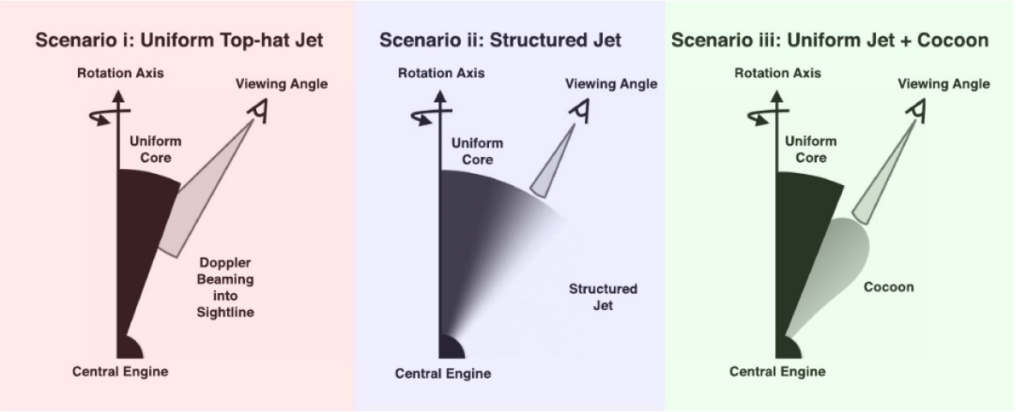

X-ray and radio counterparts are likely afterglows (synchrotron)

A. Jet off-axis by ~5 deg → excluded
   - 1.7 s delay is too short (delay to medium transparency)
   - Delayed X-rays require viewing angle ~ 13 deg
   - Radio flux x 10 larger if true

B. Structured jet (same conclusion)

C. "Hot cocoon"
   - Kilonova shows that a lot of material surrounds the binary. Jet drills into the ejecta.

Run 03
2018-2019

O3 performance: sensitivity

- BNS ranges [Mpc]

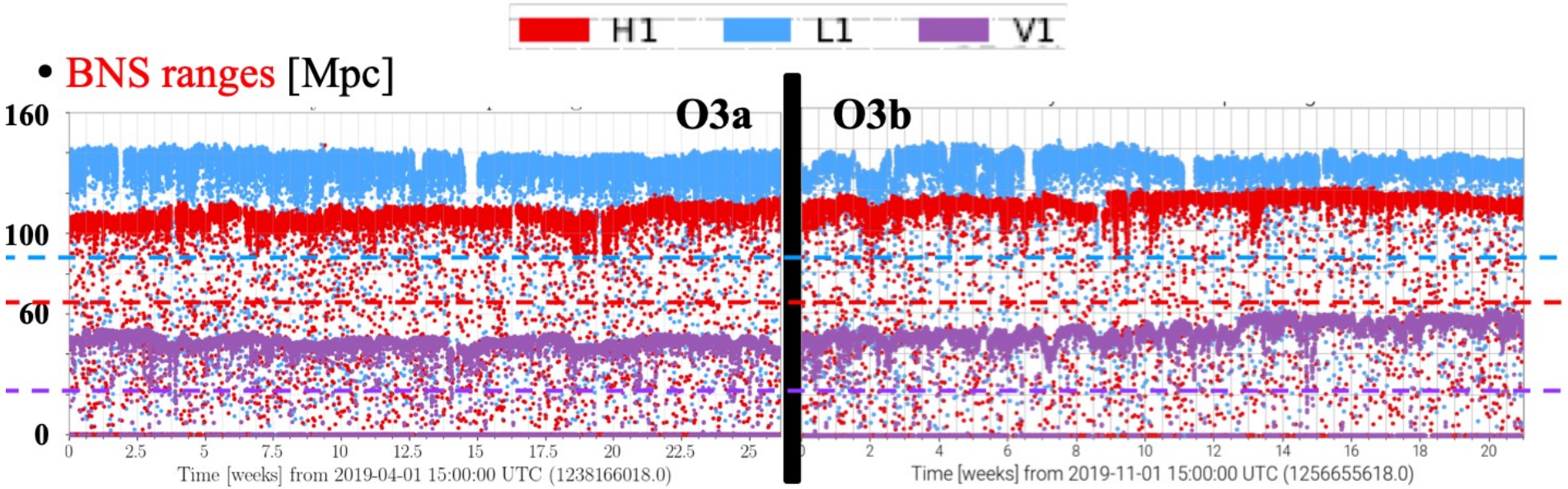

→ Dashed lines show the corresponding O2-averaged BNS ranges

- LIGO Livingston is the most sensitive detector, ahead of LIGO Hanford and Virgo

- Significant progress during the commissioning break for LIGO Hanford and Virgo
  - Point absorbers on optics for LIGO Livingston
    → Part of the lost BNS range recovered by tuning instrument

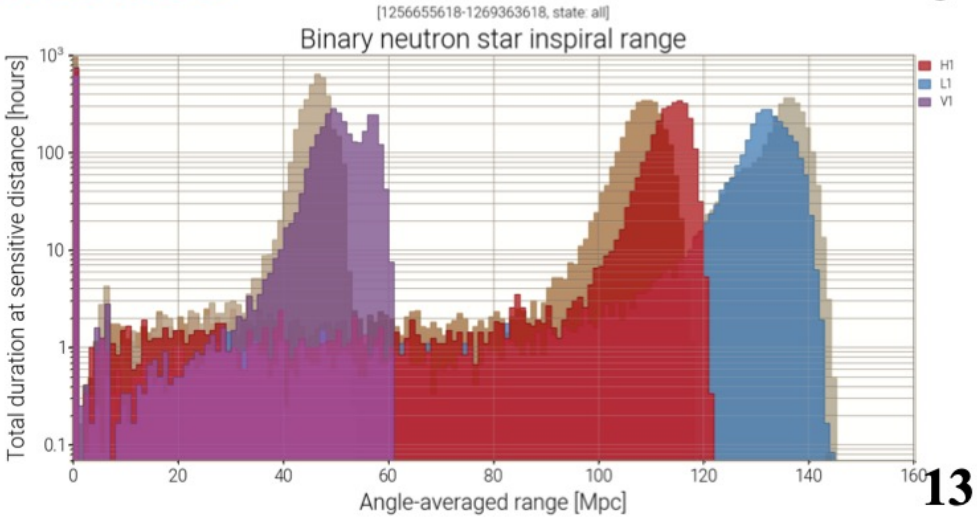

LIGO-Virgo candidate events over time

O3: 1 April 2019 — 27 March 2020

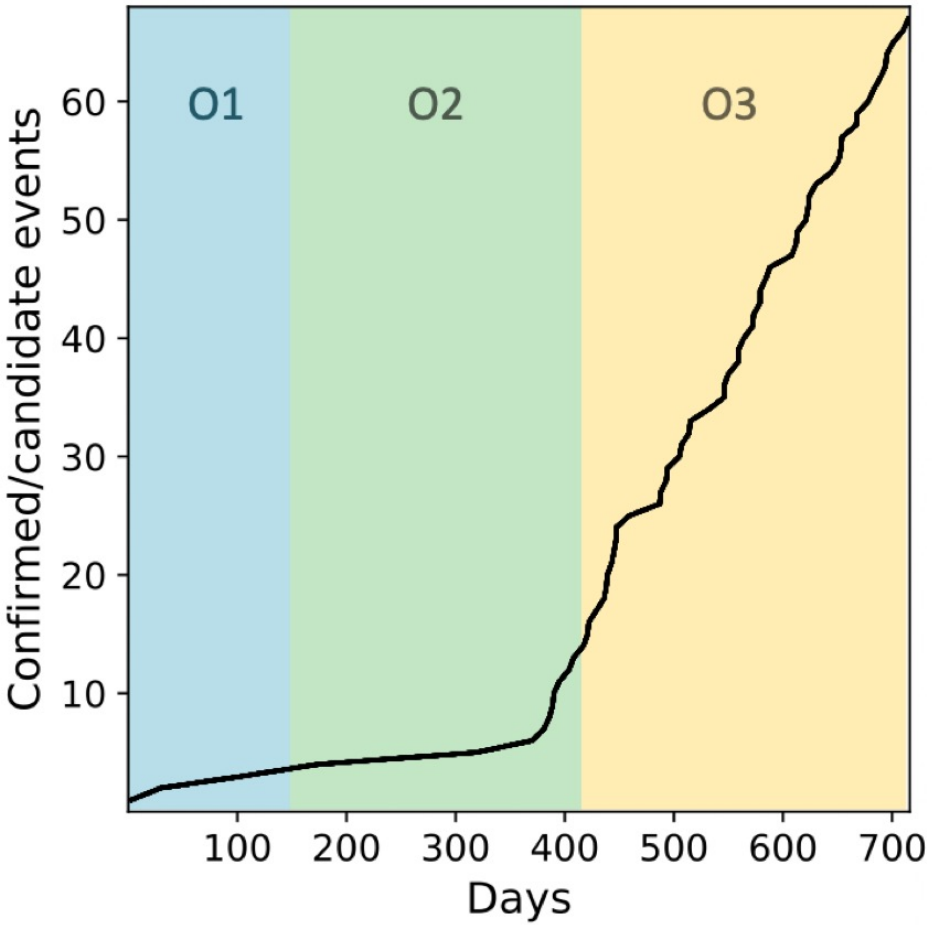

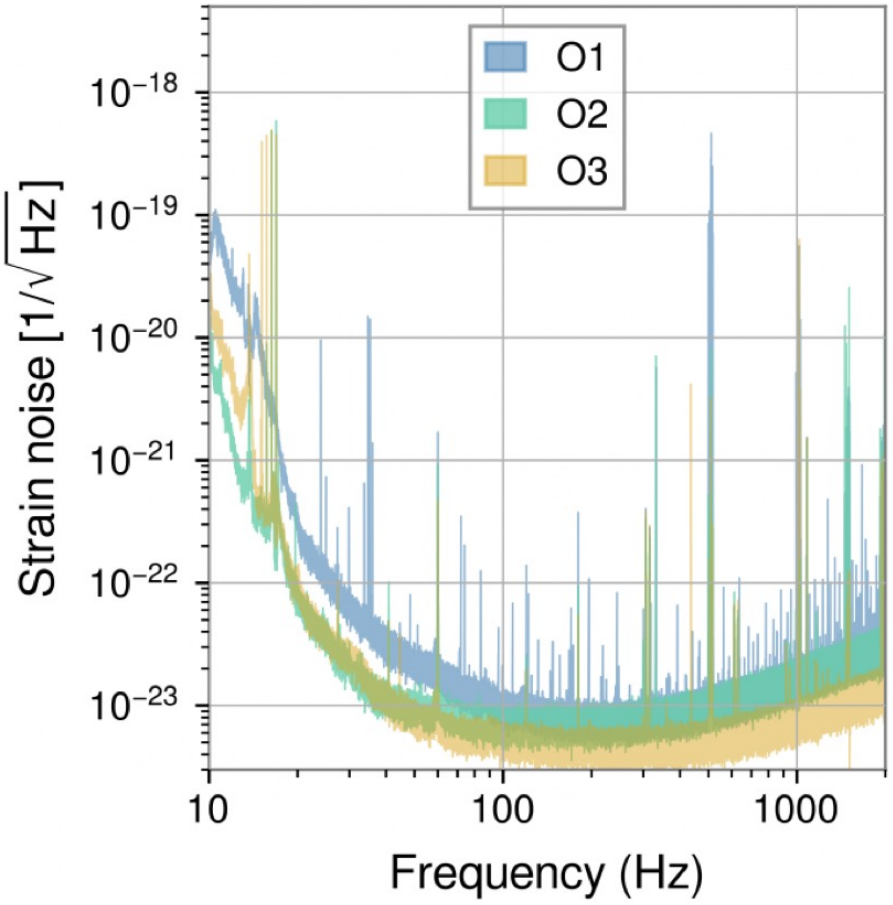

McIver & Shoemaker, in prep.

Many noteworthy transient GW signals discovered in O3

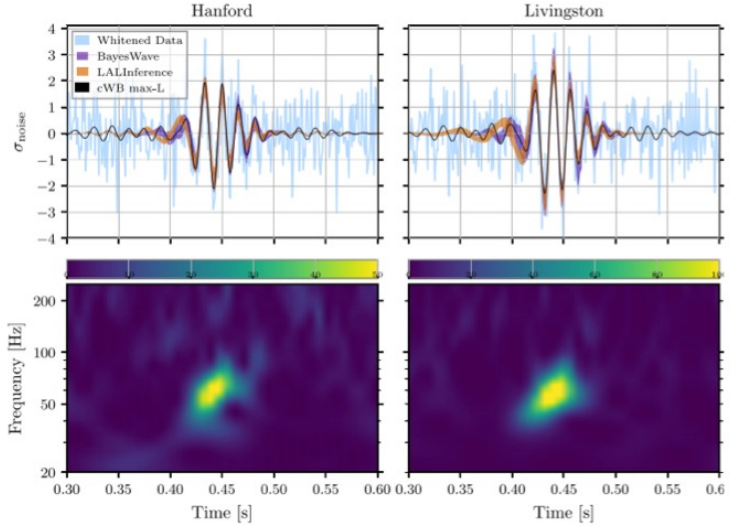

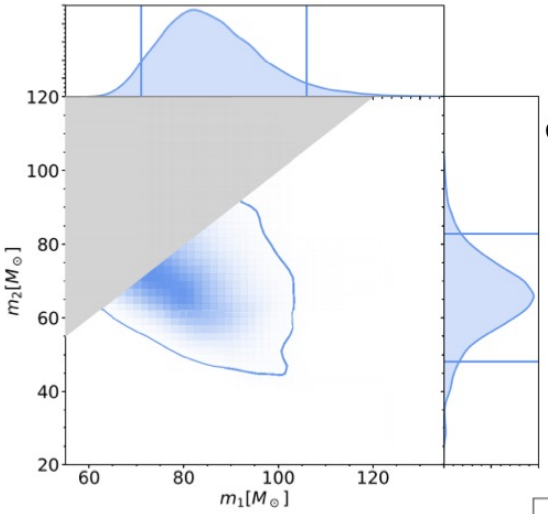

GW190521: 85, 66 $M_\odot$ system ==> 150 $M_\odot$
PISN mass gap: ~65-120 $M_\odot$
Abbott, et al., PRL **125** 101102

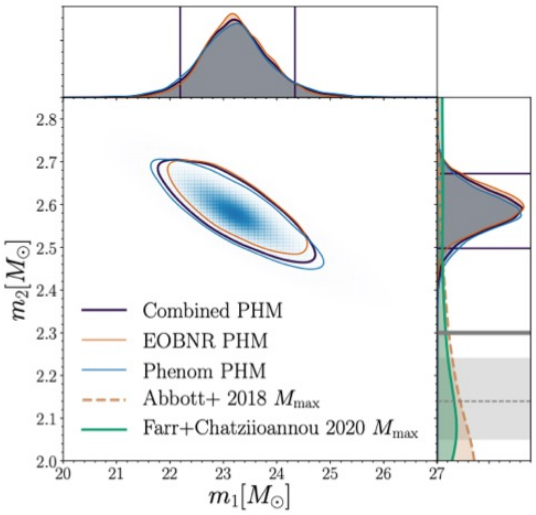

GW190814: 23, 2.6 $M_\odot$ system
Uncertain nature of companion
Abbott, et al., ApJL **896** L44

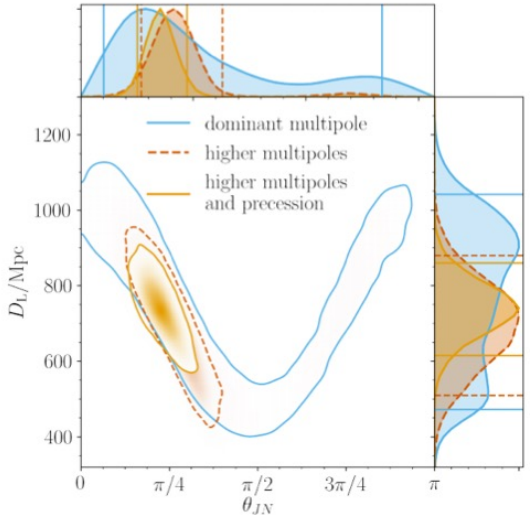

GW190421: 30, 8 $M_\odot$ system
Higher order modes
Abbott, et al., PRD **102** 043015

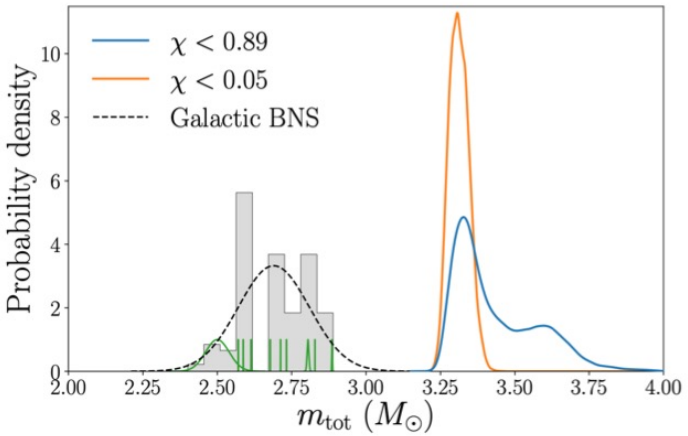

GW190425: second BNS detection
Total mass inconsistent with other galactic binary NSs
Abbott, et al., ApJL **892** L3

GWTC-2: 39 new confident detections

Mass ratio vs. total mass

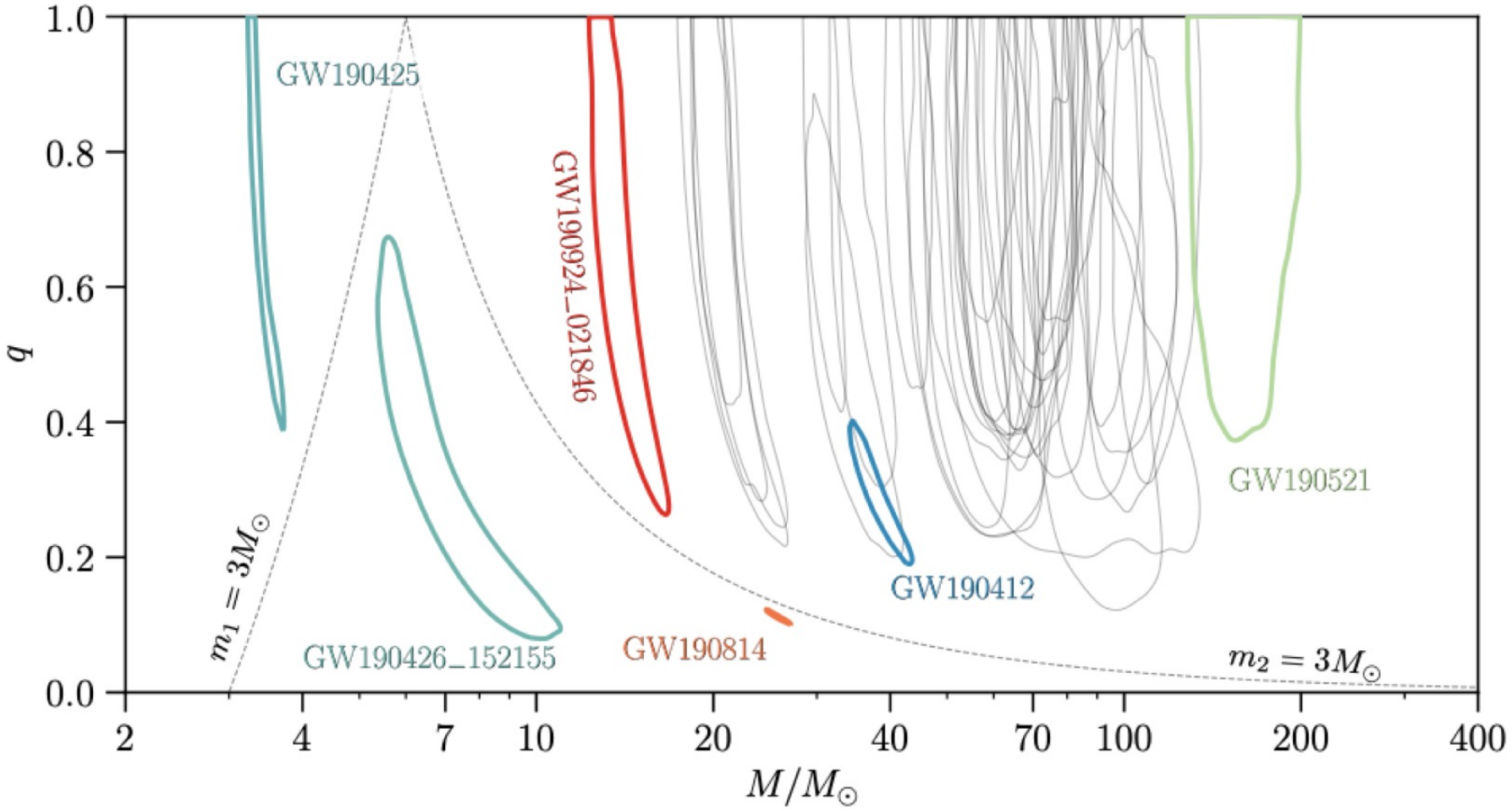

Abbott, et al., arXiv:2010.14527 [gr-qc]

Recent results for continuous wave searches

Surpassing spindown limit of millisecond pulsars

- Spindown limit benchmark for GW emission amplitude from known NSs
- First time spindown limit surpassed for millisecond pulsars
- MSPs have significantly different evolutionary history than slowly rotating pulsars
- Implications for internal magnetic field strength

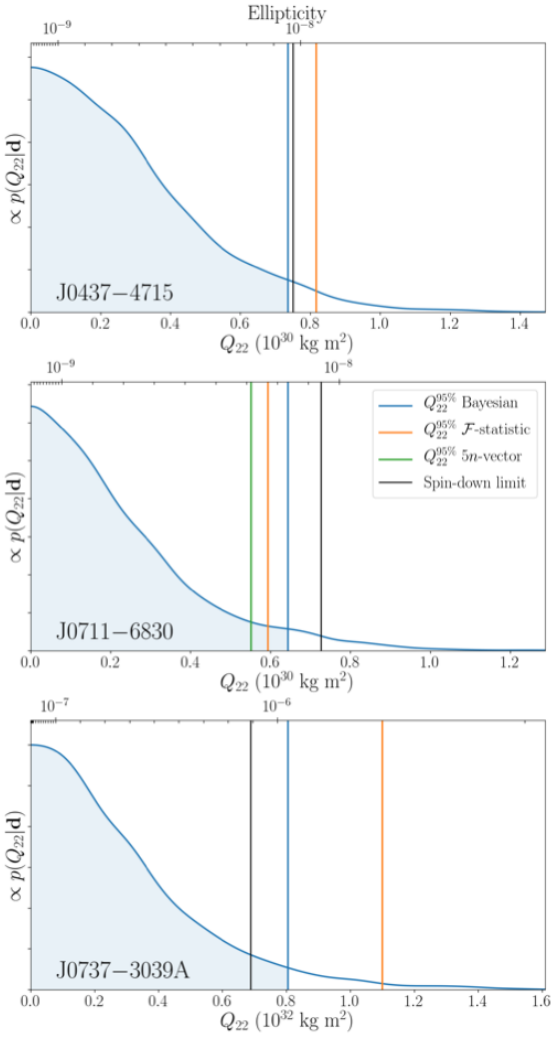

Abbott, et al., ApJL **902** L21

Screenshot

Recent results for continuous wave searches

Constraining continuous GW emission from J0537-6910

- Large spin down luminosity and frequent pulsar glitches observed
- NICER timing solution + LIGO/Virgo data ==> surpass spindown limit for first time

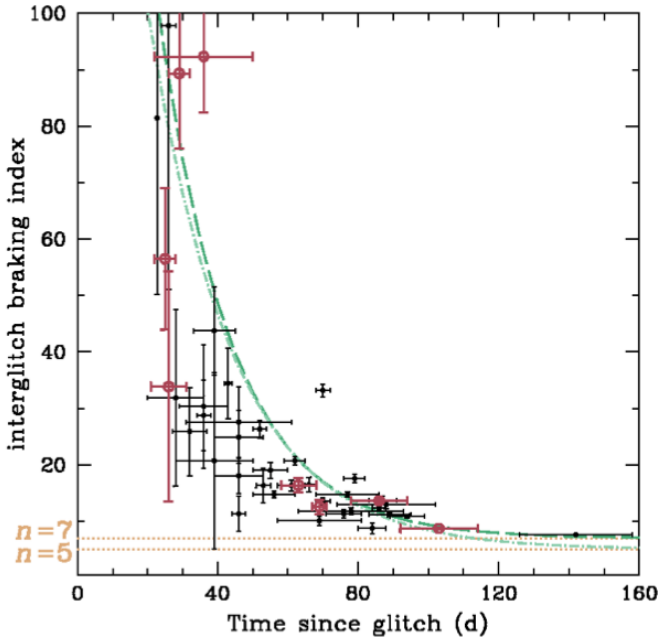

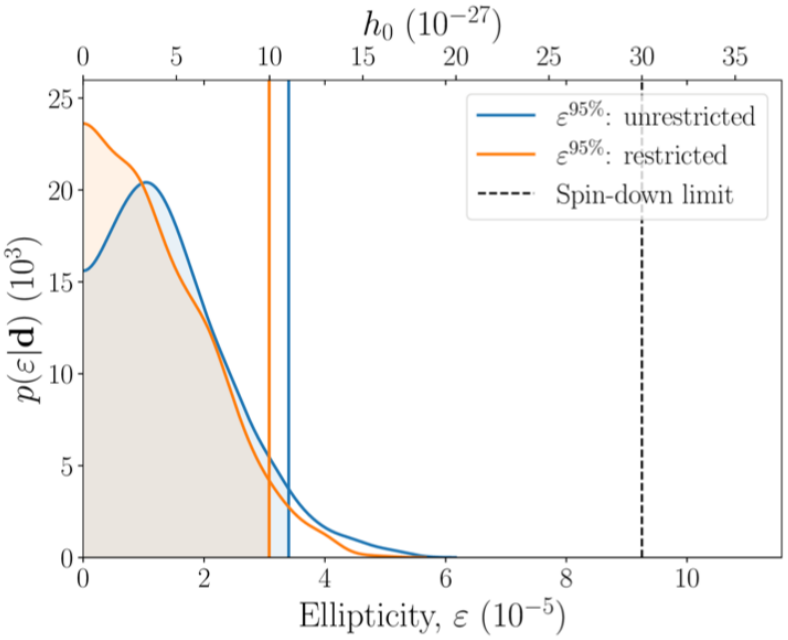

Abbott, et al. arXiv:2012.12926 [astro-ph.HE]

Recent results for continuous wave searches

All-sky search for unknown neutron stars in binary systems

- Notoriously computationally challenging search to include the additional unknown binary orbital parameters
- Most constraining results to date and probing sources in Galactic neighborhood

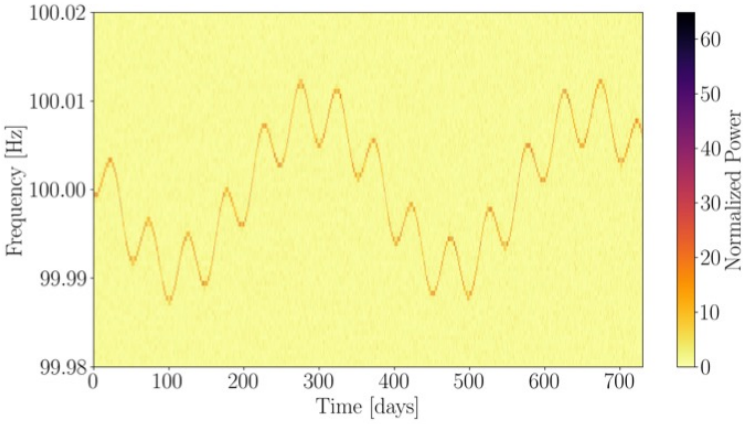

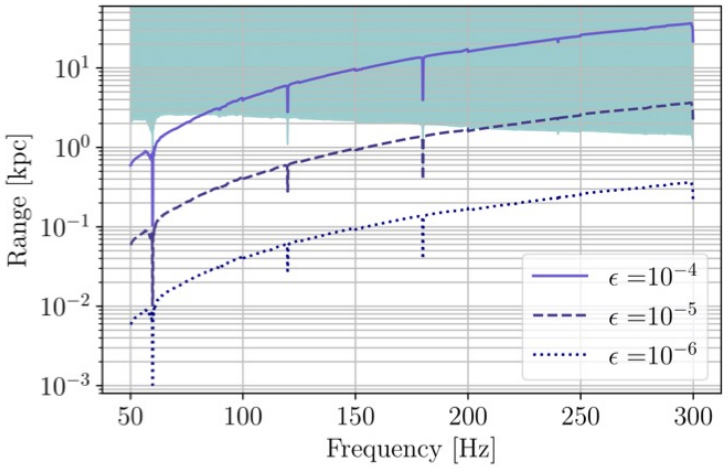

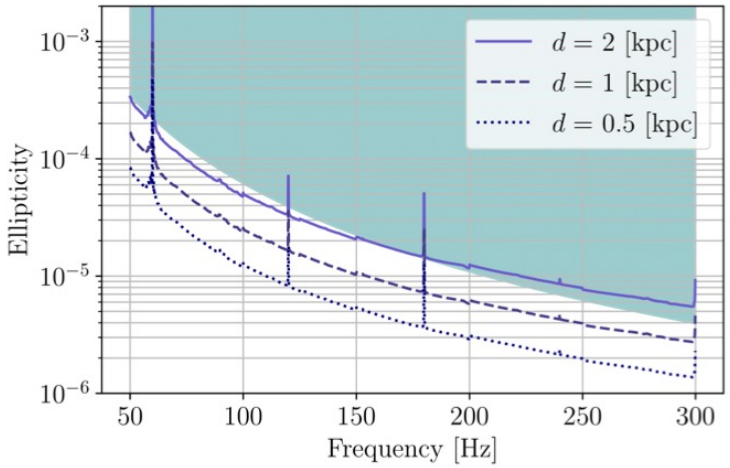

Abbott, et al., arXiv:2012.12128 [gr-qc]

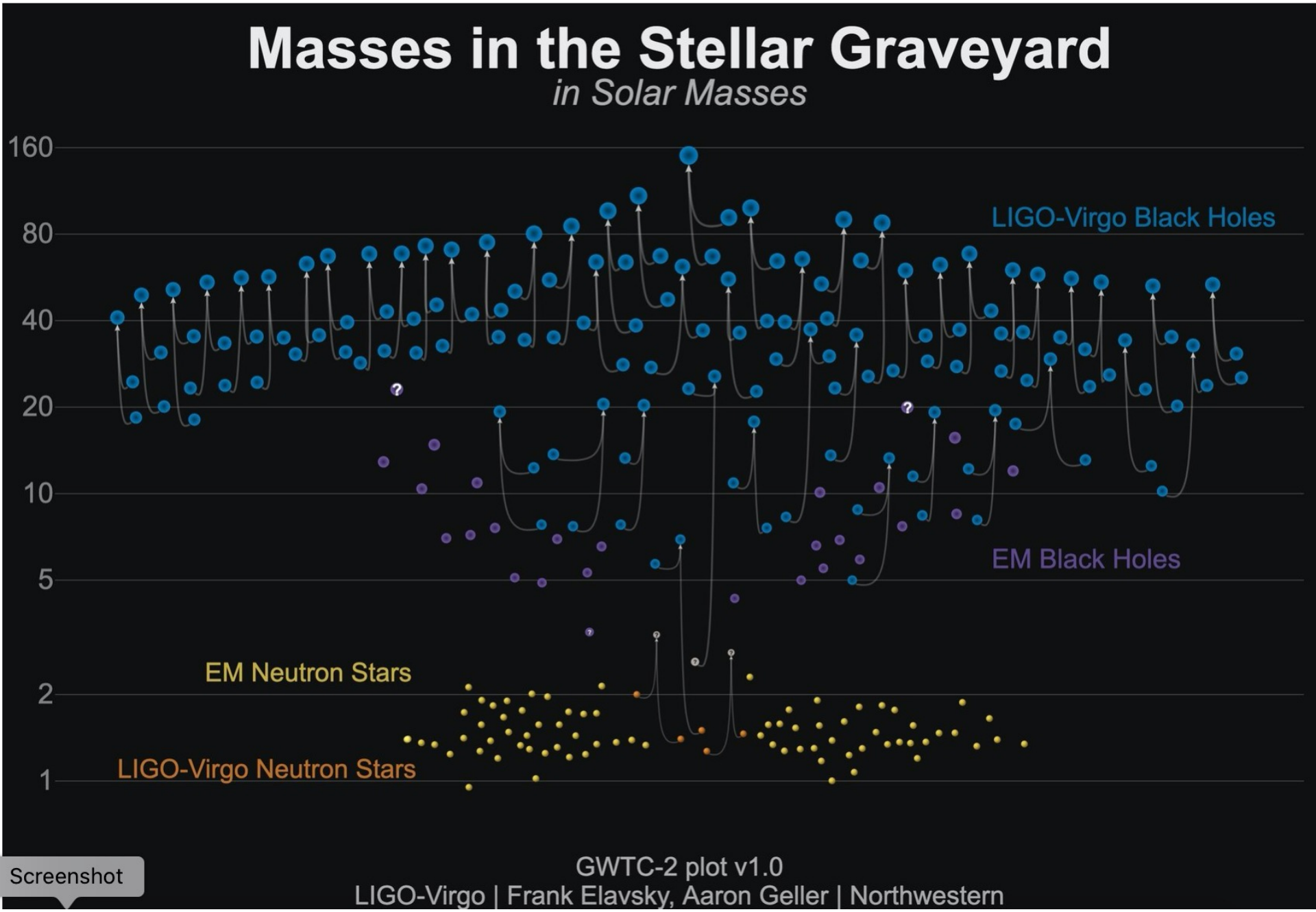
Masses in the Stellar Graveyard
in Solar Masses
160
80
40
20
10
5
2
1
LIGO-Virgo Black Holes
EM Black Holes
EM Neutron Stars
LIGO-Virgo Neutron Stars
?
?
GWTC-2 plot v1.0
LIGO-Virgo | Frank Elavsky, Aaron Geller | Northwestern

Screenshot

Conclusions

- Exceptional observation campaign after an exceptional event
  - Comprehensive picture of what happened after the merger
- Amazing predictive power of Physics (and physicists!)
  - All electromagnetic counterparts predicted
  - Kilonova (observed timescale, luminosity, color – consistent with simulations)
  - This is no the end of the story: explain gamma-rays vs X-ray and radio observations
- 30 yrs after SN1987A, entering the **golden ages of multimessenger astronomy**?
  - 80 papers published on GW170817 so far (and counting)
    https://lco.global/~iarcavi/kilonovae.html

Run 04
2023-2024
Run 5
2026-2028

Laser System Upgrade

Goal for O4: power of about 40 W at the input of the interferometer -> power of about 200 kW circulati
the arm cavities:

- 100 W monolithic fibered system -> maximum power of about 75 W injected into the interferome
- former multi-stage amplification system kept as spare

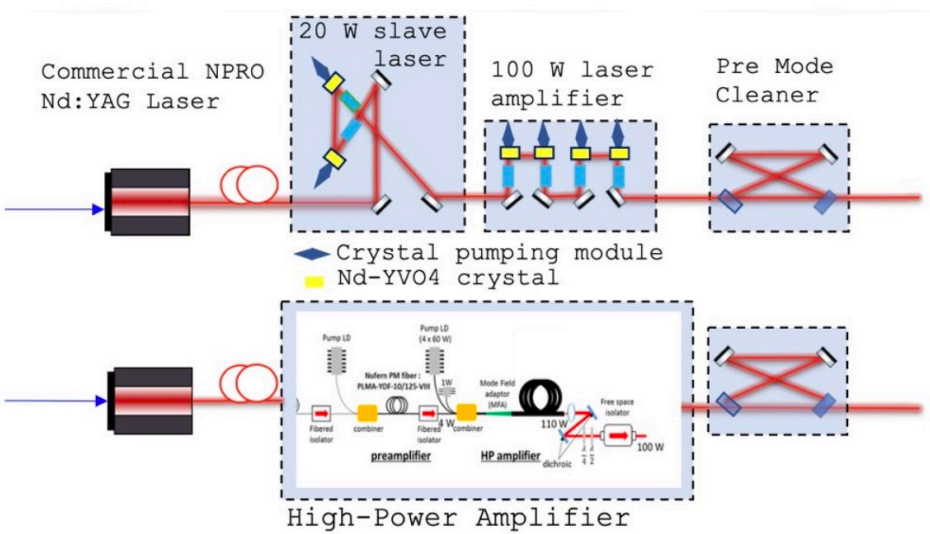

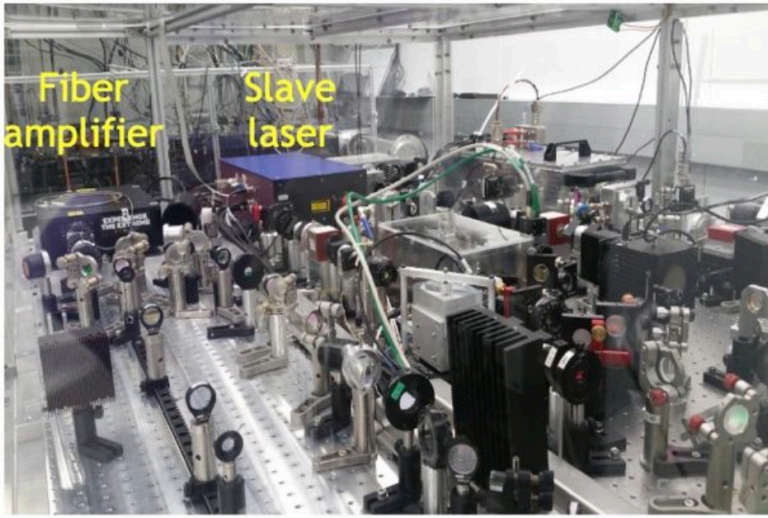

LIGO

Potential Resulting Sensitivity

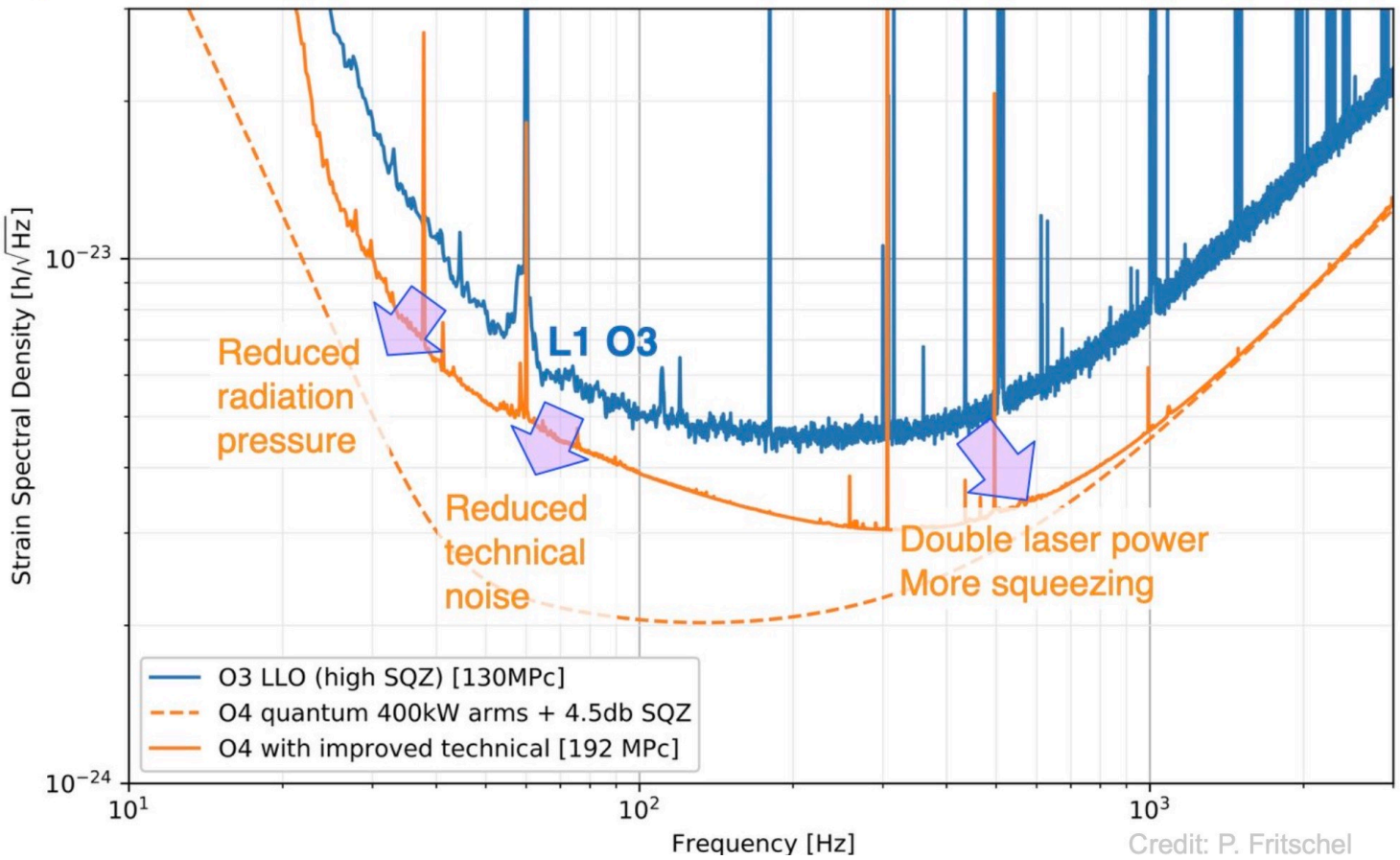

h ~ 1/r

rate ~ r^3 * T

VIRGO

Target Sensitivity Curve

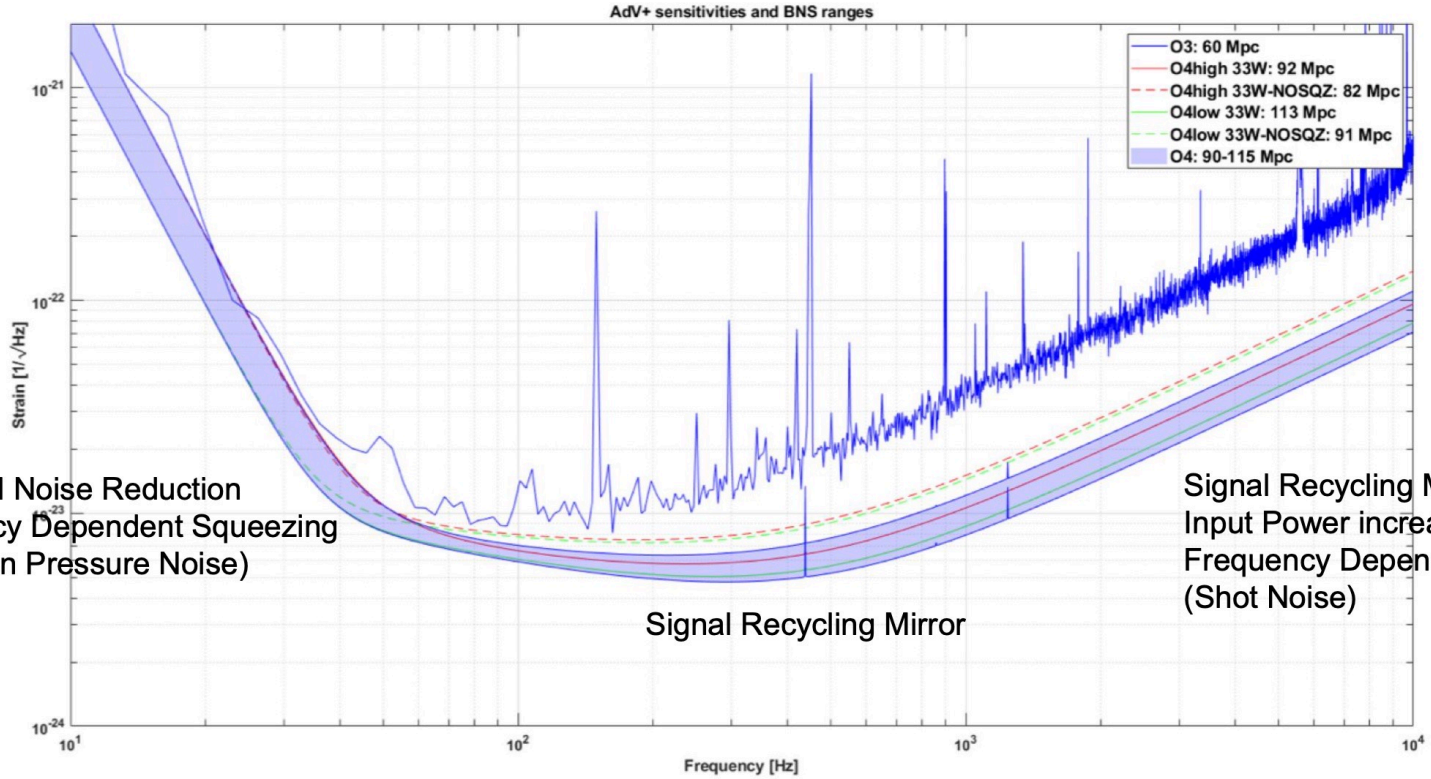

Technical Noise Reduction
Frequency Dependent Squeezing
(Radiation Pressure Noise)

Signal Recycling Mirror

Signal Recycling Mirror
Input Power increase
Frequency Dependent Squeezing
(Shot Noise)

KAGRA

O3GK Noise Budget

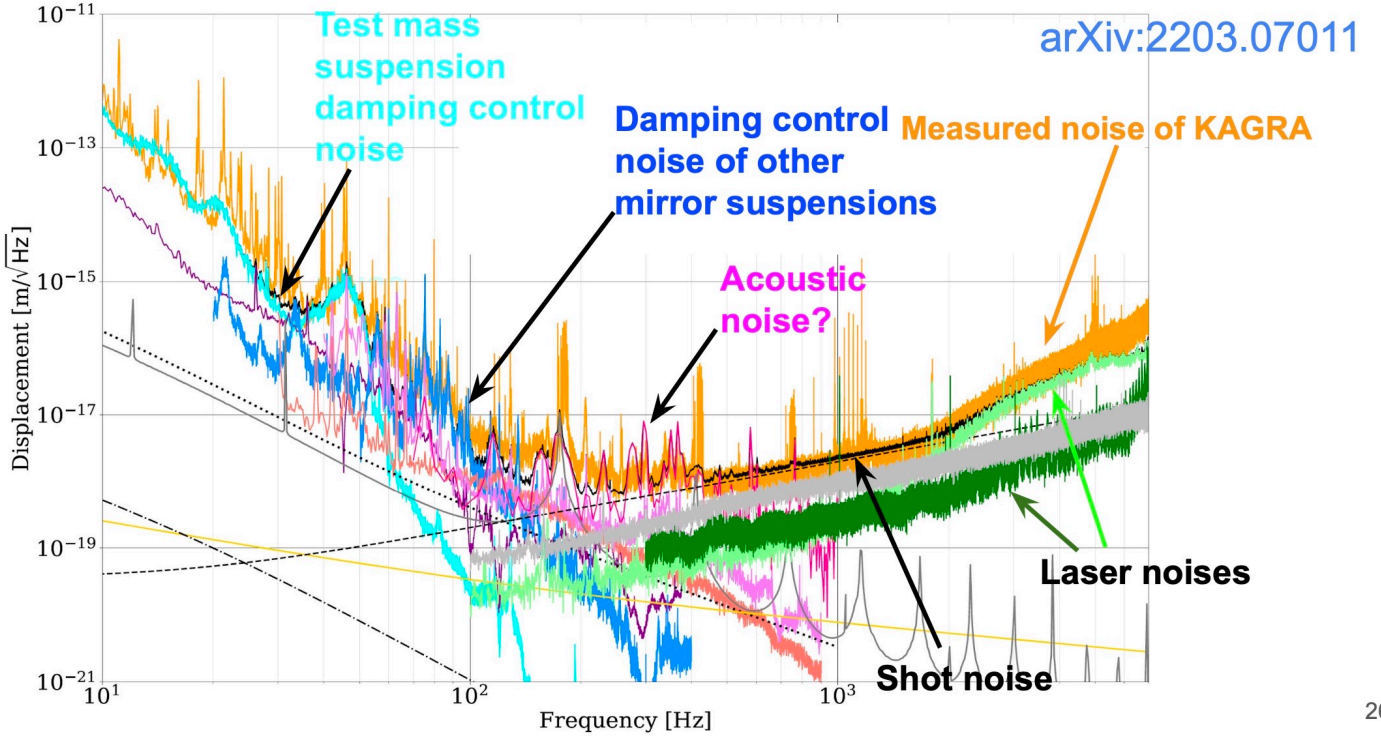

KAGRA

Possible scenarios for O4 sensitivity

O4a (1-3Mpc)
- Transparent SRM
- 1/3 technical noises

O4b (10-25Mpc)
- Cryogenic operation
- 1/25 to 1/77 technical noise reduction

KAGRA design sensitivities (128Mpc-153Mpc)

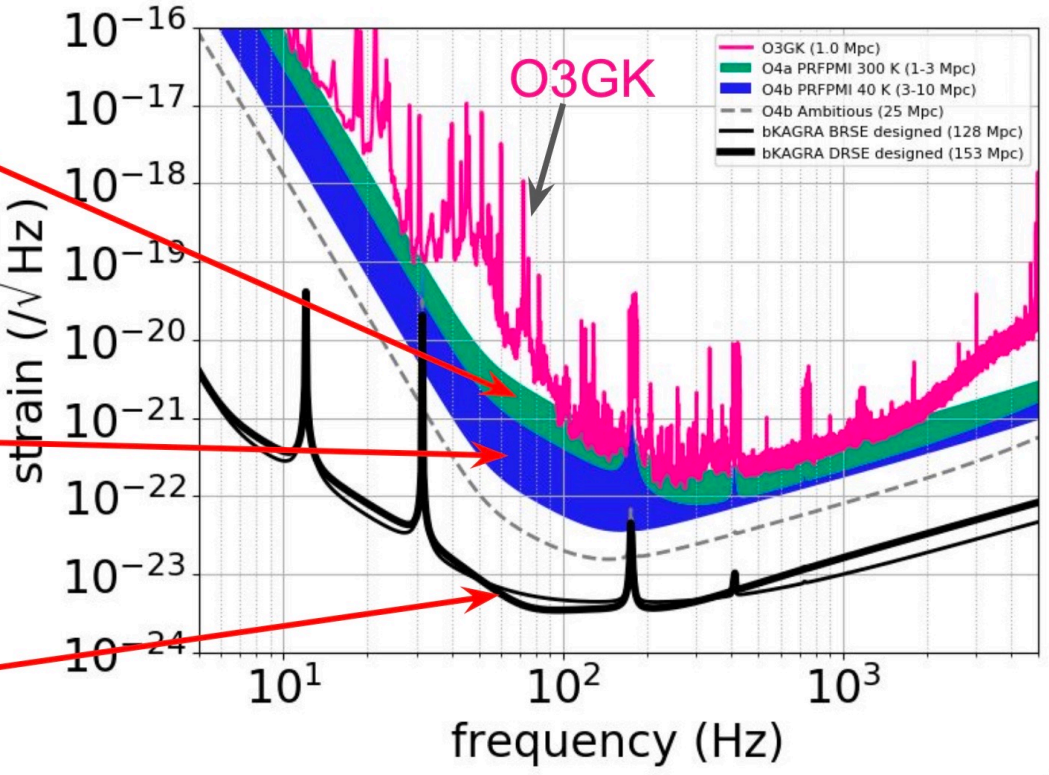

Runs 4 and 5

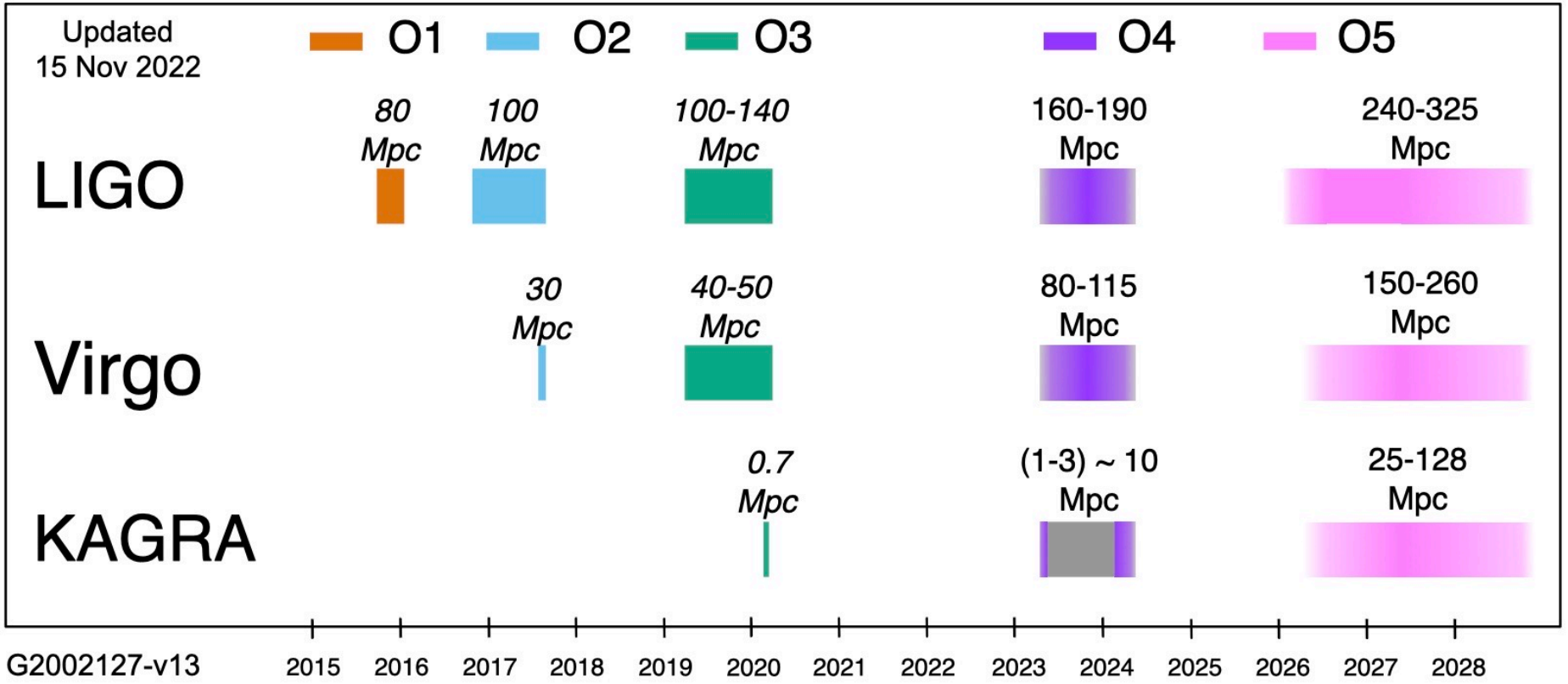
Updated
15 Nov 2022
O1
O2
O3
O4
O5
LIGO
80 Mpc
100 Mpc
100-140 Mpc
160-190 Mpc
240-325 Mpc
Virgo
30 Mpc
40-50 Mpc
80-115 Mpc
150-260 Mpc
KAGRA
0.7 Mpc
(1-3) ~ 10 Mpc
25-128 Mpc
G2002127-v13
2015
2016
2017
2018
2019
2020
2021
2022
2023
2024
2025
2026
2027
2028

MEPHI Lecture: Gravitational Waves

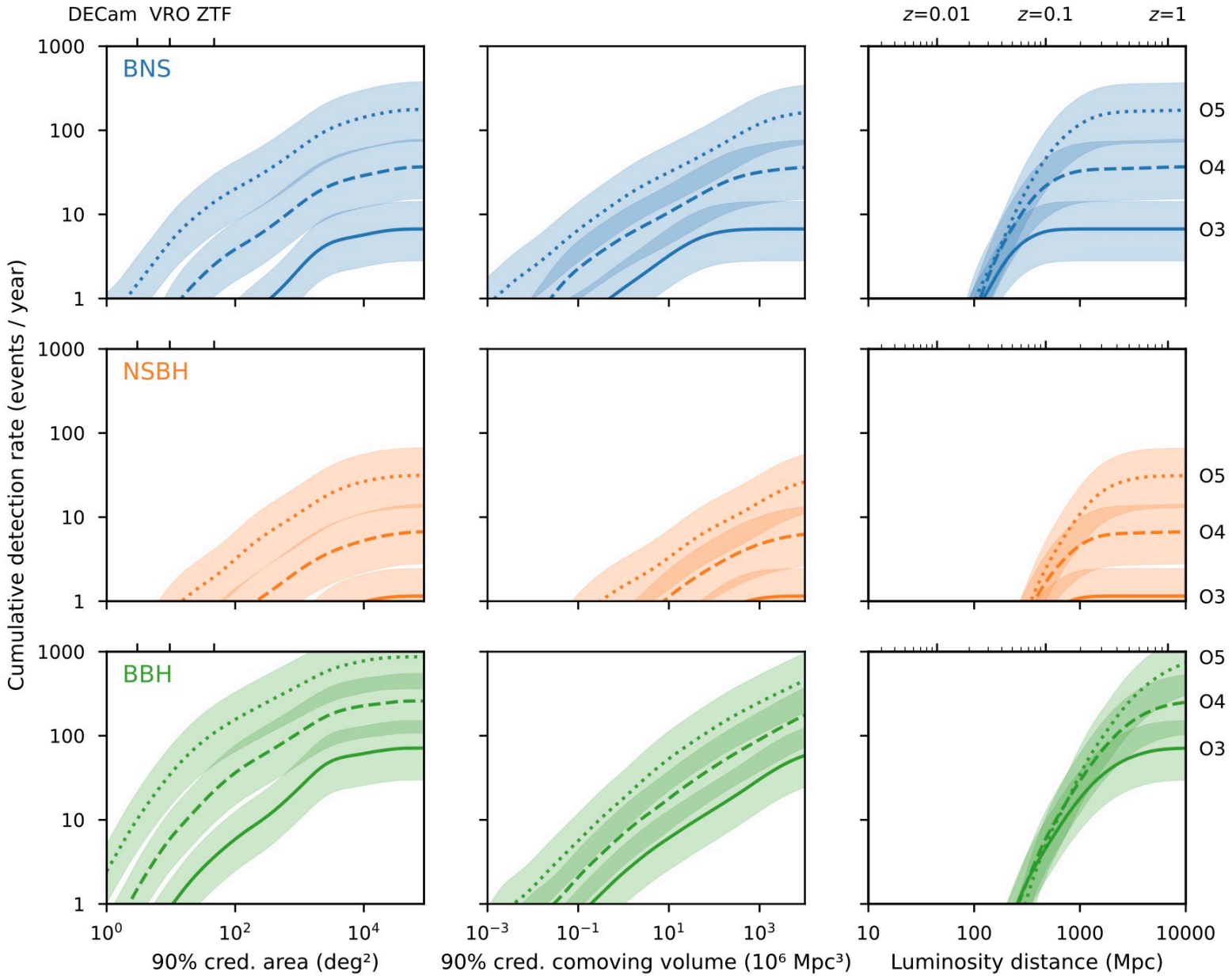

Summary

- *99 years after prediction by Einstein, gravitational waves was detected from 2 black holes merger in 2015.*
- *In 2017 extraordinary event of binary NS merger proved heavy element production and challenge gamma-ray models.*
- *This field has great future, first detections just started. Run O4 statistical properties of BH-BH and several NS-NS*

SEMINAR

For binaries with general eccentricity *e*

$$t_{GW} = \frac{5}{256}\,\frac{c^5}{G^3}\,\frac{a^4\,(1-e^2)^{7/2}}{m_1\,m_2\,(m_1+m_2)}$$

Peters 1964

Timescale depends on semi-major axis, eccentricity, masses

Timescale extremely long

EXERCISE: calculate tGW for 2 neutron stars with mass equal to the Sun mass (1 Msun) orbiting at the distance between Sun and Earth (1 AU)

NS-NS merging time

*G=6.67*1e-11 m^3/kg/s^2*

1au=150 Mkm=1.5e11 m

c=300 000 km/s=3e8 m/c

M=M_sun=10^33 g=10^30 kg

*G*M/c^2/a=6.7-11*10^30/9/10^16/1.5e11*
*m^3/s^2/m^3*s^2*

*G*M/c^2/a=5*10^-9*

*T=5/256/2*1.5e11/3e8 /(5e-9)^3 sec= 5*8 10^24*
sec =1.5 10^18 yr>> t_U